KONINKLIJK BELGISCH INSTITUUT VOOR NATUURWETENSCHAPPEN
OD NATUUR – BEHEERSEENHEID VAN HET MATEMATISCH MODEL

MOnitoring en MOdellering van het cohesieve sedimenttransport en evaluatie van de effecten op het mariene ecosysteem ten gevolge van bagger- en stortoperatie (MOMO)

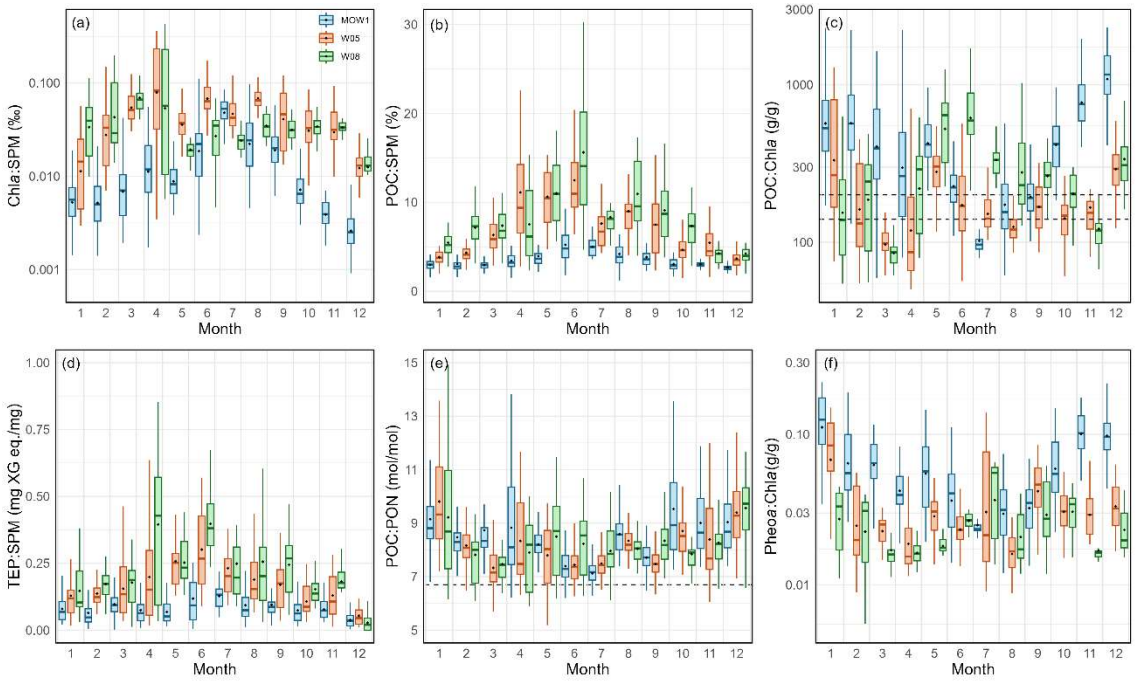

Activiteitsrapport (1 januari - 30 juni 2025)

Michael Fettweis, Xavier Desmit, Saumya Silori

MOMO/10/MF/202509/NL/AR/7

KBIN-OD Natuur - BMM
Vautierstraat 29
B–1000 Brussel
België

Inhoudstafel

1. Inleiding

1.1. Voorwerp van deze opdracht

Het MOMO-project (monitoring en modellering van het cohesieve sedimenttransport en de evaluatie van de effecten op het mariene ecosysteem ten gevolge van bagger- en stortoperatie) maakt deel uit van de algemene en permanente verplichtingen van monitoring en evaluatie van de effecten van alle menselijke activiteiten op het mariene ecosysteem waaraan België gebonden is overeenkomstig het verdrag inzake de bescherming van het mariene milieu van de noordoostelijke Atlantische Oceaan (1992, OSPAR-Verdrag). De OSPAR Commissie heeft de objectieven van haar Joint Assessment and Monitoring Programme (JAMP) gedefinieerd tot 2021 met de publicatie van een holistisch "quality status report" van de Noordzee en waarvoor de federale overheid en de gewesten technische en wetenschappelijke bijdragen moeten afleveren ten laste van hun eigen middelen.

De menselijke activiteit die hier in het bijzonder wordt beoogd, is het storten in zee van baggerspecie waarvoor OSPAR een uitzondering heeft gemaakt op de algemene regel "alle stortingen in zee zijn verboden" (zie OSPAR-Verdrag, Bijlage II over de voorkoming en uitschakeling van verontreiniging door storting of verbranding). Het algemene doel van de opdracht is het bestuderen van de cohesieve sedimenten op het Belgisch Continentaal Plat (BCP) en dit met behulp van zowel numerieke modellen als het uitvoeren van metingen. De combinatie van monitoring en modellering zal gegevens kunnen aanleveren over de transportprocessen van deze fijne fractie en is daarom fundamenteel bij het beantwoorden van vragen over de samenstelling, de oorsprong en het verblijf ervan op het BCP, de veranderingen in de karakteristieken van dit sediment ten gevolge van de bagger- en stortoperaties, de effecten van de natuurlijke variabiliteit, de impact op het mariene ecosysteem in het bijzonder door de wijziging van habitats, de schatting van de netto input van gevaarlijke stoffen op het mariene milieu en de mogelijkheden om deze laatste twee te beperken.

Voor een synthese van de resultaten uit de vergunningsperioden 2017-2021 en 2022-2026 zie de Vooruitgangsrapporten (Lauwaert et al., 2019; Fettweis et al., 2024) en het Syntheserapport (Lauwaert et al., 2021). Deze werden gepubliceerd conform art. 10 van het K.B. van 12 maart 2000 ter definiëring van de procedure voor machtiging van het storten in de Noordzee van bepaalde stoffen en materialen.

1.2. Algemene doelstellingen

Het onderzoek uitgevoerd in het MOMO project kadert in de algemene doelstellingen om de baggerwerken op het BCP en in de kusthavens te verminderen, om de effecten van het storten van baggerspecie te kwantificeren en om een gedetailleerd inzicht te verwerven van de fysische processen die plaatsvinden in het mariene kader waarbinnen deze baggerwerken worden uitgevoerd. Dit impliceert enerzijds beleidsondersteunend onderzoek naar de vermindering van de sedimentatie op de baggerplaatsen en het evalueren van alternatieve stortmethoden. Anderzijds is vernieuwend onderzoek noodzakelijk om beter de effecten van het storten van baggerspecie in te schatten. Dit onderzoek is specifiek gericht op het dynamische gedrag van slib in de waterkolom en op de bodem en de interacties tussen fysische en biologische processen en zal uitgevoerd worden met behulp van modellen, in situ metingen en remote sensing data.

De specifieke acties die binnen dit onderzoek uitgevoerd worden om de algemene doelstellingen in te vullen zijn:

1. Streven naar een efficiënter stortbeleid door een optimalisatie van de stortlocaties.

2. Continue monitoring van het fysisch en biogeochemisch milieu waarbinnen de baggerwerken worden uitgevoerd (Taak 1) en aanpassing van de monitoring aan de nog op te stellen targets voor het bereiken van de goede milieutoestand (GES), zoals gedefinieerd zal worden binnen MSFD;

3. Uitbouw en optimalisatie van het numerieke modelinstrumentarium, ter ondersteuning van het onderzoek (Taak 2.1).

1.3. Algemeen Onderzoek 2012-2026

Het onderzoek heeft als doel om de effecten van baggerspeciestortingen op het mariene ecosysteem (fysische en biogeochemische aspecten) te onderzoeken. Hiervoor worden in situ metingen verzameld, gebruik gemaakt van remote sensing data en worden numerieke modellen ingezet. Voor de vergunningsperiode 2022-2026 worden volgende taken voorzien:

1) In situ en remote sensing metingen en data-analyse

De monitoring van effecten van baggerspeciestortingen gebeurd met behulp van een vast meetstation in de nabijheid van MOW1, en met meetcampagnes met de RV Belgica (een 10-tal meetcampagnes voor het verzamelen van traject informatie, profielen en de calibratie van sensoren; en een 10-tal campagnes voor het onderhoud van het meetstation te MOW1). De geplande monitoring is gericht op het begrijpen van processen, zodoende dat de waargenomen variabiliteit en de effecten van baggerspeciestortingen in een correct kader geplaatst kunnen worden. Een belangrijk deel is daarom gericht op zowel het uitvoeren van de in situ metingen, het garanderen van kwalitatief hoogwaardige data en het archiveren, rapporteren en interpreteren ervan. Remote sensing data afkomstig van onder andere satellieten worden gebruikt om een ruimtelijk beeld te bekomen.

2) Uitbouw en optimalisatie van het modelinstrumentarium

Het tijdens de voorbije jaren verbeterde en aangepaste slibtransportmodel zal verder worden ontwikkeld. Dit zal parallel gebeuren met de nieuwe inzichten die voorvloeien uit de metingen en de procesgerichte interpretatie van de metingen.

3) Ondersteunend wetenschappelijke onderzoek

Monitoring gebaseerd op wetenschappelijke kennis is essentieel om de effecten van menselijke activiteiten (hier het storten van baggerspecie) te kunnen inschatten en beheren. Om te kunnen voldoen aan de door OSPAR opgelegde verplichtingen van monitoring en evaluatie van de effecten van menselijke activiteiten is het ontwikkelen van nieuwe monitorings- en modelleractiviteiten nodig. Dit houdt in dat onderzoek dat de actuele stand van de wetenschappelijke kennis weerspiegelt wordt uitgevoerd en dat de hieruit voortvloeiende nieuwe ontwikkelingen geïntegreerd zullen worden in zowel de verbetering van het modelinstrumentarium als voor het beter begrijpen van het kustnabije ecosysteem.

1.4. Onderzoek Januari 2022 – December 2024

Voor de periode 2019-2021 werd rekening gehouden werd met de aanbevelingen voor de minister ter ondersteuning van de ontwikkeling van een versterkt milieubeleid zoals geformuleerd in het “Syntheserapport over de effecten op het mariene milieu van baggerspeciestortingen (2021)” dat uitgevoerd werd conform art. 10 van het K.B. van 12 maart 2000 ter definiëring van de procedure voor machtiging van het storten in de Noordzee van bepaalde stoffen en materialen.

Taak 1: In situ en remote sensing metingen en data-analyse

Taak 1.1 Langdurige metingen te MOW1 en W05

Sinds eind 2009 worden er continue metingen uitgevoerd te MOW1 met behulp van een meetframe (tripode). Met dit frame worden stromingen, slibconcentratie, korrelgrootte-verdeling van het suspensiemateriaal, saliniteit, temperatuur, waterdiepte en zeebodem altimetrie gemeten. Om een continue tijdreeks te hebben, wordt gebruik gemaakt van 2 tripodes. Na ongeveer 1 maand wordt de verankerde tripode voor onderhoud aan wal gebracht en wordt de tweede op de meetlocatie verankerd. Op de meetdata wordt een kwaliteitsanalyse uitgevoerd, zodat de goede data onderscheiden kunnen worden van slechte of niet betrouwbare data.

Veranderingen in kustnabije ecosystemen zijn dikwijls gecorreleerd met veranderingen van de helderheid van het water of de concentratie aan particulair suspensiemateriaal (SPM) en dus ook met het gehalte aan particulair organisch materiaal. De zone waar de invloed van het minerale en kustnabij suspensiemateriaal overgaat in een zone met dominantie van organisch suspensiemateriaal van mariene origine is van bijzonder belang. De monitoring wordt uitgebreid met de verankering van een meetboei in locatie W05 (51°N 24.96', 2°E 48.7'). W05 is één van de drie monitoringspunten waar waterstalen en sensormetingen maandelijks worden uitgevoerd.

Taak 1.2 Calibratie van sensoren tijdens in situ metingen

Tijdens meetcampagnes met de R/V Belgica zullen een voldoende aantal 13-uursmetingen uitgevoerd worden met als hoofddoel het kalibreren van optische of akoestische sensoren en het verzamelen van verticale profielen. De metingen zullen plaatsvinden in het kustgebied van het BCP (MOW1, W05). De optische metingen (Optical Backscatter Sensor) zullen gekalibreerd worden met de opgemeten hoeveelheid materie in suspensie (gravimetrische bepalingen na filtratie) om te komen tot massa concentraties

Taak 1.3 Bio-geo-chemische monitoring van het SPM (BGCMonit)

SPM bestaat uit minerale deeltjes van fysicochemische (b.v. kleimineralen, kwarts, veldspaat) en biogene oorsprong (b.v. calciet, aragoniet, opaal), levend (bacteriën, fyto- en zoöplankton) en niet-levend organisch materiaal (b.v. fecale pellets, detritus, exopolymeren), en partikels van menselijke oorsprong (microplastiek). Het SPM kan door hydrofobe organische polluenten of metalen gecontamineerd zijn. De samenstelling en concentratie van het SPM inclusief de hydrofobe polluenten verandert in functie van de tijd en de locatie. Deze variaties worden beïnvloed door de interacties tussen de fysische processen (getij, meteo, klimaat), biologische cycli (algenbloei), chemische processen (koolstofcyclus) en menselijke activiteiten (aanvoer van nutriënten, bagger- en stortactiviteiten, offshore constructies). De samenstelling van het particulair en opgelost suspensiemateriaal zal bepaald worden tijdens meetcampagnes met de RV Belgica tijdens een 10-tal campagnes per jaar. Naast de totale hoeveelheid aan SPM worden ook de concentraties aan verschillende organische bestanddelen (POC, PON, TEP, chlorofyl en phaeofytine) bepaald. De opgeloste stoffen zijn inorganische nutriënten, DOC, DIC en alkaliniteit. Stalen van suspensiemateriaal zullen genomen worden met de centrifuge om de samenstelling ervan te bepalen.

Taak 1.4: Archivering en verwerking van de data

De meetdata worden gearchiveerd en er wordt een kwaliteitsanalyse uitgevoerd, zodat de goede data onderscheiden kunnen worden van slechte of niet betrouwbare data. Slechte data kunnen bv optreden doordat het instrument slecht heeft gewerkt en verkeerd werd ingesteld. Niet betrouwbare data zijn typisch geassocieerd met bv biofouling. De data en metadata worden gearchiveerd. De metingen worden verwerkt en geïnterpreteerd. En

zullen dienen als basis voor het verder gebruik bij wetenschappelijke vraagstellingen.

Taak 2: Uitbouw en optimalisatie van het modelinstrumentarium

Taak 2.1: Opstellen van een slibtransportmodel voor het BCP met Coherens V2

Een slibtransportmodel zal worden geïmplementeerd met de software Coherens V2. De software laat toe om rekening te houden met gemengde sedimenten en dus met de interactie tussen zand en slib en laat morfologische berekeningen toe door een verbeterde implementatie van het schema voor het massabehoud en gebruik van lagen met gemengde sedimenten. Verdere aanpassingen en verbeteringen aan het model zullen worden uitgevoerd, meer bepaald:

- Kritische bodemschuifspanning voor erosie van gemengde sedimenten,
- Formulering voor de bodemschuifspanning,
- Koppeling van het model met het TILES voxel model voor een betere voorstelling van de bodemkarakteristieken.

Taak 2.2: Validatie van het slibtransportmodel voor het jaar 2013 (stortproef)

Een eerste toepassing van het model kan het jaar 2013 zijn, waarin de terreinproef voor alternatieve stortplaats alsook een intensieve monitoring plaatsvond. Deze laatste zal gebruikt worden voor de validatie van het model. Verder zal het model vergeleken worden met andere modellen van het BCP.

Taak 2.3: Optimalisatie baggerwerken

Een operationeel stortmodel zal worden opgezet in overleg met aMT. Dit model zal geïntegreerd worden in de binnen BMM-OD Natuur beschikbare operationele modellen. Het model zal gebruikt worden om in functie van de voorspelde fysische (wind, stroming, golven, sedimenttransport, recirculatie), economische (afstand, grootte baggerschip) en ecologische aspecten op korte termijn een keuze te kunnen maken tussen de beschikbare stortlocaties. Een eerste test hiervoor werd uitgevoerd in Van den Eynde en Fettweis (2011) waarin werd aangetoond dat door een optimale positie te kiezen voor het storten van baggerspecie in functie van de meteorologische omstandigheden, een vermindering van de aanslibbing van de vaargeulen en haven van Zeebrugge kan worden verwacht.

Het model zal worden gebruikt voor de optimalisatie van de baggerwerken. Verschillende simulaties kunnen worden uitgeoefend waarbij de invloed van de verschillende mogelijke stortplaatsen kunnen worden geëvalueerd.

Taak 2.4: Flocculatiemodel

De inzichten die voortvloeien uit de in situ data (Taken 1.4, 3.1 en 3.2) zullen worden geïntegreerd in een numeriek model dat het verband tussen SPM, TEP en flocculatie langsheen temporele (getij, seizoenen) en geografische (waterkolom, onshore-offshore) schalen combineert. Het model zal worden opgezet als 1D verticaal en zal gekoppeld worden met het 2 klassen populatie model van Lee et al. (2011). Hierdoor zal de verticale verdeling van de minerale en de organische fractie van het SPM en hun interactie kunnen worden voorspeld.

Taak 3: Ondersteunend wetenschappelijk onderzoek

Monitoring gebaseerd op wetenschappelijke kennis is essentieel om de effecten van menselijke activiteiten (hier het storten van baggerspecie) te kunnen inschatten en beheren. Om te kunnen voldoen aan de door OSPAR opgelegde verplichtingen van monitoring en evaluatie van de effecten van menselijke activiteiten is een verdere implementatie van huidige en het ontwikkelen van nieuwe monitoringsactiviteiten nodig. Meer specifiek gericht op de activiteit ‘storten van baggerspecie’ worden hier – wat het fysische milieu betreft - turbiditeit, samenstelling van de zeebodem, bathymetrie en

hydrografische condities beoogt. Deze taak speelt hierop in door de ontwikkeling en de implementatie van nieuwe tools die de actuele stand van de wetenschappelijke kennis weerspiegelen teneinde de mathematische modellen te optimaliseren en verfijnen.

Taak 3.1: SPM samenstelling - minerale fractie

Door de aanwezigheid van gemengde sedimenten in de zeebodem (zand en slib) zal tijdens sterke stroming en of hoge golven ook een gemengde minerale fractie in suspensie komen. Dit heeft twee consequenties voor monitoring. Ten eerste reageren akoestische en optische sensoren verschillend op zand en slib, zodat de verzamelde tijdreeksen een grotere onnauwkeurigheid hebben tijdens zo'n momenten (Fugate & Friedrichs, 2002; Baschek et al., 2017; Schwarz et al, 2017; Fettweis et al., 2019). Ten tweede bevatten zandkorrels geen mineraal-gebonden organisch materiaal en stalen genomen tijdens dit soort momenten kunnen dus de onzekerheid van het SPM-POM model vergroten. Indien er geen rekening gehouden wordt hiermee zal de SPM concentratie onder- of overschat worden alsook de afgeleid organische fracties. Doel is om de zand en slibfractie te identificeren door gebruik te maken van innovatieve meettechnieken (Pearsons et al., 2021) die optische en akoestische sensoren combineren. Het ultieme doel is om te komen tot tijdreeksen van zand- en slibconcentratie te MOW1.

Uit visuele inspecties van de bodemsamenstelling te MOW1 tijdens de laatste jaren blijkt dat het sediment zandiger is geworden. De hypothese is, dat dit verband houdt met erosie van de vooroever na de strandopspuitingen die de voorbije jaren werden uitgevoerd. Aan de hand van de boven aangehaalde methode zal nagegaan worden of er een trend naar zandaanrijking kan vastgesteld worden in de omgeving van MOW1.

Taak 3.2: SPM samenstelling - organische fractie

Het semi-empirisch POM-SPM model (Fettweis et al., 2022) zal verfijnd worden met de nieuwe data verzameld in taak 1.3. Hierdoor zal de inschatting van de minerale en de vers en mineraal-gebonden organische fractie nauwkeuriger kunnen worden gedaan.

Op basis van dit POM-SPM model kan de samenstelling van het suspensiemateriaal (minerale fractie, vers en mineraal gebonden POC, PON en TEP) worden berekend voor de tijdreeksen te MOW (vanaf 2005) en voor de satellietdata (vanaf 1997). Dit zal toelaten om de geografische en temporele variabiliteit van de transitiezone tussen het kustgebonden turbiditeitsmaximum en de offshore wateren te kwantificeren. De dynamica van het suspensiemateriaal in beide gebieden is verschillend, wat consequenties heeft naar de modellering ervan. Verder kan uit de lange tijdsreeksen gekeken worden of het gebruik van de stortplaatsen, meer bepaald S1, geleid heeft tot een zeewaartse uitbreiding van het turbiditeitsmaximum.

Taak 3.3: Trends in SPM concentratie

Om significante statistische trends te kunnen documenteren in SPM concentratie over de laatste decades, zijn metingen nodig die een lange tijdspanne omvatten en een groot gebied omvatten. Deze data zijn helaas niet beschikbaar. Wat er wel beschikbaar is zijn de tripode metingen te MOW1 (vanaf 2005) en op andere locaties, de puntmetingen verzameld met onderzoeksschepen in het Belgisch Deel van de Noordzee sinds ongeveer 1970 (cf. Belspo 4DEMON project) en satellietbeelden (vanaf 1997). De tripode data geven de temporele variabiliteit weer, maar zijn heel beperkt wat ruimtelijke spreiding betreft. De 4DEMON en satellietbeelden zijn beschikbaar over een lange periode en over een groot gebied, maar kunnen de temporele schaal niet oplossen. Om deze heterogene datasets samen te kunnen gebruiken, zal gekeken worden naar de statistische verschillen tussen de datasets en naar een manier om deze te combineren. Doel is om mogelijke trends in de SPM concentratie te identificeren en deze te linken aan natuurlijke veranderingen of aan menselijke activiteiten.

De trendanalyse van de historische data zal de basis vormen om de verandering van de SPM concentratie in de nabijheid van de nieuwe stortplaats ZBW te kwantificeren.

Taak 4: Rapportage en outreach

Om de zes maanden zal er een activiteitenrapport worden opgesteld dat de onderzoeksresultaten beschrijft. Jaarlijks wordt er een 'factual data' rapport opgesteld van de verzamelde meetgegevens. De resultaten uit het onderzoek zullen tevens worden voorgesteld op workshops, conferenties en in de wetenschappelijke literatuur.

1.5. Aanpassing onderzoeksplan naar aanleiding van de niet beschikbaarheid van de RV Belgica

Het onderzoek uitgevoerd door het KBIN heeft als doel om de effecten van baggerspeciestortingen op het mariene ecosysteem (fysische en biogeochemische aspecten) te onderzoeken. Hiervoor worden in situ metingen verzameld, gebruik gemaakt van remote sensing data en worden numerieke modellen ingezet. Door het wegvallen van de RV Belgica sinds juni 2024 tot vermoedelijk 2026 kan het verzamelen van in situ data (monitoring) enkel deels worden uitgevoerd. Ter verantwoording van het begrootte budget voor 2024 en 2025 wordt er een overzicht over de geplande activiteiten met betrekking tot de in situ monitoring gegeven als ook extra taken beschreven die verantwoorden waarvoor het voorziene budget zal gebruikt worden.

Taak 1: In situ en remote sensing metingen en data-analyse

Taak 1.1 Langdurige metingen te MOW1 en W05

De Zeetijger zal ingezet worden voor het voortzetten van de langdurige meting met behulp van een meetframe (tripode) te MOW1. Het uitbreiden van de langdurige monitoring met een meetboei te W05 zal worden uitgevoerd.

Taak 1.5 Analysemethode TEP

De analysemethode voor de TEP (transparant exoplymeric particle) werd recent verbeterd (zie activiteitsrapport MOMO/10/MF/202410/AR/5). TEP-concentratie wordt bepaald met behulp van de kationische kleurstof Alciaan Blauw. In de literatuur wordt vermeld dat dit soort kleurstoffen zich kunnen hechten aan kleimineralen, waardoor de TEP-concentratie mogelijks verkeerd wordt bepaald. Er zal daarom onderzocht worden of de aanwezigheid van kleimineralen (zie hieronder) in het SPM een invloed kan hebben op de TEP-concentratie.

Taak 3: Ondersteunend wetenschappelijk onderzoek

Taak 3.4 SPM-samenstelling – mineralogie en interactie met organisch materiaal

Deze taak zal worden aangevuld met een mineralogische analyse van het suspensiemateriaal. We zullen hiervoor materiaal gebruiken dat in 2023 werd verzameld met een centrifuge (RV Belgica). Een mineralogische karakterisatie (bulk en kleimineralogie) van het suspensiemateriaal werd in 2004-2007 uitgevoerd en diende als basis voor een herkomstonderzoek van het slib op het BCP. Met deze nieuwe analyse willen we nagaan of er zich veranderingen hebben voorgedaan en indien ja, waarom.

Mineralen en organisch materiaal vertonen beide cohesieve eigenschappen en interacties kunnen leiden tot organo-minerale associaties. In natuurlijke systemen komen mineralen en organisch materiaal altijd samen voor en zijn organo-minerale associaties op moleculaire tot mm-schaal alomtegenwoordig. Deze interacties vinden op verschillende manieren plaats, variërend van de sorptie van kleine en grotere organische moleculen aan oppervlakken door bijvoorbeeld waterstofbruggen of van der Waals-krachten, tot intercalatie in expandeerbare kleimineralen, de occlusie in kleine kleimineraalaggregaten

(flocculi), het incorporeren van grote organische deeltjes (bijvoorbeeld fytoplankton, bacteriën) in vlokken en de vorming van biofilms. In mariene sedimenten en in het suspensiemateriaal wordt het gehalte aan organische materiaal voornamelijk bepaald door de mineralen en de beschikbaarheid van organisch materiaal. Met behulp van de mineralogische karakteristieken zal een betere beschrijving van de stabiliteit van de organische fractie kunnen worden bepaald.

Taak 3.5: Trends in SPM concentratie en stortoperaties

Doel van dit onderzoek is om mogelijke trends in de SPM concentratie te identificeren en deze te linken aan natuurlijke veranderingen of aan menselijke activiteiten. Deze bestaande taak zal worden aangevuld met een onderzoek op het effect van stortplaats ZBW. Onderzoeksvragen zijn 1) of de herlocatie van de stortplaats ZBW tot een vermindering van de aanslibbing (SPM concentratie) in de haven van Zeebugge heeft geleid en 2) wat de veranderingen in SPM concentratie ter hoogte van ZBW is. Hiervoor zullen tripode en remote sensing data worden gebruikt.

1.6. Gerapporteerde en uitgevoerde taken

Periode Januari 2022 - Juni 2022

Taak 1.1: De meetreeks te MOW1 werd verdergezet.
Taak 1.2: Calibratie van OBS sensoren werd uitgevoerd tijdens RV Begica campagnes 2022/01, 2022/03, 2022/06, 2022/09 en 2022/14.
Taak 3.1: De akoestische en optische sensoren werden gebruikt om veranderingen in sedimentsamenstelling te zien te MOW1. Eerste resultaten worden getoond in hoofdstuk 2.
Taak 3.2: Intensieve bio-geochemische monitoring werd uitgevoerd te MOW1, W05 en W08 tijdens RV Belgica campagnes 2022/01, 2022/03, 2022/07, 2022/11, 2022/14). Eerste resultaten worden besproken in hoofdstuk 3.
Taak 4: zie hoofdstuk 1.7

Periode Juli 2022 - December 2022

Taak 1.1: De meetreeks te MOW1 werd verdergezet.
Taak 1.2: Calibratie van OBS sensoren werd uitgevoerd tijdens RV Begica campagnes 2022/17, 2022/19, 2022/21, 2022/24, 2022/28 en 2022/32.
Taak 2.4: De interactie van phytoplankton en SPM resulteert in de vorming van grotere vlokken met hogerer valsnelheden. In een labo experiment werd de flocculatie bestudeerd tussen klei en phytoplankton deeltjes. Een twee-klassen flocculatiemodel werd opgesteld om de experimentele data kwantitatief te analyseren, zie paper in appendix 1.
Taak 3.2: Intensieve bio-geochemische monitoring werd uitgevoerd te MOW1, W05 en W08 tijdens RV Belgica campagnes 2022/17, 2022/19, 2022/21, 2022/24, 2022/28 en 2022/32). Eerste resultaten worden besproken in hoofdstuk 3.
Taak 3.3: Het informatieverlies van niet continue tijdreeksen werd bepaald. Dit zal de basis vormen voor de trendanalyse in SPM concentratie over een langere periode, zie hoofdstuk 2.
Taak 4: zie hoofdstuk 1.7

Periode Januari 2023 - Juni 2023

Taak 1.1: De meetreeks te MOW1 werd verdergezet.
Taak 1.2: Calibratie van OBS sensoren werd uitgevoerd tijdens RV Begica campagnes 2023/01, 2023/04, 2023/06, 2023/08 en 2023/10.
Taak 2.4: Een 2D horizontaal flocculatiemodel werd gevalideerd voor het BCP (zie appendix 3). De resultaten tonen het nut van een flocculatiemodel voor grootschalig SPM transport modellering. Tegelijkertijd onderstrepen ze tekortkomingen die het gevolg zijn van de transitie tussen kust en offshore en die zich uiten in verschillende SPM dynamica (zie ook hoofdstuk 2). Dit dient

opgenomen te worden in toekomstige modelleringen.

Taak 3: De resultaten beschreven in hoofdstuk 2 hebben mogelijks consequenties voor het storten van baggerspecie. Zij tonen immers aan dat er een duidelijk verschil tussen een kustnabije zone die gedomineerd wordt door minerale deeltjes en een offshore zone die vooral uit organische deeltjes bestaat. Er is geen (of weinig) uitwisseling tussen deze twee zones, zie hoofdstuk 3.

Taak 3.1: Analysen werden uitgevoerd gebaseerd op akoestische en optische sensoren van de tripode te MOW1 om de slib en zand fractie van het SPM te bepalen.

Taak 3.2: De biogeochemische monitoring werd verdergezet te MOW1, W05 en W08 tijdens RV Belgica campagnes 2023/01, 2023/04, 2023/06, 2023/08 en 2023/10.

<u>Periode Juli 2023 – December 2023</u>

Taak 1.1: De meetreeks te MOW1 werd verdergezet.

Taak 1.2: Calibratie van OBS sensoren werd uitgevoerd tijdens RV Belgica campagnes 2023/17 en 2023/25.

Taak 1.3: De biogeochemische monitoring werd verdergezet te MOW1, W05 en W08 tijdens RV Belgica campagnes 2023/17 en 2023/25.

Taak 2.4: De interactie tussen phytoplankton en minerale partikels werd verdergezet, resultaten werden voorgesteld op de INTERCOH conferentie (zie Appendix 1).

Taak 3.1: De analysen gebaseerd op akoestische en optische sensoren van de tripode te MOW1 om de slib en zand fractie van het SPM te bepalen, werden verdergezet. Eerste resultaten werden op de INTERCOH conferentie voorgesteld (zie Appendix 1)

Taak 3.2: De verandering in samenstelling van het SPM werd bestudeerd over de waterkolom, conclusies met betrekking tot de gehele waterkolom in turbide gebieden worden besproken in hoofdstuk 2 (en Appendices 2-12) en werden voorgesteld op de INTERCOH conferentie (zie Appendix 1).

Taak 4: zie hoofdstuk 1.7

<u>Periode Januari 2024 – Juni 2024</u>

Taak 1.1: De meetreeks te MOW1 werd verdergezet.

Taak 1.2: Calibratie van OBS sensoren werd uitgevoerd tijdens RV Belgica campagnes 2024/01 en 2024/03.

Taak 1.3: De biogeochemische monitoring werd verdergezet te MOW1, W05 en W08 tijdens RV Belgica campagnes 2024/01 en 2024/03.

Taak 3.1: De analysen gebaseerd op akoestische en optische sensoren van de tripode te MOW1 om de slib en zand fractie van het SPM te bepalen worden besproken in hoofdstuk 2 voor de langdurige meetreeks te MOW1.
De mineralogische samenstelling van het SPM werd bepaald in 4 locaties (MOW1, W03, W05 en W08).

Taak 3.2: Er werd gewerkt aan een klimatologie van de biogeochemische parameters (particulair en opgelost) langsheen de kust-offshore gradiënt.

Taak 4: zie hoofdstuk 1.7

<u>Periode Juli 2024 – December 2024</u>

Taak 1.1: De meetreeks te MOW1 werd enkel verdergezet tot september 2024, wegens het niet beschikbaar zijn van de Belgica.

Taak 1.2: idem voor de calibratie van de OBS sensoren.

Taak 1.3: idem voor de biogeochemisch monitoring te MOW1, W05 en W08.

Taak 2.4: De interactie van biologische en minerale bestanddelen werd gemodelleerd in een 0D flocculatiemodel. Het model simuleert de fytoplankton groei en de productie van organisch material, inclusief de ‘transparent exopolymer particles’ (TEP) en is gekoppeld aan het ‘two-class population balance equation’ flocculatie model zie Appendix 1;

Taak 3.1: Akoestische en optische sensoren van de tripode te MOW1 om de slib en zand fractie van het SPM te bepalen. Resultaten werden voorgesteld op de PECS concferentie, zie Appendices 2 en 3.

Taak 3.2: De studie van de biogeochemische karakterisatie van particulaire en opgeloste parameters op het BCP werd afgewerkt. Een uitgebreid verslag ervan zal in het komende rapport worden opgenomen, een samenvatting van de resultaten is te vinden in hoofdstuk 3.
Er werd meegewerkt aan een review paper over SPM dynamica, zie Appendix 4.

Taak 3.4: SPM-samenstelling – mineralogie en interactie met organisch materiaal, zie hoofdstuk 2.

Taak 3.5 Er werd verder gewerkt aan de analyse van trends en langdurige veranderingen in SPM concentratie en stortoperaties.

Taak 4: zie hoofdstuk 1.7

<u>Periode Januari 2025 – Juni 2025</u>

Taak 1.1: De meetreeks te MOW1 werd hervat vanaf April tot Juni.

Taak 1.2: Calibratie van de OBS sensoren kon niet worden uitgevoerd wegens het niet beschikbaar zijn van de Belgica of een alternatief onderzoeksschip

Taak 1.3: idem voor de biogeochemisch monitoring te MOW1, W05 en W08.

Taak 1.5 Er werd begonnen met de valorisatie van de analysemethode TEP.

Taak 3.2: De studie van de biogeochemische karakterisatie van particulaire en opgeloste parameters op het BCP werd afgewerkt, zie hoofdstuk 2.

Taak 3.5 Er werd verder gewerkt aan de analyse van trends en langdurige veranderingen in SPM concentratie en stortoperaties.

Taak 4: zie hoofdstuk 1.7

1.7. Publicaties

Hieronder wordt een overzicht gegeven van publicaties met directe betrokkenheid van het KBIN waar resultaten en data uit het MOMO project in werden gebruikt.

<u>Activiteits-, Meet- en Syntheserapporten</u>

Fettweis M, Desmit X, Silori, S. 2025. MOMO activiteitsrapport (1 januari - 30 juni 2025). BMM-rapport MOMO/10/MF/202509/NL/AR/7, 41pp + app.

Hindryckx K. 2025. Rapport van de RV Belgica Meetcampagnes en Verankering van Meetsystemen 2019. BMM-rapport OD Natuur-MDO/2025-06/MOMO/2019, 241pp.

Fettweis M, Silori S, Tran D, Desmit X. 2025. MOMO activiteitsrapport (1 juli - 31 december 2024). BMM-rapport MOMO/10/MF/202502/NL/AR/6, 34pp + app.

Fettweis M, De Witte B, Van Hoey, Seghers S, Vanermaete, Timmermanx S, Hermans L. 2024. Vooruitgangsrapport juni 2024 over de effecten op het mariene milieu van baggerspeciestortingen. MF/2024/10, 34pp.

Fettweis M, Tran D, Knockaert M, Desmit X. 2024. MOMO activiteitsrapport (1 januari - 30 juni 2024). BMM-rapport MOMO/10/MF/202410/NL/AR/5, 27pp.

Fettweis M, Silori S, Desmit X. 2024. MOMO activiteitsrapport (1 juli - 31 december 2023). BMM-rapport MOMO/10/MF/202403/NL/AR/4, 29pp + app.

Fettweis M, Desmit X. 2023 MOMO activiteitsrapport (1 januari - 30 juni 2023). BMM-rapport MOMO/10/MF/202310/NL/AR/3, 28pp + app.

Fettweis M, Desmit X. 2023 MOMO activiteitsrapport (1 juli – 31 december 2022). BMM-rapport MOMO/10/MF/202303/NL/AR/2, 27pp + app.

Fettweis M, Baeye M, Desmit X. 2022 MOMO activiteitsrapport (1 januari – 30 juni 2022). BMM-rapport MOMO/10/MF/202210/NL/AR/1, 21pp + app.

<u>Thesis</u>

Brysse F. 2024. Optimalisatie en validatie van de 'Multiskan Skyhigh spectrofotometer' voor analyse van transparante exopolymeerpartikels (TEP) in zeewater. VIVES Hogeschool Campus Roeselare, Bachelor thesis in de agro- en biotechnologie, 55pp + app.

<u>Conferenties/Workshops</u>

Fettweis M, Belliard J-P, Desmit X, Silori S, Tran D, Meysman F. 2025. Environmental conditions for alkalinity enhancement in the Belgian part of the North Sea. 56th Int. Liège Coll. on Ocean Dynamics, 26-30 May, Liège (Belgium).

Fettweis M, Silori S, Desmit M. 2025. Composition of SPM along nearshore to offshore transects. Workshop on flocculation, 21 May, TUDelft (NL).

Silori S, Desmit X, Schartau M, Terseleer N, Riethmüller R, Fettweis M. 2025. Vertical dynamics of suspended particulate matter and chlorophyll-a in a well-mixed coastal turbid system. Workshop on flocculation, 21 May, TUDelft (NL).

Desmit X, Silori S, Delhaye L, Van der Zande N, Terseleer N, **Fettweis M**, Dujardin J, De Rijcke M, Brun A, Amadei Martinez L, Vyverman W, Sabbe K, Schartau M, Riethmüller R. 2025. Organic and inorganic particle interactions and their dynamics on the North Sea shelf. VLIZ, 15 May, Ostend (Belgium).

Delhaye LJ, Taymans C, Fettweis M. 2025. Intra-annual variability in the morphology of marine flocs in the southern North Sea using in-situ high-resolution underwater imaging. EGU General Assembly, 27 April 2 May, Vienna (Austria) .

Desmit X, Riethmüller R, Silori S, Schartau M, Fettweis M. 2025. Budgeting the particulate organic matter from the suspended particulate matter in shelf seas. EGU General Assembly, 27 April - 2 May, Vienna (Austria).

Fettweis M, Belliard J-P, Maris T, Amadei Martinez L, Silori S, Desmit X. 2025. The organic matter dynamics along the salinity gradient of the Scheldt estuary. Ems-Scheldt workshop, 13-14 February, Delmenhorst (Germany).

Tran D, Verney R, Fettweis M. 2024. New insights into near-bed SPM concentration and sand/mud fraction. AGU Meeting, 9-13 December, Washington DC (USA).

Baeye M, Fettweis M, Verney R. 2024. On the effects of SPM composition on the inherent acoustic and optical particle properties of the SPM. Physics of Estuaries and Coastal Seas, 23-27 September, Bordeaux (France).

Tran D, Verney R, Fettweis M. 2024. New insights into near-bed SPM concentration and sand/mud fraction in the use of Sediment Composition Index. Physics of Estuaries and Coastal Seas, 23-27 September, Bordeaux (France).

Terseleer N, Kerimoglu O, Lee BJ, Fettweis M, Desmit X. 2024. A coupled biogeochemical-flocculation model to unravel suspended particulate matter dynamics on the Belgian shelf. Symposium on Advances in Marine Ecosystem Modelling Research, 8-11 July, Plymouth (UK).

Fettweis M. 2024. A universe of particles in a sip of water: Composition, concentration and size along the land-ocean transition. Geo-Colloquium University Kiel, 18 June, Kiel (Germany).

Fettweis M. 2024. Jerico Research Infrastructure @ RBINS. Conference on EU Research Infrastructures – Belgian Presidency EU2024. 4-5 June, Brussels (Belgium).

Desmit X, Terseleer Lillo N, Fettweis M, Kallend A, Sabbe K, Dujardin J, De Rijcke M. 2024 Impact of plankton-mineral interactions on the carbon cycle in the Southern North Sea. Particles in Belgium workshop, 3 May, VLIZ, Ostend.

Silori S, Fettweis M, Desmit X, Terseleer N, Riethmüller R, Schartau M. 2024. Vertical profiles of Chlorophyll and SPM at seasonal and tidal scales in a turbid, well-mixed coastal zone. Particles in Belgium workshop, 3 May, VLIZ, Ostend.

Tran D, Fettweis M. 2024 Characterizing the composition of sand and mud suspension in coastal and estuarine environments using combined optical and acoustic measurements. Particles in Belgium workshop, 3 May, VLIZ, Ostend.

Fettweis M, Delhaye L, Lee BJ, Riethmüller R, Schartau M, Silori S, Desmit X. 2023. Vertical variations of suspended particle composition reflect particle dynamics. INTERCOH, 18-22 September, Inha University, Incheon (Korea).

Ho QN, Fettweis M, Hur J, Lee SD, Lee BJ. 2023. The role of microalgae in cohesive sediment flocculation: Insights from stochastic modeling and laboratory experiments. INTERCOH, 18-22 September, Inha University, Incheon (Korea).

Huynh TT, Fettweis M, Lee BJ. 2023. Application of an 1-DV TCPBE model with Bayesian calibration to diagnose the flocculation potential in the laboratory experiments and field measurement. INTERCOH, 18-22 September, Inha University, Incheon (Korea).

Pham TTTP, Ho QN, Lee SD, Fettweis M, Lee BJ. 2023. Isolation and characterization of the molecular composition of algal dissolved organic matter. INTERCOH, 18-22 September, Inha University, Incheon (Korea).

Tran D, Desmit X, Verney R, Fettweis M. 2023. Application of sediment composition index

to predict suspended particulate matter concentration in the North Sea. INTERCOH, 18-22 September, Inha University, Incheon (Korea).

Kallend A, Dujardin J, De Rijcke M, Fettweis M, Sabbe K, Vyverman W, Desmit X. 2023. Interactions between phytoplankton, marine gels and suspended particulate matter in a dynamic, shallow coastal system before and during the phytoplankton spring bloom. ASLO Aquatic Sciences Meeting, 4–9 June, Palma de Mallorca (Spain).

Schartau M, Fettweis M, Desmit X, Terseleer N, Riethmüller R. 2023. From brown to blue water: Unraveling spatio-temporal variations in organic matter composition of suspended particulate matter. ASLO Aquatic Sciences Meeting, 4–9 June, Palma de Mallorca (Spain).

Baeye M, Delhaye L, Fettweis M. 2022. Acoustic and optical turbidity response to altering particle size distribution during extreme events. EuroSea/OceanPredict workshop, 29 June – 1 July, Exeter (UK).

Fettweis M, Desmit X, Terseleer N, Parmentier K, Van der Zande D, Schartau M, Lee BJ, Riethmüller R. 2022. The characteristics of the organic matter in biomineral flocs. Ocean Science Meeting, 24 February – 4 March, Honolulu (USA).

Peer reviewed artikels

Fettweis M, Silori S, Adriaens R, Desmit X. 2025. Clay minerals and the stability of organic carbon in suspension along nearshore to offshore transects. Geochimica et Cosmochimica Acta. 395, 229-237.

Huynh TT, Kim J, Lee SD, Fettweis M, Bi Q, Kim SS, Lee SY, Choi YY, Lee BJ. 2024. Spatiotemporal dynamics of suspended particulate matter in the water environment: A review. Water 16, 3613.

Desmit X, Schartau M, Terseleer N, Van der Zande D, Riethmüller R, Fettweis M. 2024. The transition between coastal and offshore areas in the North Sea unraveled by the suspended particle composition. Science of the Total Environment 915, 169966.

Escobar S, Bi Q, Fettweis M, Monbaliu J, Wongsoredjo S, Toorman E. 2023. A 2DH flocculation model for coastal domains. Ocean Dynamics 73, 333-358.

Fettweis M, Riethmüller R, Van der Zande D, Desmit X. Water quality monitoring in coastal seas: How significant is the information loss of patchy time series? Science of the Total Environment 873, 162273.

Fettweis M, Schartau M, Desmit X, Lee BJ, Terseleer N, Van der Zande D, Parmentier K, Riethmüller R. 2022. Organic matter composition of biomineral flocs and its influence on suspended particulate matter dynamics along a nearshore to offshore transect. Journal of Geophysical Research Biogeosciences, 126, e2021JG006332.

Ho NQ, Fettweis M, Hur J, Desmit X, Kim JI, Jung DW, Lee SD, Lee S, Choi YY, Lee BJ. 2022. Flocculation kinetics and mechanisms of microalgae- and clay-containing suspension in different microalgae growth phases. Water Research 226, 119300.

Ho QN, Fettweis M, Spencer KL, Lee BJ. 2022. Flocculation with heterogeneous composition in water environments: A review. Water Research. 118147.

2. Spatio-temporal variation in particulate and dissolved organic matter dynamics in the southern North Sea

Shelf seas are characterized by their dynamic nature, which leads to variability in the concentrations and composition of suspended particulate matter (SPM) across both temporal and spatial scales. A typical observation is the cross-shore gradient in SPM concentrations, characterised by lower particulate organic matter (POM) content of SPM in nearshore turbid waters compared to higher POM content offshore (e.g. Eisma and Kalf 1979; Jago et al. 1993). Schartau et al. (2019) proposed a semi-empirical model to identify a mineral-associated POM fraction that varies closely with SPM concentrations, and a fresh POM fraction, representing seasonally produced and degraded matter. The mineral-associated POM fraction, as calculated by Schartau et al. (2019), likely comprises a combination of resuspended benthic POM and organic molecules adsorbed onto clay mineral surfaces (Keil et al. 1994; Keil and Mayer 2014; Fettweis et al. 2025).

Organic matter, whether allochthonous or autochthonous, is classified into particulate (POM) and dissolved (DOM) fractions based on the filtration properties. POM, which includes phytoplankton, large bacterial cells, marine gels, detritus, and fecal pellets is retained on filters with pore sizes ranging from 0.2 to 1 µm (Verdugo 2012) and, along with mineral particles, forms the SPM in the water column. In contrast, DOM passes through these filters and forms the primary source of energy and nutrients for a diverse group of heterotrophic bacteria (Hansell and Carlson 2014). DOM comprises a wide variety of molecules transformed by biotic and abiotic processes, with lifetimes varying from minutes to millennia. In the euphotic zone, its concentrations are typically an order of magnitude higher than POM (Middelburg, 2019). As a dissolved component, DOM is transported differently compared to POM in the aquatic systems, leading to distinct dynamics. Despite their differing dynamics, DOM and POM are interconnected through the continuous exchange of material via aggregation, disaggregation and degradation processes (Kharbush et al., 2020). One such mechanism is the adsorption and desorption of DOM molecules onto mineral surfaces, which shifts organic matter between the dissolved and particulate phases, maintaining a dynamic equilibrium. This phenomenon is particularly notable in the variation of POM content within total organic matter as a function of SPM concentrations (Hermann and Heip 1999; Abril et al. 2002). Evidence suggests that the incorporation of organic molecules within mineral matrices protects them from bacterial exo-enzymes and rapid remineralization (Hemingway et al. 2019), although transformations of the organic molecules still occur at the organic-mineral interface (Kleber et al. 2021). Yet, the potentially long-term storage of organic carbon on sediment mineral surfaces can have substantial implications for organic matter lability and preservation in the ocean (Mayer 1994; Hemingway et al. 2019). It is, thus, relevant to quantify the mineral-associated organic carbon fraction, which constitutes a significant component of POM pool in turbid waters.

Common approaches for delineating POM sources in coastal systems and estimating their contributions include analysing particulate organic carbon (POC) and particulate organic nitrogen (PON) elemental ratios and stable carbon isotopic ratios ($\delta^{13}C_{POC}$). These methods are particularly effective when sources exhibit distinct signatures, such as marine phytoplankton-derived POM (POC:PON ≈ 6–10 mol mol^{-1}; $\delta^{13}C_{POC}$ > −24 ‰) and terrestrial POM (POC:PON > 12 mol mol^{-1}; $\delta^{13}C_{POC}$ < −26 ‰) in temperate regions (Savoye et al. 2003; Goñi et al. 2009). This is often supplemented with POC to chlorophyll *a* ratios (POC:Chl*a*), which aid in estimating the contribution of phytoplankton biomass to the POM pool (Savoye et al., 2003; Liu et al., 2018). Generally, the POC:Chl*a* ratios have been used to distinguish between living phytoplankton, typically exhibiting values around 40–140 g g^{-1} or

phytoplankton-dominated POM, generally indicated by ratios below 200 g g^{-1}, and non-phytoplankton material, which is characterized by higher ratios exceeding 200 g g^{-1} (Savoye et al., 2003). This can be further supplemented with Pheophytin-a (Pheo*a*) to Chl*a* ratio, which is a degradation product of Chl*a* usually produced due to phytoplankton mortality via different ways and hence an indicator of physiological state of phytoplankton community. However, in shelf waters where riverine and macrophyte inputs are minimal, phytoplankton-derived POM dominates, contributing up to 75–97% of the total POM pool (Liénart et al., 2017; 2018). In shallow, well-mixed water columns, tidal currents resuspend benthic POM, making it a significant contributor to the overall POM pool (Modéran et al., 2012). Benthic POM primarily consists of a mixture of benthic primary producers, detritus from pelagic primary producers, organic molecules adsorbed onto clay mineral surfaces, and where present, contributions from macrophytes (Dubois et al., 2012; Keil & Mayer, 2014). Additionally, terrestrial organic matter sorbed onto mineral surfaces is exchanged with marine organic matter as sediments are transported into the marine environment (Keil et al., 1997; Blattmann et al., 2019). Consequently, the POC composition in shelf waters will be primarily shaped by the biomass and detritus of both primary and secondary producers, along with organic molecules adsorbed onto clay mineral surfaces. In shallow shelf waters, where mineral particles (e.g., quartz, feldspars, carbonates, clay minerals) constitute a substantial portion of suspended matter, ratios such as POC:SPM and Chl*a*:SPM serve as useful indicators of the relative contribution of organic material and, in the case of Chl*a*:SPM, algal versus non-algal particles. These ratios are useful for characterising marine particles as "organic-dominated" (POC:SPM > 0.25), "mineral-dominated" (POC:SPM < 0.06), or of "mixed composition" (POC:SPM = 0.06–0.25) (Wozniak et al. 2010).

The main aim of the study is to characterize and quantify various contributors to POM in turbid shelf seas, where significant interactions between organic matter and fine-grained sediments occur. We have utilized established methods to estimate phytoplankton biomass (POC_{phyto}), heterotrophic biomass (POC_{het}), and POC adsorbed onto mineral surfaces ($POC_{mineral}$). Estimating the POM components, particularly POC_{phyto} component, is needed to understand the seasonal and spatial variations in POM composition proxies such as POC:PON and POC:Chl*a* ratios, especially when a large fraction of POM is phytoplankton derived. This analysis is based on multi-year (2019-2023) SPM, POC, PON and Chl*a* concentration data collected at three sampling locations across the Belgian coastal-offshore gradient of SPM concentration. While the seasonal variability of SPM, POM and Chl*a* concentrations in Belgian waters has been described (Rousseau et al., 2006; Desmit et al. 2020; Fettweis et al., 2022), the variability of the different fractions composing POM (i.e. the compositional dynamics) remains poorly understood. The Belgian Coastal Zone, in the southern North Sea, experiences a spring phytoplankton bloom following the relaxation of winter light limitation. This bloom, peaking in April or May, is dominated by diatoms, with the haptophyte *Phaeocystis globosa* becoming particularly prominent at its peak (Rousseau et al., 2006). The increase in phytoplankton production coincides with a reduction in suspended particulate matter (SPM) concentrations. Enhanced flocculation, driven by phytoplankton-derived exopolymers, leads to lower tidal-averaged SPM levels during the spring and summer, despite seasonal fluctuations in wind conditions and wave heights (Fettweis & Baeye, 2015; Fettweis et al., 2022). In this study, we hypothesize that the different POM fractions (POC_{phyto}, POC_{het}, $POC_{mineral}$ and the residual fraction, which is detritus) vary in space and time. Some of this variability could be related to the nearshore to offshore gradient of SPM concentration that will affect each POM fraction differently. Another part of the variability in POC composition should be due to the seasonality in phytoplankton production and its impact on SPM concentrations in the water column.

2.1. Materials and methods

2.1.1. Study area and sampling frequency

Situated in the Southern Bight of the North Sea, the Belgian coastal waters are relatively shallow, with an average depth of ~10 m nearshore and a maximum depth of ~45 m offshore. Strong tidal currents (>1 m s^{-1}) and frequent wind forcing, result in well-mixed conditions throughout most of the year (). These waters exhibit a pronounced cross-shore gradient in SPM concentrations, with turbidity decreasing towards the offshore (Figure 2.1a). Atlantic inflow via the English Channel accounts for ~96% of the Belgian coastal water mass, with the remainder mainly supplied by the Rhine, Scheldt, and Seine rivers, among which the Rhine is the dominant freshwater source (Lacroix et al., 2004; Dulière et al., 2017). River discharge exhibit seasonal maximum during winter and early spring. The influence of freshwater input shows notable interannual variability, often attributed to the North Atlantic Oscillation (NAO). A positive NAO phase is associated with stronger south-westerly winds, enhancing the north-eastward dispersion of the Scheldt and Rhine plumes and reducing their influence in coastal waters. Simultaneously, increased precipitation over the Scheldt basin may enhance nutrient delivery to the coastal zone (Breton et al., 2006). Residual flow in the Belgian coastal zone is directed north-eastward; however, oscillating tidal currents induce substantial horizontal dispersion, influencing net transport patterns (Lacroix et al. 2004).

Water samples were collected hourly or every 1.5 hours over half or full tidal cycles at three stations from January 2019 to December 2023 (Table 2.1 and Figure 2.1a). Figure 2.1b shows the months during which these tidal cycles were sampled. During most months, data collection represents one half or full tidal cycle per station, except in April 2023 when two tidal cycles were sampled at all stations. The three stations (MOW1, W05, and W08, shown in Figure 2.1a) were positioned along a cross-shore transect, ranging from the nearshore coastal turbidity maximum at MOW1 (~10 m water depth) to W05 (~20 m water depth), located at the outer margin of the coastal turbidity maximum, and further offshore to W08 (~25m water depth), influenced primarily by the channel waters (Figure 2.1a). During each sampling event, water was collected at 1–2 m below the surface and 2–3 m above the seabed using 5- or 10-L Niskin bottles mounted on a Sea-Bird SBE09 CTD carousel. For dissolved parameters, sampling was performed at a single depth (1-2 m below the surface), assuming uniform mixing, as density stratification is uncommon in these waters (Lacroix et al., 2004).

Table 2.1: Number of samples for various parameters collected hourly or 1.5 hourly over several half and full tidal cycles at MOW1, W05, and W08 between January 2019 and December 2023.

	Number of samples		
	MOW1	W05	W08
Dissolved inorganic nitrogen (DIN)	407	270	74
Dissolved inorganic phosphate (DIP)	414	301	145
Dissolved inorganic silicate (DSi)	404	311	179
Suspended particulate matter (SPM)	886	649	409
chlorophyll *a* (Chl*a*)	813	602	370
Particulate organic carbon (POC)	825	634	392
Pheophytin *a* (Pheo*a*)	840	606	307
Particulate organic nitrogen (PON)	782	579	332
Transparent Exopolymer Particles (TEP)	685	541	314
Dissolved organic carbon (DOC)	392	297	180

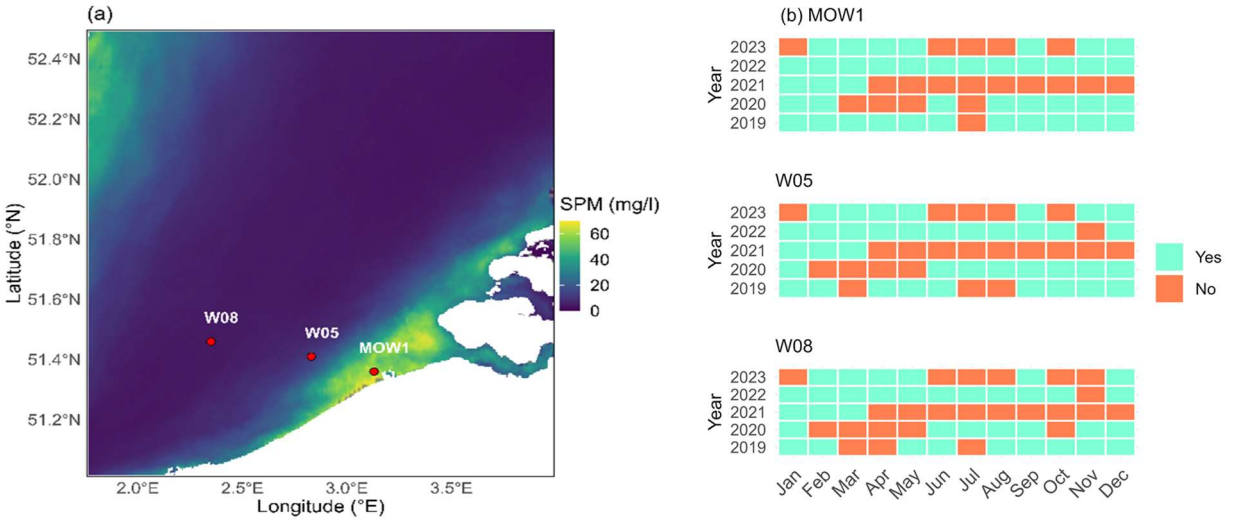

Figure 2.1: a) Map of the sampling stations MOW1, W05, and W08. The background shows the multi year (2017-2021) average surface SPM concentrations (mg/l) (Earth Observation SPM) for the winter months (monthly averages for December, January, and February). ***b****) Timeline of monthly sampling between 2019 and 2023 across three stations in the Belgian Coastal Zone. Months marked "Yes" indicate hourly or 1.5 hourly sampling over a full or half tidal cycle, with April 2023 including two distinct tidal cycles sampled at each station*

2.1.2. In-situ sample collection and analysis

Water samples for dissolved inorganic nitrogen (nitrate+nitrite+ammonia: DIN), phosphate (DIP), silicate (DSi), dissolved organic carbon (DOC) and total dissolved nitrogen (TDN) were filtered onboard using a GF/C filter and subsequently frozen for further analysis in the laboratory. For DOC, filtration was performed using GF/C filters with a pore size of 1.2 µm. Dissolved inorganic nutrient samples were then analysed using standard colorimetric methods using a Skalar autoanalyzer (van der Zee & Chou, 2005). TDN was measured following oxidation in alkaline persulfate, and total nitrogen (TN) was calculated as the sum of TDN and PON.

Water samples for SPM, POC, PON, Chl*a* and Pheo*a* were filtered on board and subsequently analysed in the laboratory. During each sampling event, three subsamples for SPM concentration were collected and filtered using pre-weighted and pre-combusted (405°C for 24 hours) 47 mm GF/C filters. After sample filtering, the filters were rinsed with ultrapure water (resistivity 18.2 MΩcm normalized at 25°C) and immediately stored at -20°C. The filters were fumigated with HCl to remove traces of particulate inorganic carbon (if any) and the filters were then dried at 50°C for 24 hr and weighted to obtain the concentrations. The uncertainty (expressed as the RMSE of the triplicates divided by the mean value) decreases with increasing concentration from 8.5% (SPM concentration <5 mg/l) to 6.7% (<10 mg/), 3.5% (10–50 mg/l), and 2.1% (>100 mg/l) and represent the random error related to the lack of precision during filtrations. Pretreated (similar to SPM) 25 mm GF/C filters were used for POC and PON filtration and stored at -20°C immediately. The samples were subsequently analysed using a Thermo Finnigan Flash EA1112 elemental analyser (Ehrhardt & Koeve, 1999). GF/C filters (47 mm) were used to collect Chl*a* and Pheo*a*, and were stored in liquid nitrogen thereafter. The concentrations were then determined using ultra high-performance liquid chromatography with fluorometric detection. The analytical uncertainty for POC is 12% and for PON, Chl*a* and Pheo*a* is 18%. We assume that the filtration error uncertainty is comparable to that observed for SPM, which ranges between 2.1% and 3.5% for SPM concentrations greater than 10 mg/l.

The smaller filtration uncertainty results in the total uncertainty for these parameters approximating the analytical uncertainty.

During each sampling event, three subsamples for TEP concentration were filtered through 25 mm polycarbonate filters with a pore size of 0.4 µm, under vacuum pressure below 200 hPa. After filtration, the filters were immediately stained with Alcian blue and stored at −20°C. The stained particles were quantified to determine their weight equivalent based on the anion density of TEP, standardized using xanthan gum (Passow & Alldredge 1995; Passow, 2002). TEP concentrations were reported in units of mg xanthan gum equivalents per litre (mg XG eq./l), with an assumed uncertainty comparable to that of POC measurements.

2.1.3. Estimation of different POC components

2.1.3.1. Phytoplankton carbon biomass

To estimate phytoplankton carbon biomass (POC_{phyto}), we use the empirical model from Danish waters, as described by Jakobsen & Markager (2016), to predict C:Chl*a* ratios for temperate coastal phytoplankton. The monthly variation in C:Chl*a* ratios is modelled using a sinusoidal function that accounts for changes in temperature, irradiance, and total nitrogen.

$$C{:}\,Chla = win + amp\left(\frac{cos\left(\frac{month-0.5-pe\quad time}{12}\times 2\pi-\pi\right)+1}{2}\right) \tag{2.1}$$

The winter minimum (win) value for C:Chla ratios is typically set at 15 for temperate waters. For the peak time, representing the temporal position of the summer phytoplankton peak relative to 1st July, we used 0.20 ± 0.11, derived from estuarine and open waters observations in Danish waters (Jakobsen & Markager, 2016). Consistent with seasonal trends observed in Danish estuarine stations, we observe the summer peak in phytoplankton biomass (Chla concentrations) in July at MOW1. The stations W05 and W08, are comparable to the open water stations in that summer peak in the biomass occurs significantly later. The amplitude (amp) between summer and winter C:Chla is estimated using a non-linear fit between amp and annual mean of total nitrogen [n] (R^2= 0.53).

$$amp = Z + \frac{C}{[n]} \tag{2.2}$$

where parameters Z and C are 15.07±5.6 and 793.1±159, respectively.

Table 2.2: Mean and standard deviation of $POC_{mineral}$ content of SPM for spring (April) and winter (December) months obtained from the mineral specific surface area (Fettweis et al. 2025).

Stations	April 2023 $POC_{mineral}$ content (%)	December 2023 $POC_{mineral}$ content (%)
MOW1	0.71±0.27	0.86±0.33
W05	0.46±0.18	0.43±0.17
W08	0.48±0.18	0.39±0.16

2.1.3.2. POC adsorbed onto mineral surfaces ($POC_{mineral}$)

The $POC_{mineral}$ concentrations in the current study are based on estimates from Fettweis et al. (2025). These estimates were derived from the clay mineral composition at the three Belgian coastal stations, along with literature data on mineral-specific surface area and organic carbon content per surface area. Non-clay minerals (quartz and feldspar), biogenic minerals (carbonates and opal) and clay minerals (smectite, illite, kaolinite, and chlorite) make up the bulk mineralogical composition of the SPM in the Belgian waters. The available

data covers spring (April) and winter (December) months (Table 2.2). As the variability in mineral composition between seasons is small, we used an average of both months to calculate the monthly $POC_{mineral}$ concentrations.

2.1.3.3. Heterotrophic carbon biomass

The estimation of heterotrophic carbon biomass (POC_{het}) is based on the relationship between heterotrophic:autotrophic biomass ratios and autotrophic biomass in coastal waters (Gasol et al., 1997; Duarte et al., 2000). Gasol et al. (1997) include heterotrophic bacteria, microzooplankton, and mesozooplankton in the heterotrophic biomass, while autotrophic biomass comprises phytoplankton. POC_{phyto} concentrations calculated using the C:Chl*a* ratios (Section 2.3.1), are taken as the autotrophic biomass concentrations.

$$log\left(\frac{POC_{het}}{POC_{phyto}}\right) = -0.43 log POC_{phyt} + 1.19 \quad (2.3)$$

Although the dataset used to derive the relationship includes data from the southern North Sea and mesocosm studies (incorporating benthic heterotrophs), the majority of it was derived from deeper coastal waters (100–200 m). Consequently, the contribution of benthic heterotrophs may be underestimated, particularly in the study area, which is shallow and well-mixed.

2.1.3.4. Detrital carbon biomass

Detrital carbon biomass (POC_{det}) is calculated by subtracting POC_{phyto}, $POC_{mineral}$, and POC_{het} from the measured POC in water samples.

2.1.4. Redundancy Analysis

We conducted redundancy analyses (RDA) with two primary objectives: (1) to identify the environmental variables (salinity, temperature, DIN, DIP, and DSi) driving variation in biological variables (POC, Chl*a*, POC:PON, Chl*a*:SPM, POC:SPM, and POC:Chl*a*) and (2) to assess the influence of measured variables (salinity, temperature, DIN, DIP, DSi, POC, and Chl*a*) on the relative contributions of different POC components along the cross-shore gradient. The RDA was performed using the "vegan" package in R. The data was scaled before the analysis to ensure an even contribution from the variables, preventing variables with larger values or ranges from dominating. RDA can be viewed as a constrained form of principal component analysis (PCA), where the canonical axes, formed as linear combinations of the response variables are restricted to also be linear combinations of the explanatory variables as determined through multiple linear regression (Legendre & Legendre, 1998).

2.1.5. Organic matter partitioning into dissolved and particulate pool

The partitioning of organic matter in turbid waters is strongly influenced by SPM concentrations. Herman & Heip (1999) introduced the following equations to describe the balance between the adsorption and desorption of organic matter on mineral particles.

$$k_1.SPM.DOC - k_2.POC = 0 \quad (2.4)$$

where k_1 and k_2 represent the first-order rate constant for adsorption and desorption, respectively. Eq. 4 can be rewritten as:

$$\frac{POC}{TOC} = \frac{SPM}{SPM+K} \quad (2.5)$$

where $K = k_2/k_1$.

2.2. Results

2.2.1. Seasonal and spatial variations

2.2.1.1. Physico-chemical parameters

The concentrations of the dissolved inorganic nutrients (DIN, DIP, and DSi) displayed a consistent distribution pattern, declining from nearshore (MOW1) to offshore (W08), indicative of dominant riverine nutrient sources. A common trend observed across all three stations was elevated concentrations during winter months (Figures 2.2a, 2.2b, 2.2c), followed by a gradual decrease in spring, reaching the lowest levels in summer, and subsequent regeneration and increased riverine loads of nutrients during autumn months. At W05 and W08, DIN concentrations reached their lowest levels in April and remained low throughout summer. However the lowest concentrations are observed much later in July at MOW1 and W05. Notably, DIN:DIP ratios at all three stations exceeded the canonical Redfield ratio of 16 for most of the year, except during July, August, and September when values dipped below or approached 16 (Figure 2.2d). Similarly, the lowest DIN:DSi ratios were predominantly observed towards late summer, often close to or less than 1 (Figure 2.2e).

2.2.1.2. Concentrations and characteristics of suspended particulate matter

SPM concentrations exhibit a gradient, progressively decreasing from MOW1 situated within the coastal turbidity maximum, towards W05 and further at W08, reflecting a gradient in bathymetry and SPM transport (Figure 2.2f). At MOW1, SPM concentrations can reach several hundreds of mg/l, with values below 10 mg/l being rare. In contrast, concentrations exceeding 10 mg/l are uncommon at W08. Despite the substantial variability observed across the three stations, SPM concentrations exhibit a typical seasonal trend, characterized by a decline in SPM concentrations towards the end of spring, reaching a minimum during summer (June-July), followed by a subsequent increase to reach winter-spring high values by October.

Chl*a* concentrations were generally highest closest to the coast at MOW1. It was only during the peak of the spring bloom in April, that Chl*a* concentrations at W05 (14.7±11.0 µg/l) and W08 (7.9±7.6 µg/l) were comparable to those at MOW1 (12.7±7.4 µg/l). Despite the difference in Chl*a* concentrations, the seasonal trends were somewhat similar across the three stations, with low concentrations in winter, a sharp increase during the spring bloom, a decrease in May, and a second bloom later in summer (Figure 2.2g). The main difference was in the timing and intensity of the second peak at MOW1, it peaked in July (15.7±3.4 µg/l) and high values persisted until October. While at W05 and W08, the late summer-autumn peak concentrations where lower in magnitude (W05: 4.5±1.6 µg/l; W08: 1.6±0.2 µg/l) and occurred later.

Similar to the SPM and Chl*a* concentrations, POC and PON (not shown) concentrations display a cross-shore gradient (Figure 2.2h). The distribution patterns of POC and PON (not shown) are quite similar, hence only POC is elaborated here. POC concentrations greater than 1 mg/l were commonly observed at MOW1, whereas such concentrations were rare at the other sampled stations. The monthly variation in POC concentrations at MOW1 mirrored the SPM pattern, with a distinct reduction towards the end of spring and beginning of summer (June: 1.7±0.9 mg/l), followed by a gradual increase, reaching high values (3-4 mg/l) in October, consistent with measurements during other months. Unlike the two distinct peaks in the annual Chl*a* distribution, such discernible increases are not observed in POC concentrations at MOW1. At W05 and W08, the monthly POC pattern slightly differed from the SPM pattern. Similar to the Chl*a* buildup during the spring months and subsequent decline in summer, a gradual buildup and decline in POC concentrations was

noticeable at W05 (Apr: 1.2±0.4 mg/l) and W08 (Apr: 0.6±0.2 mg/l), but this was less evident at MOW1. The second peak in POC towards the end of the summer, which again was not evident at MOW1, was recognizable at W05 (September: 0.6±0.1 mg/l) and W08 (August: 0.4±0.1 mg/l), and the concentrations were higher compared to the winter values.

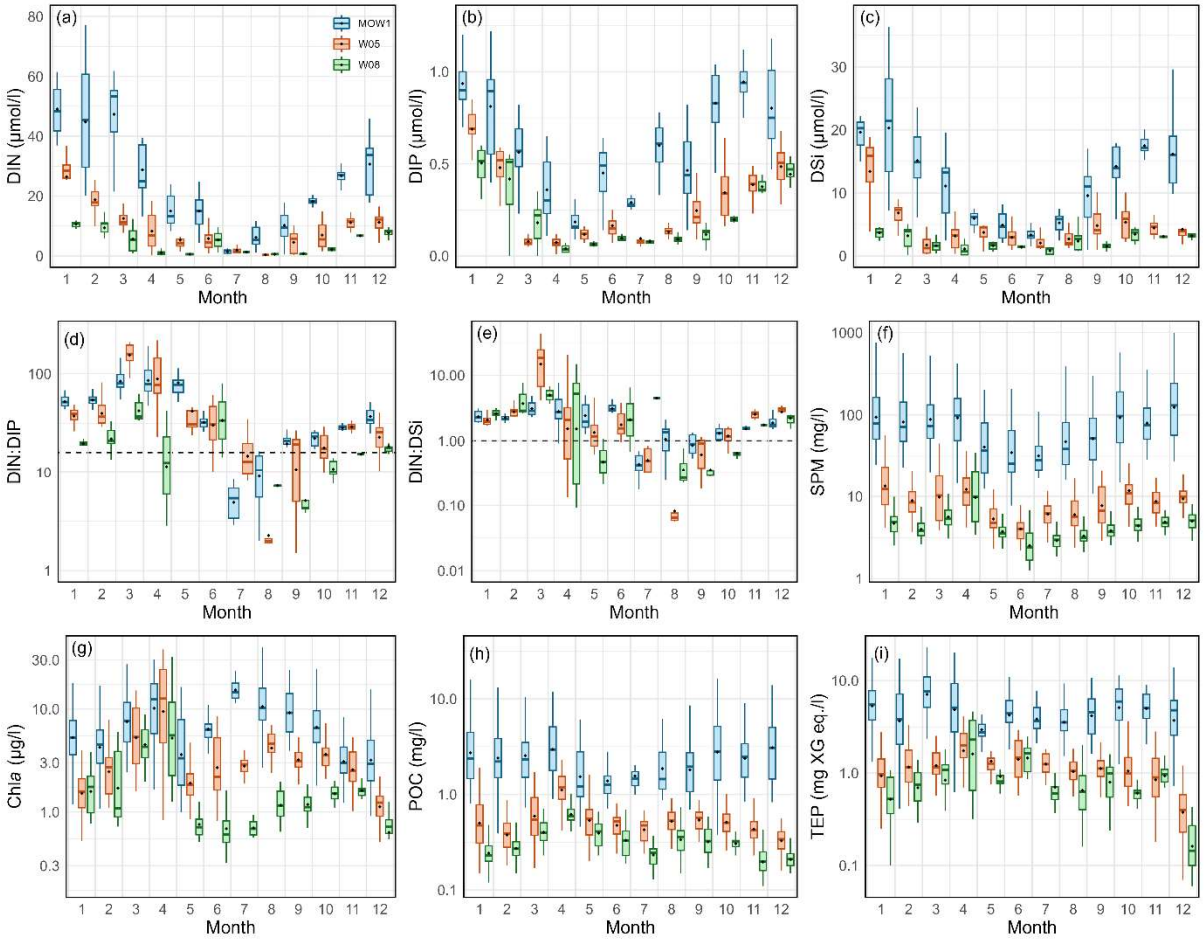

Figure 2.2: Annual variations (mean 2019-2023) in a) DIN (µmol/l), b) DIP (µmol/l), c) DSi (µmol/l), d) DIN:DIP, e) DIN:DSi, f) SPM (mg/l), g) Chla (µg/l), h) POC (mg/l), and i) TEP (mg XG eq./l) at MOW1, W05, and W08. Boxplots show minimum, first quartile, median, third quartile, and maximum, filled black circles display mean values. Values outside the interquartile range have not been displayed. Note the log scale used for panels f-i. Dashed line indicates the Redfield-Brzezinski nutrient ratio (N:P = 16 and N:Si = 1)

TEP concentrations displayed a decreasing trend with distance from the coast (Figure 2.2i). The highest monthly averages were observed at MOW1 (3.6-8.6 µg/l), followed by W05 (0.5-2.0 µg/l), and the lowest at W08 (0.1-2.2 µg/l). At MOW1, TEP concentrations generally followed the trends in SPM and POC, with a notable decline in May and during the summer months, while remaining comparable during other months. Conversely, at W05 and W08, the lowest TEP concentrations were recorded during the winter months. These values gradually increased to peak in April, then declined slightly, maintaining moderately high levels until the end of autumn.

2.2.1.3. Suspended particulate matter composition

The Chl*a* content of SPM (Chl*a*:SPM) did not increase consistently with distance from the coast (Figure 2.3a). At MOW1, the values ranged from 0.03 to 0.51 ‰, the lowest amongst the stations. In contrast, W05 and W08 showed similar ranges (0.14-1.31 ‰ and 0.14-1.23

‰, respectively), but values greater than 0.4 ‰ were more frequent at W05. At MOW1, Chl*a*:SPM ratios exhibited a distinct seasonal pattern, differing from the seasonal progression of Chl*a* concentrations. During the spring bloom, values increased slightly to 0.16±0.13 ‰ (April) from the winter low of 0.06±0.03 ‰ (December). A more significant rise occurred in summer, reaching 0.51±0.17 ‰ (July), followed by a gradual decline to the low winter levels. The monthly progression at W05 and W08 differed from that at MOW1. At these stations, values increased from the winter low to peak in April, unlike the summer peak observed at MOW1.

The POC content of SPM (POC:SPM), generally increased with distance from the coast (Figure 2.3b). The lowest values were observed at MOW1 (2.6-5.2 %), followed by W05 (3.6-12.4 %), and peaking at W08 (4.2-15.6 %). The monthly variation in POC:SPM ratios was broadly similar across the three stations, increasing from winter minima to peak in June. At W05 and W08, this was followed by a notable decline in July, a small increase in August and, a subsequent gradual decrease toward winter levels. Values increased gradually from the low winter levels. The spring and summer increase in POC:SPM ratios was more prominent at W05 and W08.

Notably, the peaks in POC:SPM ratios did not coincide with the peaks in POC concentrations at any of the stations. The POC:Chl*a* ratios (g/g) did not display a cross-shore gradient and exhibited different seasonal patterns across the stations (Figure 2.3c). At MOW1, values above 200, indicative of detritus dominated or non phytoplankton material were prevalent from January to June with maximum values in December (1281±647), except in April when a portion of data fell between 140 and 200, suggesting phytoplankton dominated but detritus influenced POC (Savoye et al., 2003). The ratio dropped below 140, typical of living phytoplankton, in July (105 ±30), while values between 140 and 200 were observed in August and September, before returning to ratios greater than 200 from October onward. At W05, values above 200 were common in winter (e.g., Jan: 457±355), while values below 140 were common in early spring (e.g., March: 100±26). The ratio increased slightly by May, and throughout summer and autumn, it typically ranged between 140 and 200. In contrast, W08 exhibited the highest values at the end of spring (595±300) and start of summer (June: 681.6±326.1), with the lowest values in early spring (March: 85±22).

The TEP content of SPM (TEP:SPM) was lowest at MOW1, ranging from 0.04 to 0.13 mg XG eq./mg, compared to W05 (0.05 to 0.30 mg XG eq./mg) and W08 (0.03 to 0.40 mg XG eq./mg) (Figure 2.3d). At MOW1, the highest TEP content was measured in summer, with other periods showing comparable values between 0.06-0.07 mg XG eq./mg. In contrast, W05 and W08 exhibited greater variability, with TEP:SPM increasing from winter lows to a high values in June, then gradually declining back to the winter levels.

A clear spatial trend was not evident in POC:PON ratios (mol/mol) across the three stations, with most values ranging between 6 and 12 (Figure 2.3e). However, a seasonal trend, with the highest POC:PON ratios in winter and lower values during spring and summer, was observed at the three stations. At MOW1, the POC:PON ratios showed a gradual decline from January (9.1±1.3) to the lowest values in summer (July: 7.1±0.6). In contrast, at W05 and W08, the high values in January (9.8±1.7 and 9.4±2.5, respectively) declined rapidly, reaching their lowest in March (7.3±0.8 and 7.5±0.8, respectively).

The Pheo*a*:Chl*a* ratios at MOW1 were highest during the winter months, gradually declining through spring and reaching their lowest levels in summer (Figure 2.3f). In contrast, at W05 and W08, the high winter values dropped sharply, reaching their minimum during spring. Subsequently, ratios comparable to winter levels reappeared after early summer.

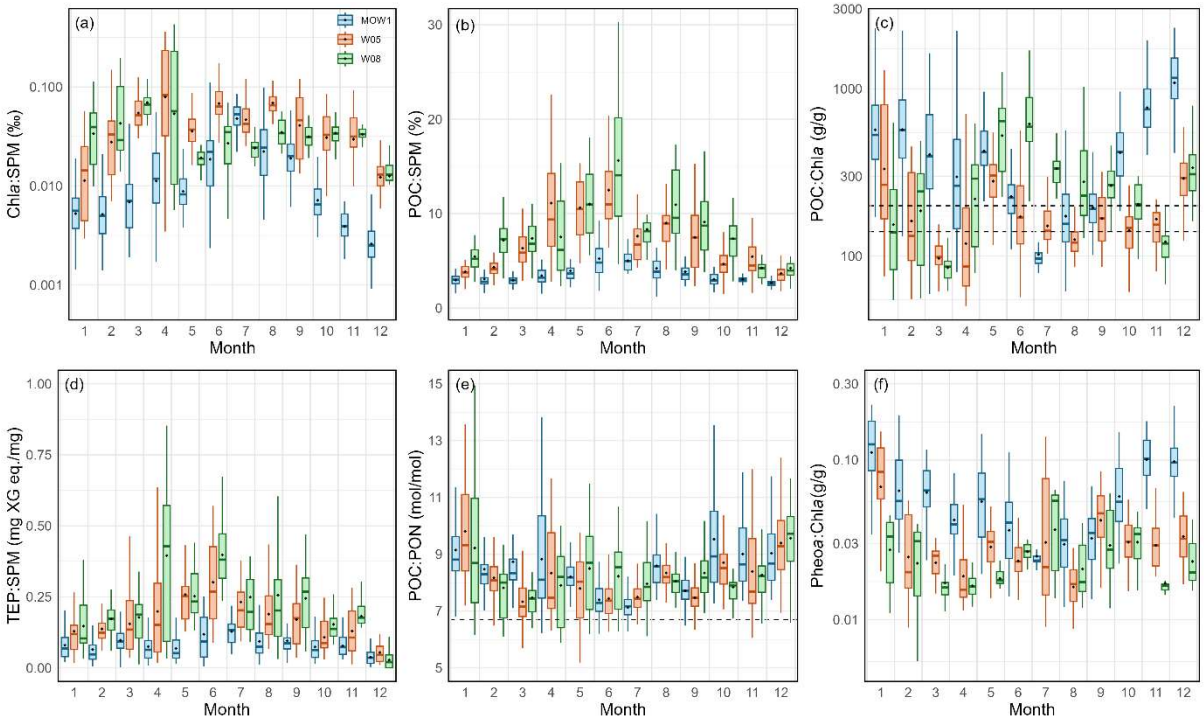

Figure 2.3: Annual variations (mean 2019-2023) in a) Chla:SPM (‰), b) POC:SPM (%), c) POC:Chla (g/g), d) TEP:SPM (mg XG eq./mg), e) POC:PON (mol/mol), and f) Pheoa:Chla (g/g) at MOW1, W05, and W08. Boxplots show minimum, first quartile, median, third quartile, and maximum, filled black circles display mean values. Values outside the interquartile range have not been displayed. Data has been collected between 2019-2023. Dashed lines in panel c indicate 200 and 140 g/g, the upper bounds of POC:Chla ratios range assigned to living phytoplankton POC (40-140 g/g) and phytoplankton-dominated POC but potentially including contributions from secondary producers, detritus and others (140-200 g/g), and the dashed line in panel e indicates the canonical Redfield ratio (POC:PON = 6.7)

2.2.1.4. Particulate organic carbon components

POC_{phyto}, calculated using an empirical model for C:Chl*a* ratios in Danish coastal waters (see section 2.1.3.1 and Figure 2.4a), shows seasonal variation somewhat similar to Chl*a* concentrations across all three stations. At MOW1, POC_{phyto} ranges from 0.08 to 0.67 mg/l, with a first peak in April and a second, higher peak in July (Figure 2.4b). In contrast, W05 and W08 display lower ranges (0.02–0.43 mg/l at W05 and 0.01–0.31 mg/l at W08), with a comparable first peak in April but a delayed, smaller second peak in August. The estimated POC_{phyto}:POC (%) values at MOW1 were generally lower than at the other stations, ranging from 1.2% to 40.1% with values exceeding 15only during summer and early autumn (Figure 2.4c). At W05, low winter values (January: ≈ 3.85 %) steadily increased, with high value in April (≈35.29 %) and remained high through summer (35.39–46.88%), before gradually declining into winter. Similarly, at W08, winter lows steadily rise to a peak in April (≈ 48.83 %), but the values then decrease, with only a slight summer increase (17.46–27.45 %) (Figure 2.4c). The monthly average POC:PON and POC:Chl*a* ratios at all three stations showed significant negative logarithmic correlations with the POC_{phyto}:POC (%) ($p < 0.01$), suggesting that the higher fractions of POC_{phyto} are associated with lower POC:PON and POC:Chl*a* ratios (Fig. 4d, 4e). Conversely, both TEP:SPM ratio demonstrated a positive linear correlation with POC_{phyto}:POC ($p < 0.01$) (Figure 2.4f).

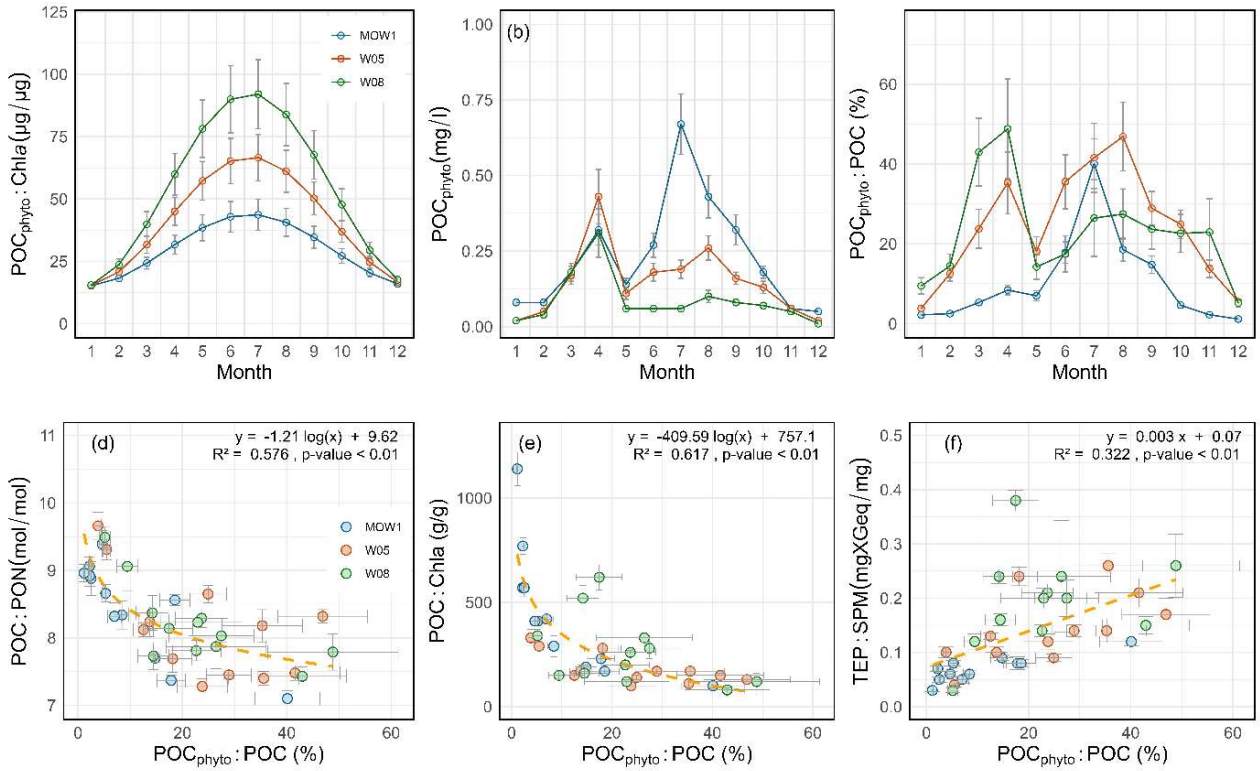

Figure 2.4: Monthly mean values (climatology 2019-2023) of a) POC_{phyto}:Chla (µg/µg), b) POC_{phyto} (mg/l), and c) POC_{phyto}:POC (%) at the three stations. Error bars represent the standard error from the monthly mean. Linear regression of monthly means of d) POC:PON (mol/mol), e) POC:Chla (g/g), and f) TEP:SPM (mg XG eq./mg) as a function of POC_{phyto}:POC (%) at the three stations. Error bars represent the standard error from the monthly mean.

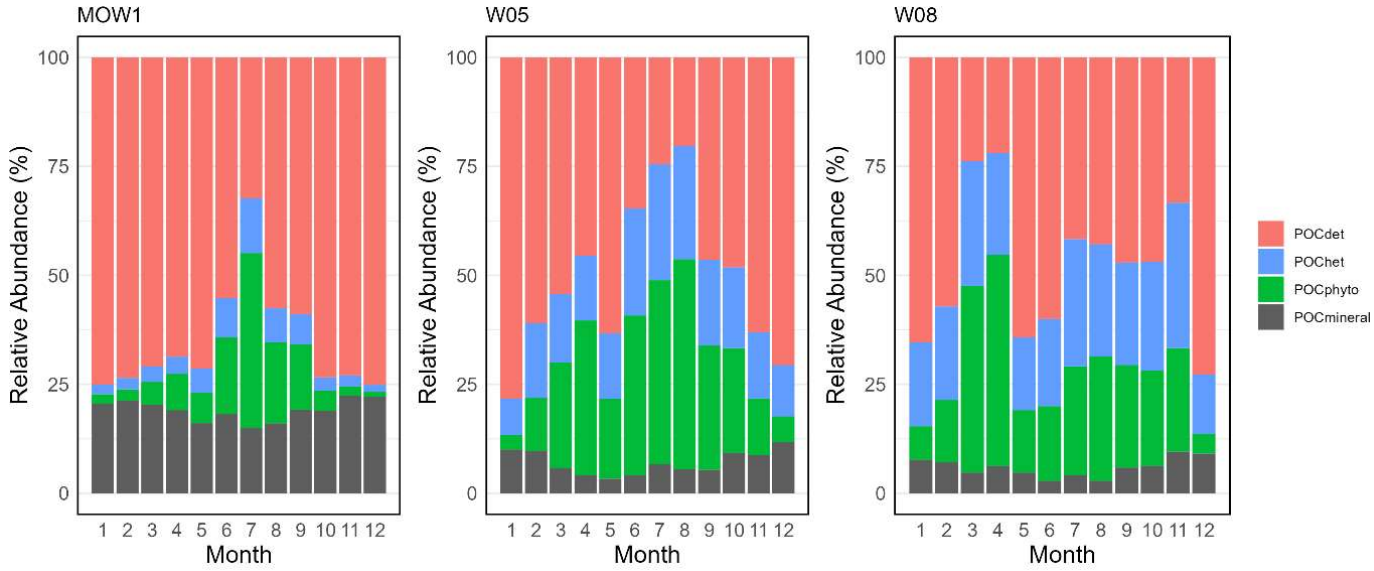

Figure 2.5 Relative abundance of POC components over a climatological year (2019-2023) at MOW1, W05, and W08. POC_{det} stands for detritic organic matter (calculated after subtracting other components from measured POC). POC_{het} stands for heterotrophic biomass. POC_{phyto} stands for phytoplankton biomass. $POC_{mineral}$ stands for mineral-associated organic matter (based on clay specific surface area available for organic matter adsorption).

At MOW1, POC_{det} and $POC_{mineral}$ contribute substantially to the water column POC pool for most of the year, with POC_{phyto} making a notable contribution (25–50 %) only during the summer months (Figure 2.5). In contrast, at the other two stations, $POC_{mineral}$ remains consistently low (3–12 %) year-round, reaching its lowest relative contribution in summer. At W05, POC_{phyto} shows comparable relative abundance (30-55 %) in spring and summer, while, POC_{det} dominates in late autumn and winter (60–80%). At W08, POC_{phyto} peaks (50–60%) in March and April, followed by lower values (25–35%) in summer, whereas POC_{det} remains the dominant fraction (45–75%) throughout the year, except during the spring peak.

2.2.1.5. Dissolved organic carbon concentrations

Similar to its particulate counterpart, DOC concentrations were highest at MOW1 with monthly averages ranging between 1.13-1.89 mg/l, decreasing progressively at W05 (0.72-1.64 mg/l) and then at W08 (0.72-1.02 mg/l) (Figure 2.6a). The seasonal variation of the DOC concentrations seemed to be similar at all three stations: lowest values were observed in winters, followed by an increase in values from April onwards with the highest values generally observed in summer, after which the concentrations gradually declined to lower values in winter (Figure 2.6a). At W05, however, the peak concentration was observed earlier in May, after which the concentrations gradually declined to lower winter values (Figure 2.6a). At W05 and W08, DOC formed the larger part of the total organic carbon (POC+DOC = TOC) pool, with POC:DOC ratios consistently less than 1 (Figure 2.6b). It is only during the peak of the spring bloom in April that there is a slight increase in the POC:DOC ratios. In contrast, at MOW1, POC seems to be the larger carbon fraction in the TOC pool, with POC:DOC ratios greater than 1, except at the end of the spring phytoplankton bloom and towards the summer when POC:DOC ratios lower than 1 were observed. The monthly averages of the DOC:TOC ratios showed a significant negative correlation (p<0.01) with the monthly SPM averages, with a stronger correlation at MOW1 than at W05 and W08 (Figure 2.6c). At the offshore W05 and W08 stations, the DOC:TOC ratios also correlate negatively with the POC_{phyto} concentrations, while it correlates positively at inshore MOW1 station (Figure 2.6d).

2.2.2. Tidal and Spatial Variations

2.2.2.1. Relationships between suspended particulate matter components

Hourly or 1.5 hourly tidal data of SPM concentrations shows peaks close to the highest current velocities and minimum concentrations near the lowest velocities, with the greatest range between maximum and minimum values observed at MOW1. At MOW1, minimum SPM concentrations can be as low as 3-20 % of the maximum, increasing offshore to 15-50 % at W05 and 30-60 % at W08. At MOW1, Chl*a* concentrations generally follow SPM concentrations over the tidal cycles throughout the year, though the y-intercepts for linear regression in winter are lower than in spring, reflecting higher background Chl*a* concentrations in spring, while the correlation weakening in summer (Figure 2.7a, 2.7b, 2.7c). Similarly, POC and SPM concentrations are significantly correlated at MOW1 during most of the year, in summer, however, this relationship tends to weaken, during periods when SPM concentrations are at the lowest relative to other times of the year (Figure 2.8a, 2.8b, 2.8c). At W05, Chl*a* and SPM concentrations show a good correlation during some tidal cycles in winter, though poor correlations are observed, particularly with lower SPM concentrations (Figure 2.7d). This relationship weakens in spring and summer (Figure 2.7e, 2.7f). POC concentrations exhibit excellent correlation with SPM concentrations in winter (Figure 2.8d) but the correlation deteriorates in spring and is weakest in summer (Figure 2.8e, 2.8f). At W08, the correlations between Chl*a*, POC, and SPM concentrations are

generally moderate to weak during most tidal cycles (Figures 2.7g, 2.7h, 2.7i and 2.8g, 2.8h, 2.8i). POC and PON concentrations were closely related during most tidal cycles throughout the year at all three stations (not shown).

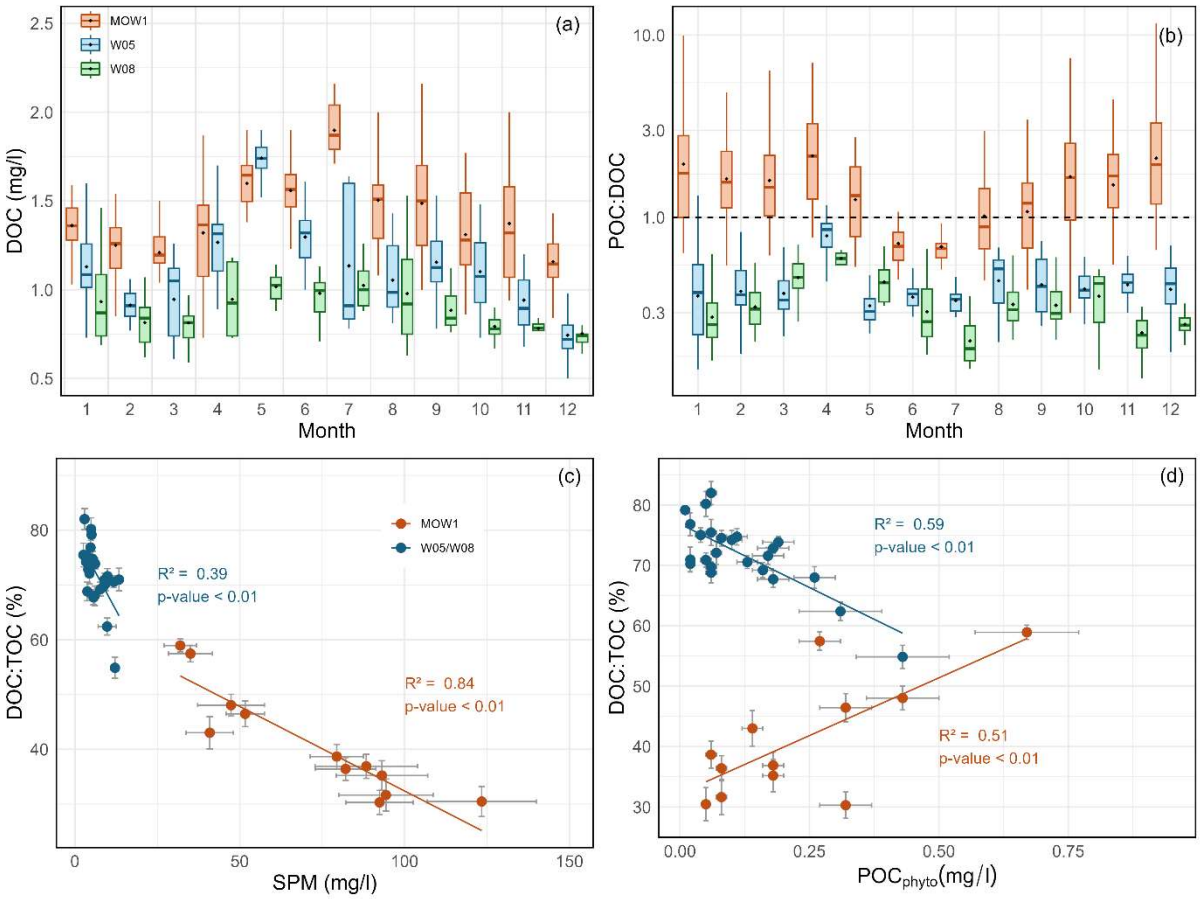

Figure 2.6: Monthly mean values (climatology 2019-2023) of a) DOC (mg/l), and b) POC:DOC ratios at the three stations. Boxplots show minimum, first quartile, median, third quartile, and maximum, filled black circles display mean values. Dashed line in panel b indicates the 50 % mark where DOC concentrations are equal to POC concentrations. Linear regression of monthly means of c) DOC:TOC (%) and SPM (mg/l), and d) DOC:TOC (%) and POC_{phyto} (mg/l). Error bars represent the standard error from the monthly mean.

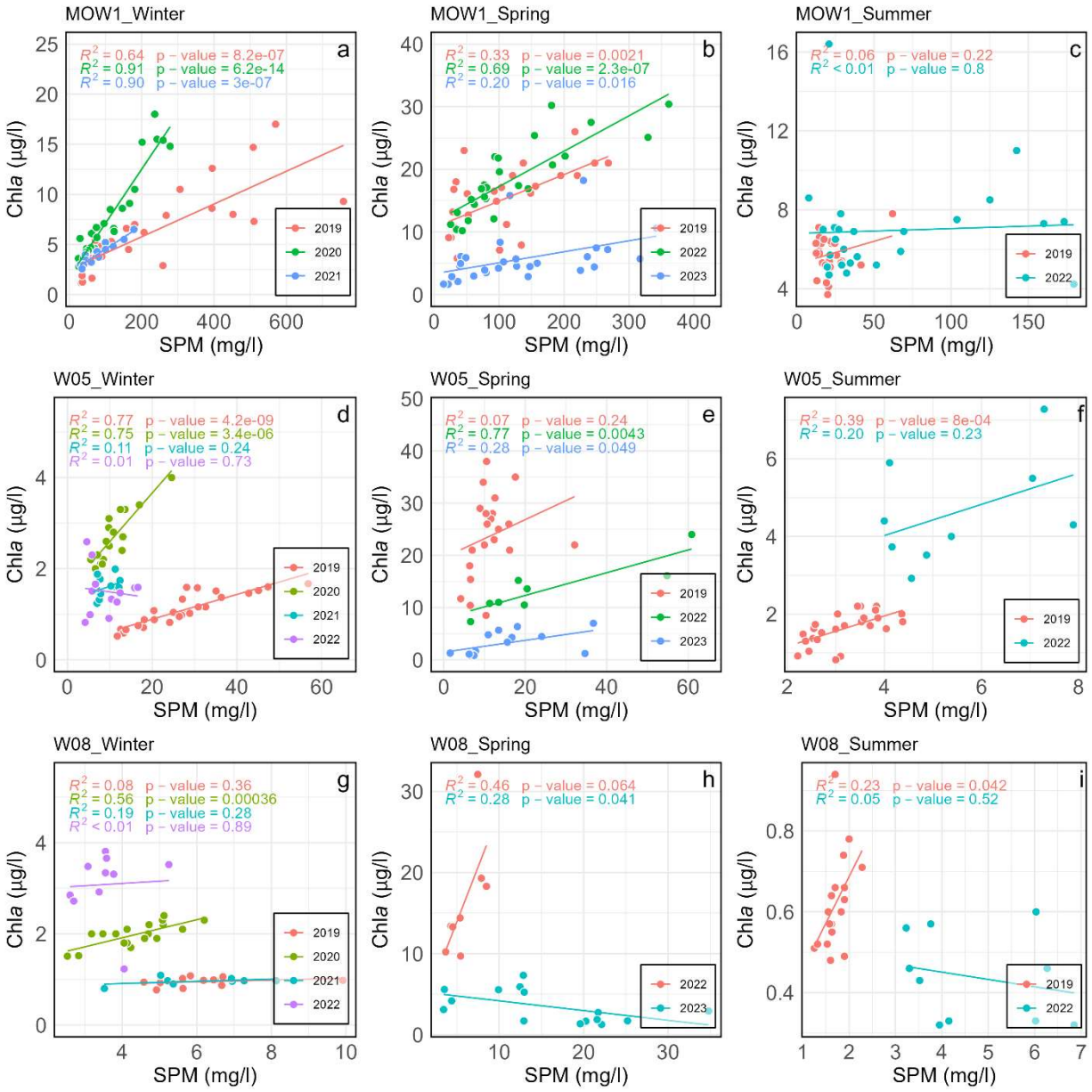

Figure 2.7: Linear Regression relationships between Chla and SPM concentrations at MOW1 (a-c), W05 (d-f), and W08 (g-i) during winter, spring and summer. The data for winter, spring, and summer represents tidal cycles sampled during January, April, and June, respectively, over the period from 2019 to 2023 (see legend).

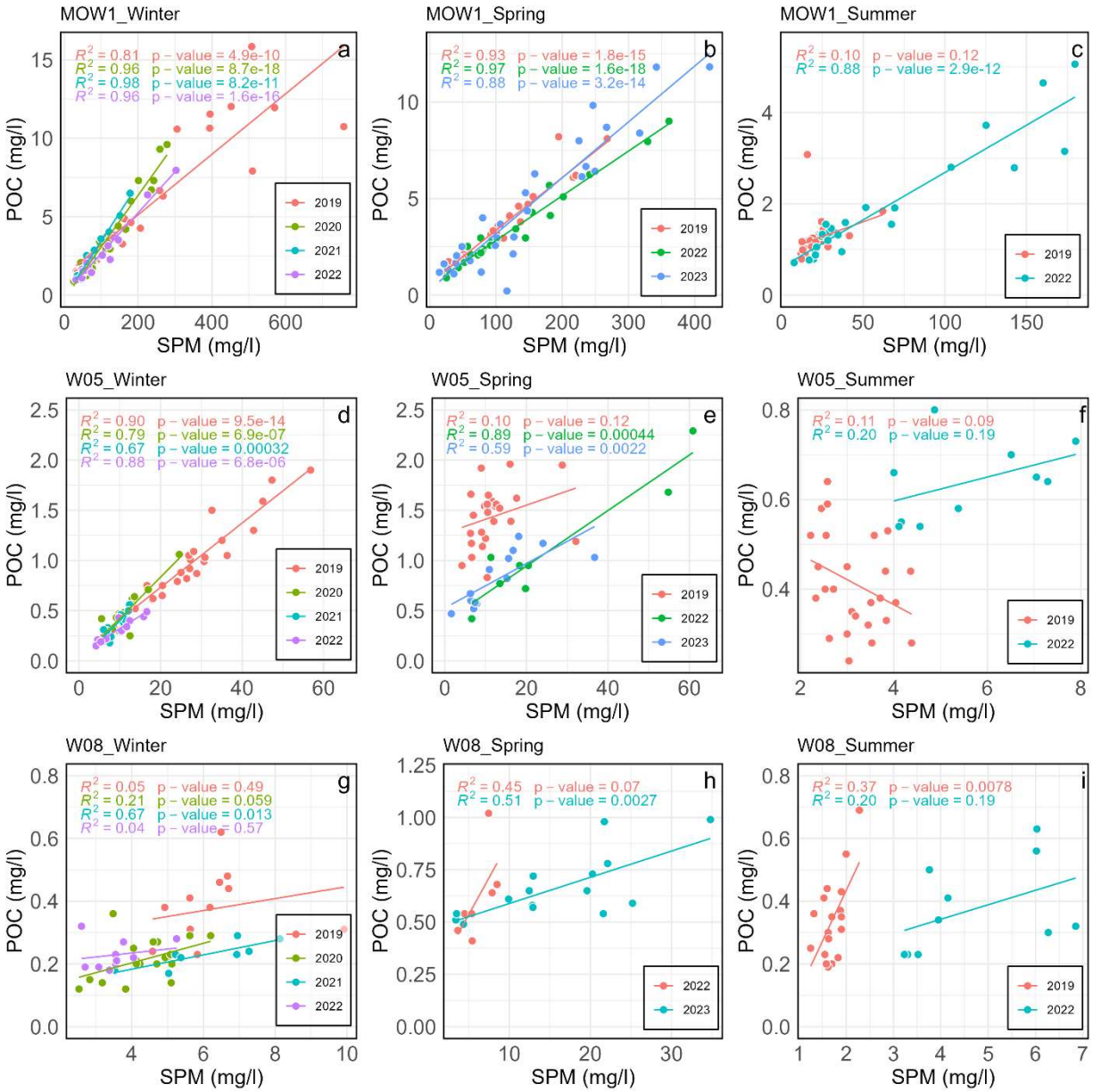

Figure 2.8: Linear Regression relationships between POC (mg/l) and SPM (mg/l) concentrations at MOW1 (a-c), W05 (d-f), and W08 (g-i) during winter, spring and summer. The data for winter, spring, and summer represents tidal cycles sampled during January, April, and June, respectively, over the period from 2019 to 2023

2.2.3. Redundancy analysis

The RDA analysis considering salinity, temperature, DIN, DIP, and DSi as environmental variables and POC, Chl*a*, POC:PON, Chl*a*:SPM, POC:SPM, and POC:Chl*a* as response variables shows that the first RDA axis is characterized by high biplot scores for SPM (0.95), salinity (0.52), and dissolved inorganic nutrients(DIN: 0.56, DIP: 0.63, DSi: 0.68), with salinity suggesting that this axis represents the coastal-offshore gradient (Figure 2.9a). The second RDA axis shows high biplot scores for temperature (0.68) and dissolved inorganic nutrients(DIN: 0.36, DIP: 0.56, DSi: 0.38), likely reflecting seasonal evolution. High species scores for all response variables across both axes indicate the influence of both seasonal and cross-shore gradients. However, Chl*a* concentrations and POC:PON ratios appear to be more strongly influenced by seasonal patterns, while other response variables are more affected by the cross-shore gradient.

The RDA analysis of the influence of environmental variables on the relative contribution of different POC components reveals distinct patterns (Figure 2.9b). The first RDA axis, with high biplot scores for temperature, Chl*a*, and dissolved inorganic nutrients, represents a seasonal gradient. The second RDA axis, characterized by high biplot scores for salinity, SPM, POC, and inorganic nutrients, reflects a cross-shore gradient. The relative contributions of POC_{det} and POC_{het} are influenced by both seasonal and cross-shore gradients, while POC_{phyto} is predominantly shaped by the seasonal gradient, and $POC_{mineral}$ is largely influenced by the cross-shore gradient.

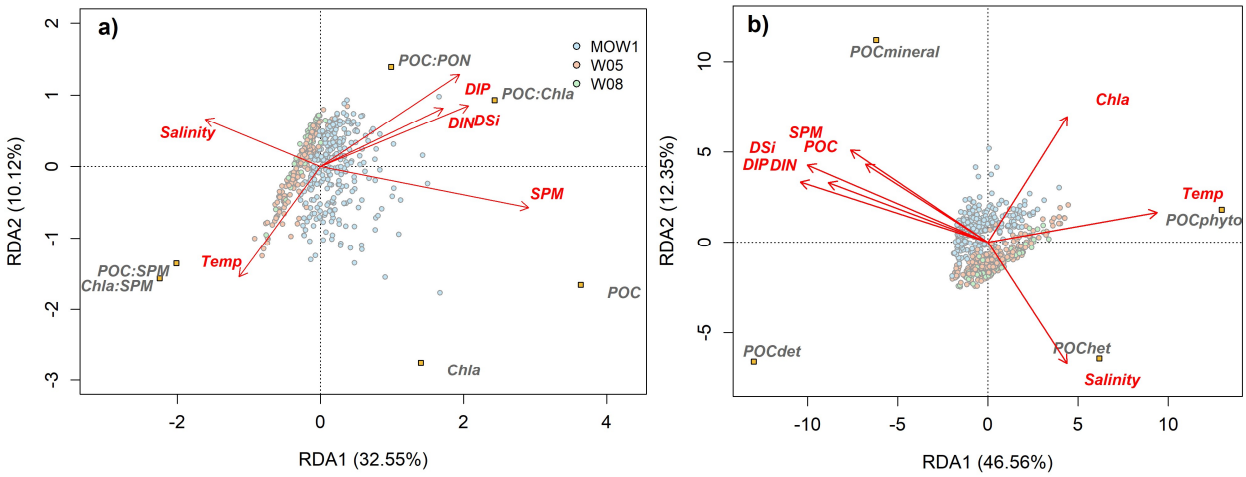

Figure 2.9: Redundancy analyses performed by considering a) salinity, temperature, DIN, DIP, and DSi as environmental variables and POC, Chla, POC:PON, Chla:SPM, POC:SPM, and POC:Chla as response variables and (b) salinity, temperature, DIN, DIP, DSi, POC, and Chla as explanatory variables and the relative contributions (%) of different POC components (POC_{phyto}, POC_{het}, POC_{det}, and $POC_{mineral}$) as response variables.

2.3. Discussion

2.3.1. Spatial variation in particulate organic matter composition

Dominance of phytoplankton-derived POC in marine-influenced coastal systems is a widely observed phenomenon (Cresson et al., 2012, Berto et al., 2013, Lowe et al., 2014; Liénart et al., 2017). In Belgian waters, however, the higher phytoplankton production at the coast, although important, is not the only factor contributing to variations of the POC composition. It is evident from the RDA analysis, (Figure 2.9) that MOW1, the station closest to the shore, exhibits notably different POC composition compared to offshore W05 and W08 stations. The first RDA axis, reflecting a spatial gradient, separates MOW1 characterised by higher SPM concentrations, lower salinity and higher POC:Chl*a* ratios from W05 and W08, which are associated with higher salinity and higher POC:SPM and Chl*a*:SPM ratios. Among the POC components, the relative abundance of $POC_{mineral}$ seems to influenced by the spatial gradient, and the relative abundance of POC_{het} increase with salinity (Figure 2.9b). A substantial difference in the POC composition along the cross-shore gradient lies in the contribution of $POC_{mineral}$ to the bulk POC pool (Figures 2.5, 2.10b). At MOW1, the station closest to shore, $POC_{mineral}$ can contribute up to a quarter of the POC pool. This contribution, however, decreases significantly at the offshore stations (Figure 2.5) and is driven by the higher availability of SPM and the greater organic matter per specific mineral surface area nearshore (Table 2.2). At MOW1, $POC_{mineral}$ and POC_{det} constitute the majority of the POC pool, with POC_{det} originating from primary and secondary producers. Since $POC_{mineral}$ is

defined as organic matter adsorbed onto mineral surfaces (primarily clay minerals), correlation between $POC_{mineral}$ and SPM is expected. However, the observed correlation between SPM and POC during the tidal cycles further suggests that POC_{det}, like $POC_{mineral}$, follows the same settling-resuspension dynamics as SPM at MOW1.

The transition zone between coastal and offshore waters in the southern North Sea, generally located around the 20 m water depth, represents a distinct regime in terms of particle dynamics (Maerz et al., 2016; Desmit et al., 2024). As bathymetry controls the propagation of the turbulent kinetic energy in the water column, the transition zone exhibits a decrease in turbulence that promotes particle settling. Depending on the cross-shore system, particles may be transported back to the coast during the tidal cycle, thus enhancing their coastal-offshore gradient. In turn, this drives a separation between turbid coastal and clear offshore waters (Desmit et al., 2024). In the Belgian waters, the transition zone encompasses station W05. While coastal particles are likely to be retained at the coast by alongshore tidal currents and because their transport to the offshore is limited by the transition zone, dissolved substances, such as inorganic nutrients and DOC, are not subject to such limitations and can be transported to the offshore waters. With mineral particles mostly confined at the coast, the relative contribution of POC_{phyto} and POC_{het} is comparatively higher at W05 and W08. Dissolved inorganic nutrients exhibit concentration gradients due to dilution. As a result, the Chl*a* content of SPM does not exhibit the same offshore increase observed for the POC content of SPM. While SPM concentrations decline substantially between stations MOW1 and W05, Chl*a* concentrations decrease primarily between W05 and W08 as nutrient supplies decrease to the offshore. The relatively high Chl*a* content of SPM at W05 is reflected in the highest relative contribution of POC_{phyto}, particularly during the summer months (Figure 2.4c). POC:Chl*a* ratios at W05 also provide insight into the dominance of living phytoplankton in the POC pool. For most of the year, POC:Chl*a* ratios at W05 remain below 200 g/g, indicative of a phytoplankton-dominated POC pool (Savoye et al., 2003). This contrasts with the offshore station W08, where POC:Chl*a* ratios exceed 200 g/g, suggesting a detritus-dominated POC pool most likely a result of inorganic nutrient limitation.

2.3.2. Seasonal variation in particulate organic matter composition

Chl*a* concentrations indicate that there are two annual phytoplankton blooms in the Belgian waters. The spring bloom develops earlier at W05 and W08, with significant nutrient depletion in March, while at MOW1 nutrients are minimum in the period between April-June. The earlier phytoplankton development offshore is likely driven by the earlier relaxation of the winter light limitation in less turbid waters. Muylaert et al. (2006) also noted a similar temporal shift along the coast, with earlier development in the southwest attributed to lower turbidity compared to the more turbid northeast waters closer to the Scheldt estuary. Nutrient ratios further indicate phosphorus limitation as a potential driver of spring bloom termination, consistent with previous studies (van der Zee & Chou 2005; Billen et al., 2011; Desmit et al., 2018). The second Chl*a* peak varies in timing and intensity across the cross-shore transect, driven by inorganic nutrient availability. It occurs earlier (July–August) at the nearshore MOW1 station and later (October–November) with lower intensity at the offshore W08 station. At MOW1, riverine inputs sustain moderate DIN levels after spring bloom, while offshore DIN concentrations remain low until summer remineralization. Similarly, DIP concentrations reach their lowest in May but increase earlier at MOW1, remaining low offshore until after summer.

The seasonal variability of POC concentrations differ from those in Chl*a* concentrations, particularly at MOW1. During the winter, physical forcings play a dominant role in shaping the distribution of both POC and Chl*a* in the coastal zone (MOW1). Here, the strong

correlations between POC, Chl*a*, and SPM concentrations during winter suggest that, in the absence of production, resuspended sediments drive the relatively high concentrations of POC and Chl*a* in the water column. With a relatively low POC_{phyto}, the winter POC pool is likely to be more refractory. In spring, the dynamics begins to shift with Chl*a* concentrations gradually increasing. Yet, this rise is not accompanied by a substantial increase in POC concentrations (POC_{phyto} fraction in April at MOW1 = 8% of the POC pool). The decoupling between Chl*a* and POC is also reflected by comparing the poor correlations between Chl*a* and SPM concentrations with the positive correlation between POC and SPM concentrations at MOW1. While the POC concentration background is largely controlled by resuspended sediments, the POC_{phyto} fraction remains relatively small at the coast despite the substantial spring phytoplankton bloom. At W05, strong correlations between POC and SPM or Chl*a* and SPM concentrations are observed during winter, when the POC_{phyto} fraction is still low, indicating that SPM dynamics, mainly tidal resuspension, control their concentrations. However, as the contribution of the POC_{phyto} fraction increases in spring and summer, these correlations weaken. At W08, the same correlations are weak throughout the year, even during winter. This highlights the relatively low impact of tidal resuspension on POC and Chl*a* distribution in the deeper offshore waters, where diel Chl*a* production and horizontal transport of phytoplankton communities dominate (Blauw et al. 2018). Thus, the contribution of the POC_{phyto} fraction influences the composition of SPM and the quality of the bulk POC pool seasonally, with different outcomes along the cross-shore gradient of SPM concentrations, that is, an important increase of the organic fraction of SPM offshore during the growing season and a relatively reduced impact in coastal waters despite a higher phytoplankton production.

2.3.3. Origin of coastal organic matter

POC:PON ratios, along with other proxies, are commonly used to determine the sources of organic matter in coastal systems. Typically, POC:PON ratios greater than 12 indicate terrestrial organic matter, while ratios between 6 and 10 suggest marine phytoplankton origins (Savoye et al. 2003). In this study, even at MOW1, POC:PON values rarely exceed 12.5, which suggests that terrestrial organic matter may not be a major contributor. Vanaverbeke et al. (2008) reported $\delta^{13}C_{POC}$ values at the coastal station 115bis (51° 09.2'N, 02° 37.2'E, located next to MOW1) ranging from -22 to -18 ‰, further indicating minimal terrestrial influence. The RDA analysis shows the influence of seasonal variation, inferred from second axis (Fig 9a), on POC and SPM compositional ratios, including POC:PON, POC:Chl*a*, POC:SPM, and Chl*a*:SPM. At the same time, the increase in POC_{phyto} relative abundance with increasing temperature (Figure 2.9b), indicative of higher phytoplankton production in spring and summer, likely drives these seasonal shifts in POC and SPM composition. The negative correlation between the POC_{phyto} fraction and POC:PON ratio indicates the lowering of POC:PON ratios due to the addition of freshly produced phytoplankton biomass to a relatively more refractory resuspended winter POC pool. At all three stations, the highest POC:PON and Pheo*a*:Chl*a* ratios are observed during winter, likely due to a larger resuspended detrital fraction. Detritus typically shows higher POC:PON ratios compared to phytoplankton biomass, as nitrogen is preferentially mineralized over carbon (Savoye et al., 2003; Harmelin-Vivien et al., 2008). However, the lowest POC:PON ratios were observed during the spring bloom at the offshore stations but later in summer at MOW1, consistent with the POC_{phyto} fraction of the POC pool. At MOW1, the large $POC_{mineral}$ pool may also influence the POC:PON ratios. Composed of DOC molecules adsorbed onto clay mineral particles (Herman & Heip, 1999; Fettweis et al., 2025), the $POC_{mineral}$ pool may exhibit higher C:N ratios due to the carbon-rich nature of the dissolved pool (~6–21; Biddanda & Benner, 1997). However, POC:PON ratios at MOW1 were not

significantly higher than at other stations. This could be due to (i) greater seasonal variations in POC:PON ratios masking spatial differences (Figure 2.9a), and/or (ii) relatively low C:N ratios (<15) of the dissolved pool in Belgian coastal waters, particularly in summer (Painter et al. 2018), which would make it difficult to distinguish from the marine POC pool.

2.3.4. Dissolved and particulate forms of organic matter

The southern North Sea, particularly along the Belgian coast, has some of the highest DOC concentrations in the North Sea, and a substantial fraction of this organic pool has marine origins (Van Engeland et al., 2010; Painter et al., 2018). While the Scheldt river is a concentrated DOC source, its impact is geographically limited. In contrast, the Rhine and Meuse rivers, the second significant freshwater inputs to the Belgian coast, serve as a more dilute source of DOC (Lacroix et al., 2004; Dai et al., 2012). Autochthonous production, in turn driven by the cross-shore gradient in nutrients, also influences the distribution of DOC. The highest DOC concentrations observed after the peak of the spring phytoplankton bloom towards summer (Figure 2.6a) have been previously noted and attributed in part to extracellular phytoplankton release (Suratman et al., 2009; Sintes et al., 2010). This release typically occurs toward the end of the bloom when nutrients are depleted, causing the excess dissolved inorganic carbon fixed by phytoplankton to be released as DOC (Toggweiler, 1993). The delayed rise in DOC concentrations has also been linked to the degradation of phytoplankton biomass rather than excretion (Wetz et al., 2008). In Belgian waters, the spring-summer increase in DOC concentrations over the winter background level is especially important at the coast, where production is more important, and is relatively lower at the offshore station (W08). This is further reflected in the contrasting relationships between DOC:TOC ratio and POC_{phyto} concentrations across stations (Figure 2.6d). At offshore stations, POC_{phyto} production leads to increase in both POC and DOC, but a greater increase in POC concentrations relative to winter POC levels results in negative correlation between the two. In contrast, at MOW1, where background POC concentrations from mineral and detrital sources remain high, the relative increase in POC_{phyto} during phytoplankton growth is minimal, whereas DOC concentrations rise significantly, leading to a positive correlation between DOC:TOC and POC_{phyto} concentrations. Furthermore, it is apparent that the partitioning of organic matter into particulate and dissolved pools differs significantly between coastal and offshore waters at all seasons (Figure 2.6b). In offshore waters, POC:DOC ratios remained below 1, consistent with the commonly observed dominance of DOC in marine systems, where it typically constitutes ~90% of the organic carbon pool (Hansell et al. 2009). POC becomes a more notable fraction only during periods of high phytoplankton productivity (Wetz & Wheeler, 2003; Engel et al., 2012). Conversely, at the turbid coastal station MOW1, POC:DOC ratios exceeded 1, a pattern also observed in turbid waters elsewhere (Abril et al., 2002; Zhao & Gao, 2019). To summarize, the cross-shore gradient of the POC:DOC ratio (Figure 2.6b) is partly driven by higher phytoplankton production and significant presence of $POC_{mineral}$ near the coast compared to offshore areas. As explained in section 2.3.1, particles tend to be retained in the coastal zone whereas dissolved substances are transported and diluted across the cross-shore axis. Such a difference in transport dynamics supports the less pronounced cross-shore gradient in DOC concentrations compared to POC, and accounts for the observed POC:DOC ratio gradient (Figure 2.6b).

2.3.5. Dynamic exchange between DOC and $POC_{mineral}$

Previous studies carried out in estuarine systems and focused on the turbidity maxima demonstrate a positive relationship between the POC fraction of TOC and the SPM concentrations in the turbid estuarine waters (Herman & Heip, 1999; Abril et al., 2002;

Middleburg & Herman, 2007). This observation aligns with the Freundlich isotherm model (eq. 2.4), which has been widely used to describe the sorption of organic matter onto mineral surfaces, reinforcing the role of SPM in governing organic matter partitioning in aquatic systems. Despite the substantial variation in POC:SPM ratios across these estuaries (Middleburg & Herman, 2007), ranging from lower values in the Gironde estuary (<5%) to higher ratios in the Scheldt estuary (~5–15 %), the overall data aligns well with Eq. 2.4. The K values (the ratio of desorption to adsorption rate constants) remain comparable among the different estuaries (Figure 2.10). Even though data from MOW1 aligns with Eq. 2.4, the value of K (~40) differs from that observed in the tidal estuaries (Figure 2.10). A smaller K value in Belgian coastal waters suggests that POC remains dominant over DOC at lower SPM concentrations compared to estuarine turbid waters; hence, the switch to DOC dominance occurs offshore at SPM concentrations equal to ~40 mg/l. Such a situation, that is, the POC:TOC ratio increasing faster with SPM concentrations, would imply a higher organic matter content of the mineral particles in Belgian coastal waters compared to the estuaries. Since the organic matter content is strongly influenced by the specific surface area of mineral particles, which is in turn governed by mineral composition (Keil et al. 1997), the variability in K values between the coastal and estuarine waters could imply differences in mineral composition. However, it remains to be seen whether the different estuaries considered have a similar mineralogical composition on average, which may or may not be the case given a large range in POC:SPM ratios in these estuaries. Hence the differences in the mineralogical composition may not completely explain the observed differences and similarities in the K values. This points to the need to consider other factors that differ between coastal and estuarine waters, such as the origin and quality of organic matter (marine vs. terrestrial) and physicochemical conditions like ionic strength (salinity), and pH, which are known to influence the adsorption and exchange of organic matter (Henrichs, 1995; Keil et al., 1997; Blattman et al., 2019).

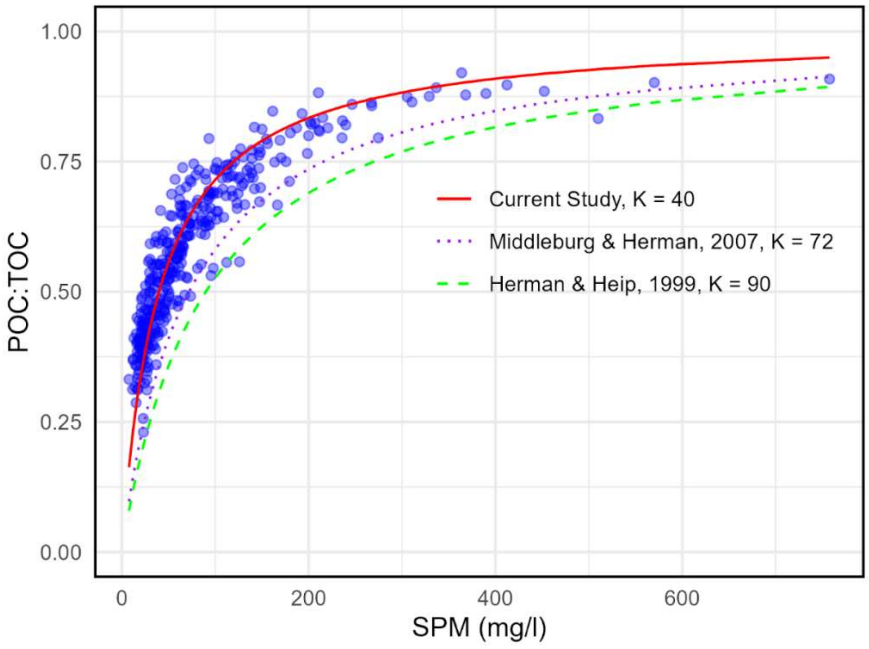

Figure 2.10: POC:TOC ratio as a function of SPM concentrations with all fitted lines representing a non-linear regression fit to Eq. (2.4). The blue dots in the figure represent observations from this study, which include data from MOW1 only (fitting red curve R^2 = 0.81). Herman & Heip (1999) presented data from high turbidity zones in the Elbe, Scheldt, and Gironde Estuaries. Middelburg & Herman (2007) expanded their dataset to include additional estuaries such as the Ems, Thames, Rhine, Loire, Douro, and Sado.

2.3.6. Estimating particulate organic matter components

C:Chl*a* ratios often form the basis of estimating POC_{phyto} from Chl*a* observations, but are tedious to obtain from field observations, requiring microscopy and biovolumes estimates. Consequently data capturing the seasonal variability in C:Chl*a* ratios in temperate coastal waters are limited (Calvo-Díaz et al., 2008; Vázquez-Domínguez et al., 2013; Jakobsen & Markager, 2016). Despite that, the available field observations across environments from coastal to open-ocean waters show a wide range of C:Chl*a* ratios (6–333) (Cloern et al., 1995; Sathyendranath et al., 2009). The trends in field observations along with experimental studies indicate that C:Chl*a* ratios generally decrease under light limitation due to increased Chl*a* production, while higher light availability promotes greater carbon accumulation relative to Chl*a* (Geider, 1987). Similarly, nitrogen limitation tends to increase C:Chl*a* ratios by constraining Chl*a* production more than carbon fixation, while the effect of temperature is complex and appears to be controlled by nitrogen availability (Geider, 1987). The empirical model developed by Jakobsen & Markager (2016) for C:Chl*a* ratios is based on observational data from the Kattegat-Belt Sea, the Wadden Sea, and various Danish estuaries. Although a number of factors would influence the light climate in the water column, the model is relevant to Belgian coastal waters, as the dataset encompasses a range of water column turbidity and seasonal surface irradiance patterns comparable to ours. Furthermore, although the phytoplankton community structure is likely to be different, the seasonal pattern of phytoplankton bloom is similar. Chl*a* concentrations at MOW1 indicate two major blooms, one in spring and another in summer, similar to those in the Wadden Sea and Danish estuaries. In contrast, offshore stations in the Kattegat-Belt Sea exhibit seasonal dynamics comparable to relatively offshore stations W05 and W08, with a pronounced spring bloom but a less distinct bloom in late summer or autumn. This spatial gradient in bloom pattern is most likely regulated by nutrient availability, as such at MOW1, the annual range of DIN concentrations (1.5-50 µmol l^{-1}) is comparable to the range observed in the Wadden Sea and Danish estuarine waters (3-50 µmol l^{-1}) and the spring phytoplankton bloom in both regions appears to be phosphate-limited rather than nitrogen-limited. While the annual temperature range in Belgian (5-22°C) waters is higher than Danish waters (1-18°C), the relatively warmer southern Bay of Biscay (Spain) exhibits a sinusoidal pattern in C:Chl*a* values (12–120 g g^{-1}; coastal station 20m depth; Vázquez-Domínguez et al., 2013) similar to the Danish waters. Moreover, the empirical model closely reproduces these seasonal dynamics in the Bay of Biscay, suggesting a stronger influence of nutrient and light availability than temperature and supporting the applicability of the model in temperate waters (Jakobsen & Markager, 2016). The winter minimum C:Chla (15) used in the current study is based on the estimate suggested for temperate waters, which is consistent with observations from the Bay of Biscay (~12) and laboratory studies under low light, high nutrient conditions typical of temperate coastal waters in winters (Geider, 1987; Calvo-Díaz et al., 2008; Jakobsen & Markager, 2016).

POC_{het} to POC_{phyto} ratio has been shown to vary systematically with POC_{phyto}, based on a meta-analysis of data from open-ocean (e.g., Mediterranean, North Atlantic, tropical Pacific) and coastal regions (e.g., North Sea, Skagerrak, Peru upwelling) (Gasol et al., 1997). POC_{phyto} is generally governed by nutrient availability, which subsequently regulates POC_{het}, consequently, in eutrophic systems, primary producers often dominate the biomass pool, substantially exceeding that of heterotrophs (Duarte et al., 2000; Yuan & Pollard, 2018). This is typically represented in ecological studies as biomass pyramids with a broad base formed by autotrophs. In contrast, oligotrophic waters frequently exhibit inverted biomass pyramids, where POC_{het} is comparable to or even greater than POC_{phyto}, reflecting a tight coupling between primary and secondary producers (Gasol et al., 1997; Leblanc et al.,

2012). Despite its broad scope, the relationship proposed by Gasol et al. (1997) holds at more localized scales too. For instance, in the Baltic Sea, the observed heterotrophic biomass was of the same order of magnitude as that predicted by Gasol et al. (1997) based on measured POC_{phyto} (Scheffold & Hense, 2020). Similarly, mesocosm experiments using Mediterranean coastal plankton community showed that heterotrophic biomass scaled with autotrophic biomass to the 1/5th power, which is similar to the empirical relationship proposed by Gasol et al. (1997). Thus, while the latter relationship may not reflect all local processes, it offers a useful first-order approximation of POC_{het} based on broadly accepted ecological principles, particularly in the absence of detailed seasonal data.

2.3.7. Relevance of this study for the dumping of dredged material

Dumping operations may significantly alter physicochemical parameters in the water column and in the sediments (Donázar-Aramendía et al., 2024). The spatio-temporal variations of SPM concentration, nutrients, POC concentration and composition and DOC concentration due to tides and seasonal changes have high natural variabilities. The study presented here provides a better understanding of these dynamics as these parameters may be relevant for assessing the effect of dredging and dumping activities on the distribution and characteristics of the OM in suspension and on the bottom. Dredging and dumping can resuspend bottom sediments, releasing POC and DOC into the water column, leading to oxidation of OM and CO_2 emissions, affecting water quality and nutrient cycling, and potentially impacting aquatic life. However, it is not clear yet what the impact of dredging and dumping is on these processes, as the spatio-temporal variation in these parameters is significantly influenced by the system's noise. Can we decipher this noise, which is inherent to nonlinear chaotic systems such as the POC and DOC dynamics, from the natural variability and the impact of anthropogenic disturbances in our low-temporal POC and DOC measurements, remains to be investigated (see Elliott & Quinino, 2007). Also to be investigated remains if the possible effects of this disturbance are of the same order or less than those of natural ones.

2.4. Conclusion

POC composition varies with SPM concentrations, showing clear differences between nearshore turbid and offshore clearer waters. Nearshore waters exhibit higher POC concentrations and elevated SPM concentrations and frequent tidal resuspension result in higher relative contributions of $POC_{mineral}$ and POC_{det}. These components, often more refractory, mask seasonal variations in the bulk POC pool. $POC_{mineral}$ represents organic matter adsorbed onto mineral surfaces, limiting enzymatic degradation, while POC_{det} consists of a mixture of organic compounds at various degradation stages. In contrast, offshore waters show reduced contributions of $POC_{mineral}$ and a higher relative abundance of fresher, more labile POC_{phyto}. Tidal resuspension has a limited influence here, as indicated by weaker correlations between POC, Chl*a*, and SPM concentrations at tidal scales. Instead, processes like horizontal advection of phytoplankton biomass and diurnal Chl*a* variability play more dominant roles in controlling POC dynamics offshore. Hence, the POC_{phyto} fraction alters the composition and quality of the bulk POC pool differently along the cross-shore SPM gradient, with a marked increase in the organic fraction offshore during the growing season and a comparatively limited effect in coastal waters despite higher phytoplankton production. Furthermore, the partitioning between dissolved and particulate organic fractions also varies along the SPM concentration gradient, with POC dominating the TOC pool in nearshore turbid waters, whereas DOC prevails offshore. The POC:TOC ratio follows a similar nonlinear trend with SPM concentration in coastal and estuarine systems. Yet, the POC content of SPM is higher in Belgian coastal waters than in estuaries. This discrepancy

may result from differences in clay particle composition, organic matter characteristics, and physicochemical properties of the water column.

3. Referenties

Abril G, Nogueira M, Etcheber H, Cabeçadas G, Lemaire E, Brogueira MJ. 2002. Behaviour of organic carbon in nine contrasting European estuaries.Estuarine, coastal and shelf science 54, 241-262.

Barbier EB, Hacker SD, Kennedy C, Koch EW, Stier AC, Silliman BR. 2011. The value of estuarine and coastal ecosystem services. Ecological Monographs 81, 169-193.

Berto D, Rampazzo F, Noventa S, Cacciatore F, Gabellini M, Aubry FB, Girolimetto A, Boscolo Brusà R. 2013. Stable carbon and nitrogen isotope ratios as tools to evaluate the nature of particulate organic matter in the Venice lagoon. Estuarine, Coastal and Shelf Science 135, 66-76.

Biddanda B, Benner R. 1997. Carbon, nitrogen, and carbohydrate fluxes during the production of particulate and dissolved organic matter by marine phytoplankton. Limnology and Oceanography 42, 506-518.

Billen G, Silvestre M, Grizzetti B, Leip A, Garnier J, Voss M, Howarth R, Bouraoui F, Lepistö L, Kortelainen P, Johnes P, Curtis C, Humborg C, Smedberg E, Kaste Ø, Ganeshram R, Beusen A, Lancelot C. 2011. Nitrogen flows from European regional watersheds to coastal marine waters. In: Sutton M, Britton C, Erisman JW, Billen G, Bleeker A, Greenfelt P, van Grinsven H, Grizzetti B (Eds.). The European Nitrogen Assessment : Sources, Effects and Policy Perspectives. Cambridge University Press, 271-297. JRC57853.

Blattmann TM, Liu Z, Zhang Y, Zhao Y, Haghipour N, Montluçon DB, Eglinton TI. 2019. Mineralogical control on the fate of continentally derived organic matter in the ocean. cience 66, 742-745.

Blauw AN, Benincà E, Laane RW, Greenwood N, Huisman J. 2018. Predictability and environmental drivers of chlorophyll fluctuations vary across different time scales and regions of the North Sea. Progress in Oceanography 161, 1-18.

Breton E, Rousseau V, Parent JY, Ozer J, Lancelot C. 2006. Hydroclimatic modulation of diatom/Phaeocystis blooms in nutrient-enriched Belgian coastal waters (North Sea). Limnology and Oceanography 51, 1401-1409.

Calvo-Díaz A, Morán XAG, Suárez LÁ. 2008. Seasonality of picophytoplankton chlorophyll a and biomass in the central Cantabrian Sea, southern Bay of Biscay. Journal of Marine Systems 72, 271-281.

Cloern JE, Grenz C, Vidergar-Lucas L. 1995. An empirical model of the phytoplankton chlorophyll: carbon ratio-the conversion factor between productivity and growth rate. Limnology and Oceanography 40.

Cresson P, Ruitton S, Fontaine MF, Harmelin-Vivien M. 2012. Spatio-temporal variation of suspended and sedimentary organic matter quality in the Bay of Marseilles (NW Mediterranean) assessed by biochemical and isotopic analyses. Marine Pollution Bulletin 64, 1112-1121.

Dai M, Yin Z, Meng F, Liu Q, Cai WJ. 2012. Spatial distribution of riverine DOC inputs to the ocean: an updated global synthesis. Current Opinion in Environmental Sustainability 4, 170-178.

Desmit X, Thieu V, Billen G, Campuzano F, Dulière V, Garnier J, Lassaletta L, Ménesguen A, Neves R, Pinto L, Silvestre M, Sobrinho JL, Lacroix G. 2018. Reducing marine eutrophication may require a paradigmatic change. Science of the Total Environment, 635, 1444-1466.

Desmit X, Nohe A, Borges AV, Prins T, De Cauwer K, Lagring R, Van der Zande D, Sabbe K. 2020. Changes in chlorophyll concentration and phenology in the North Sea in relation to de-eutrophication and sea surface warming. Limnology and Oceanography 65, 828-847.

Desmit X, Schartau M, Riethmüller R, Terseleer N, Van der Zande D, Fettweis M. 2024. The transition between coastal and offshore areas in the North Sea unraveled by suspended particle composition. Science of the Total Environment 915, 169966.

Duarte CM, Agustí S, Gasol JM, Vaqué D, Vazquez-Dominguez E. 2000. Effect of nutrient supply on the biomass structure of planktonic communities: an experimental test on a Mediterranean coastal community. Marine Ecology Progress Series 206, 87-95.

Dubois S, Savoye N, Grémare A, Plus M, Charlier K, Beltoise A, Blanchet H. 2012. Origin and composition of sediment organic matter in a coastal semi-enclosed ecosystem: An elemental and isotopic study at the ecosystem space scale. Journal of Marine Systems 94, 64-73.

Dulière V, Gypens N, Lancelot C, Luyten P, Lacroix G. 2019. Origin of nitrogen in the English Channel and Southern Bight of the North Sea ecosystems. Hydrobiologia **845**, 13–33.

Ehrhardt M, Koeve W. 1999. Determination of particulate organic carbon and nitrogen. In: Grasshoff K, Kremling K, Ehrhardt M (Eds.) Methods of Seawater Analysis, 437-444.

Eisma D, Kalf J. 1979. Distribution and particle size of suspended matter in the Southern Bight of the North Sea and the Eastern Channel. Netherlands Journal of Sea Research 13, 298-324.

Elliott M, Quintino V. 2007. The estuarine quality paradox, environmental homeostasis and the difficulty of detecting anthropogenic stress in naturally stressed areas. Marine Pollution Bulletin 54,640-645.

Engel A, Harlay J, Piontek J, Chou L. 2012. Contribution of combined carbohydrates to dissolved and particulate organic carbon after the spring bloom in the northern Bay of Biscay (North-Eastern Atlantic Ocean). Continental Shelf Research 45, 42-53.

Fettweis M, Baeye M. 2015. Seasonal variation in concentration, size, and settling velocity of muddy marine flocs in the benthic boundary layer. Journal of Geophysical Research: Oceans 120, 5648-5667.

Fettweis M, Schartau M, Desmit X, Lee BJ, Terseleer N, Van der Zande D, Parmentier K, Riethmüller R. 2022. Organic matter composition of biomineral flocs and its influence on suspended particulate matter dynamics along a nearshore to offshore transect. Journal of Geophysical Research: Biogeosciences 127, e2021JG006332.

Fettweis M, De Witte B, Van Hoey, Seghers S, Vanermaete, Timmermanx S, Hermans L. 2024. Vooruitgangsrapport juni 2024 over de effecten op het mariene milieu van baggerspeciestortingen. MF/2024/10, 34pp.

Fettweis M, Silori S, Adriaens R, Desmit X. 2025. Clay minerals and the stability of organic carbon in suspension along coastal to offshore transects. Geochimica et Cosmochimica Acta 395, 229-237.

Gasol JM, Del Giorgio PA, Duarte CM. 1997. Biomass distribution in marine planktonic communities. Limnology and Oceanography 42, 1353-1363.

Geider RJ. 1987. Light and temperature dependence of the carbon to chlorophyll a ratio in microalgae and cyanobavteria: Implications for physiology and growth of phytoplankton. New Phytologist 106, 1-34

Hansell DA, Carlson CA, Repeta DJ, Schlitzer R. 2009. Dissolved organic matter in the ocean: A controversy stimulates new insights. Oceanography 22, 202-211.

Hansell DA, Carlson CA. (Eds.). 2014. Biogeochemistry of marine dissolved organic matter. Academic press.

Harmelin-Vivien M, Loizeau V, Mellon C, Beker B, Arlhac D, Bodiguel X, Ferraton F, Hermand R, Philippon X, Salen-Picard C. 2008. Comparison of C and N stable isotope ratios between surface particulate organic matter and microphytoplankton in the Gulf of Lions (NW Mediterranean). Continental Shelf Research 28, 1911-1919.

Hemingway JD, Rothman DH, Grant KE, Rosengard SZ, Eglinton TI, Derry LA, Galy VV. 2019. Mineral protection regulates long-term global preservation of natural organic carbon. Nature 570(7760), 228-231.

Herman PM, Heip CH. 1999. Biogeochemistry of the MAximum TURbidity Zone of Estuaries (MATURE): some conclusions. Journal of Marine Systems 22, 89-104.

Jago CF, Bale AJ, Green MO, Howarth MJ, Jones SE, McCave IN, Millward GE, Morris AW, Rowden AA, Williams JJ. 1993. Resuspension processes and seston dynamics, southern North Sea. Philosophical Transactions of the Royal Society of London. Series A: Physical and Engineering Sciences 343, 475-491.

Jakobsen HH, Markager S. 2016. Carbon-to-chlorophyll ratio for phytoplankton in temperate coastal waters: Seasonal patterns and relationship to nutrients. Limnology and Oceanography 61, 1853-1868.

Kharbush JJ.Close, HG, Van Mooy BAS, Arnosti C, Smittenberg RH, Le Moigne FAC, Mollenhauer G, Scholz-Böttcher B, Obreht I, Joch BP, Becker KW, Iversen MH, Mohr W.

Particulate organic carbon deconstructed: Molecular and chemical composition of particulate organic carbon in the ocean. Frontiers in Marine Science 7, 518.
Keil RG, Mayer LM. 2014. Mineral Matrices and Organic Matter. In: Turekian HDHK (Ed.) Treatise on Geochemistry, 2nd Edn., Elsevier, 337–359.
Keil RG, Mayer LM, Quay PD, Richey JE, Hedges JI. 1997. Loss of organic matter from riverine particles in deltas. Geochimica et Cosmochimica Acta 61, 1507-1511.
Keil RG, Montluçon DB, Prahl FG, Hedges JI. 1994. Sorptive preservation of labile organic matter in marine sediments. Nature 370, 549-552.
Kleber M, Bourg IC, Coward EK, Hansel CM, Myneni SC, Nunan N. 2021. Dynamic interactions at the mineral–organic matter interface. Nature Reviews Earth & Environment 2, 402-421.
Lacroix G, Ruddick K, Ozer J, Lancelot C. 2004. Modelling the impact of the Scheldt and Rhine/Meuse plumes on the salinity distribution in Belgian waters (southern North Sea). Journal of Sea Research 52, 149-163.
Lauwaert B, Fettweis M, De Witte B, Van Hoei G, Timmermans S, Hermans L. 2019. Vooruitgangsrapport (juni 2019) over de effecten op het mariene milieu van baggerspeciestortingen (Vergunningsperiode 01/01/2017 – 31/12/2021). RBINS-ILVO-AMT-CD rapport. BL/2019/01, 28pp.
Lauwaert B, De Witte B, Festjens F, Fettweis M, Hermans L, Lesuisse A, Le H-M, Seghers S, Timmermans S, Vanavermaete D, Van Hoey G. 2021. Synthesis report on the effects of dredged material dumping on the marine environment (licensing period 2017-2021). RBINS-ILVO-AMT-AMCS-FHR report BL/2021/10, 67pp.
Lee B, Toorman E, Molz F, Wang J. 2011.Atwo-class population balance equation yielding bimodal flocculation of marine or estuarine sediments. Water Research 45, 2131e2145.
Legendre P, Legendre L. 1998. Numerical Ecology. 3rd Ed. Elsevier, Amsterdam, 853pp.
Liénart C et al. 2017. Dynamics of particulate organic matter composition in coastal systems: A spatio-temporal study at multi-systems scale. Progress in Oceanography 156, 221-239.
Liénart C et al. 2018. Dynamics of particulate organic matter composition in coastal systems: forcing of spatio-temporal variability at multi-systems scale. Progress in Oceanography 162, 271-289.
Liu Q, Kandasamy S, Lin B, Wang H, Chen CTA. 2018. Biogeochemical characteristics of suspended particulate matter in deep chlorophyll maximum layers in the southern East China Sea. Biogeosciences 15, 2091-2109.
Lowe AT, Galloway AW, Yeung JS, Dethier MN, Duggins DO. 2014. Broad sampling and diverse biomarkers allow characterization of nearshore particulate organic matter. Oikos, 123, 1341-1354.
Maerz J, Hofmeister R, van der Lee EM, Gräwe U, Riethmüller R, Wirtz KW. 2016. Maximum sinking velocities of suspended particulate matter in a coastal transition zone. Biogeosciences 13, 4863-4876.
Mayer LM. 1994. Surface area control of organic carbon accumulation in continental shelf sediments. Geochimica et Cosmochimica Acta 58, 1271-1284.
Middelburg JJ, Herman PM. 2007. Organic matter processing in tidal estuaries. Marine Chemistry 106, 127-147.
Middelburg JJ. 2019. Marine Carbon Biogeochemistry: A Primer for Earth System Scientists. Springer, 118pp.
Modéran J, Bouvais P, David V, Le Noc S, Simon-Bouhet B, Niquil N, Miramand P, Fichet, D. 2010. Zooplankton community structure in a highly turbid environment (Charente estuary, France): Spatio-temporal patterns and environmental control. Estuarine, Coastal and Shelf Science 88, 219-232.
Muylaert K, Gonzales R, Franck M, Lionard M, Van der Zee C, Cattrijsse A, Sabbe K, Chou L, Vyverman W. 2006. Spatial variation in phytoplankton dynamics in the Belgian coastal zone of the North Sea studied by microscopy, HPLC-CHEMTAX and underway fluorescence recordings. Journal of Sea Research 55, 253-265.
Painter SC, Lapworth DJ, Woodward EMS, Kroeger S, Evans CD, Mayor DJ, Sanders RJ. 2018. Terrestrial dissolved organic matter distribution in the North Sea. Science of the Total Environment 630, 630-647.
Passow U, Alldredge AL. 1995. A dye-binding assay for the spectrophotometric

measurement of transparent exopolymer particles (TEP). Limnology and Oceanography 40, 1326-1335.
Passow U. 2002. Transparent exopolymer particles (TEP) in aquatic environments. Progress in Oceanography 55, 287-333.
Rousseau V, Park Y, Ruddick K, Vyverman W, Parent JY, Lancelot C. 2006. Phytoplankton blooms in response to nutrient enrichment. Current status of eutrophication in the Belgian coastal zone. Presses Univ. de Bruxelles, 45-59.
Sathyendranath S, Stuart V, Nair A, Oka K, Nakane T, Bouman H, Forget MH, Maass H, Platt T. 2009. Carbon-to-chlorophyll ratio and growth rate of phytoplankton in the sea. Marine Ecology Progress Seres 383, 73-84.
Savoye N, Aminot A, Tréguer P, Fontugne M, Naulet N, Kérouel R. 2003. Dynamics of particulate organic matter δ15N and δ13C during spring phytoplankton blooms in a macrotidal ecosystem (Bay of Seine, France). Marine Ecology Progress Series 255, 27-41.
Schartau M, Riethmüller R, Flöser G, van Beusekom JEE, Krasemann H, Hofmeister R, Wirtz K. 2019. On the separation between inorganic and organic fractions of suspended matter in a marine coastal environment. Progress in Oceanography 171, 231-250.
Sintes E, Stoderegger K, Parada V, Herndl GJ. 2010. Seasonal dynamics of dissolved organic matter and microbial activity in the coastal North Sea. Aquatic Microbial Ecology 60, 85-95.
Suratman S, Weston K, Jickells T, Fernand L. 2009. Spatial and seasonal changes of dissolved and particulate organic C in the North Sea. Hydrobiologia 628, 13-25.
Toggweiler JR. 1993. Carbon overconsumption. Nature 363, 210-211.
van der Zee C, Chou L. 2005. Seasonal cycling of phosphorus in the Southern Bight of the North Sea. Biogeosciences 2, 27-42.
Van Engeland T, Soetaert K, Knuijt A, Laane RWPM, Middelburg JJ. 2010. Dissolved organic nitrogen dynamics in the North Sea: a time series analysis (1995–2005). Estuarine, Coastal and Shelf Science 89, 31-42.
Vanaverbeke J, Franco M, Van Oevelen D, Leon M, Provoost P, Steyaert M, Soetaert K, Vincx M. 2008. Benthic responses to sedimentation of phytoplankton on the Belgian Continental Shelf. In: Current status of eutrophication in the Belgian coastal zone, 73-90. Presses Universitaires de Bruxelles.
Vázquez-Domínguez E, Morán XAG, López-Urrutia A. 2013. Photoacclimation of picophytoplankton in the central Cantabrian Sea. Marine Ecology Progress Series 493, 43-56.
Verdugo P. 2012. Marine microgels. Annual Review of Marine Science 4, 375-400.
Wetz MS, Wheeler PA. 2003. Production and partitioning of organic matter during simulated phytoplankton blooms. Limnology and Oceanography 48, 1808-1817.
Wetz MS, Hales B, Wheeler PA. 2008. Degradation of phytoplankton-derived organic matter: Implications for carbon and nitrogen biogeochemistry in coastal ecosystems. Estuarine, Coastal and Shelf Science 77, 422-432.
Woźniak SB, Stramski D, Stramska M, Reynolds RA, Wright VM, Miksic EY, Cichocka M, Cieplak AM. 2010. Optical variability of seawater in relation to particle concentration, composition, and size distribution in the nearshore marine environment at Imperial Beach, California, Journal of Geophysical Research 115, C08027
Zhao L, Gao L. 2019. Dynamics of dissolved and particulate organic matter in the Changjiang (Yangtze River) estuary and the adjacent East China Sea shelf. Journal of Marine Systems 198, 103188.

COLOPHON

Dit rapport werd voorbereid door de BMM in september 2025
Zijn referentiecode is MOMO/10/MF/202509/NL/AR/7

De scheepstijd met de RV Belgica werd voorzien door BELSPO en KBIN-OD Natuur

Indien u vragen hebt of bijkomende copies van dit document wenst te verkrijgen, gelieve een e-mail te zenden naar mfettweis@naturalsciences.be, met vermelding van de referentie, of te schrijven naar:

Koninklijk Belgisch Instituut voor Natuurwetenschappen
OD Natuur – BMM
t.a.v. Michael Fettweis
Vautierstraat 29
B–1000 Brussel
België
Tel: +32 2 627 41 83

APPENDIX 1

Bijdrage voor

Ems-Scheldt Workshop, 13-14 February 2025, Delmenhorst (Germany)

The organic matter dynamics along the land-ocean aquatic continuum of the Scheldt estuary

Michael Fettweis[1], Jean-Philippe Belliard[1,2], Xavier Desmit[1], Tom Maris[2], Luz Amadei Martínez[3], Saumya Silori[1]

[1] ODNature, Royal Belgian Institute of Natural Sciences, Brussels, Belgium
[2] ECOSPHERE, Department of Biology, University of Antwerp, Antwerp, Belgium
[3] Laboratory of Protistology and Aquatic Ecology, Department of Biology, Ghent University, Ghent, Belgium

Suspended particulate matter (SPM) occurs generally as flocs composed of minerals and organic matter. Along the continuum from rivers to estuaries and coasts, flocs are dominated by of mineral particles in estuarine and nearshore turbidity maximum zones, while they contain more organic matter and low-density aggregates in the low turbid offshore zones. Further along this estuary-coast continuum, the particulate organic carbon (POC) content of the SPM decreases exponentially with increasing SPM concentration, implying that there is a positive correlation between the POC and SPM concentrations. Yet, SPM composition between the brackish and freshwater zones of the Scheldt estuary seem to depart from this overall pattern (Figure 1). The change in composition of particles along the SPM concentration gradient and the high variability at especially lower SPM concentrations can be explained by physical (tidal hydrodynamics, waves, river discharge, residence time), biological (primary and secondary production), and chemical processes (salinity, characteristics of the mineral and organic matter) that act on various spatial and temporal scales. We will discuss the processes responsible for these observed differences in POC content along the salinity gradient of the Scheldt estuary using data on salinity, nutrients, chlorophyl, dissolved organic carbon and mineralogy.

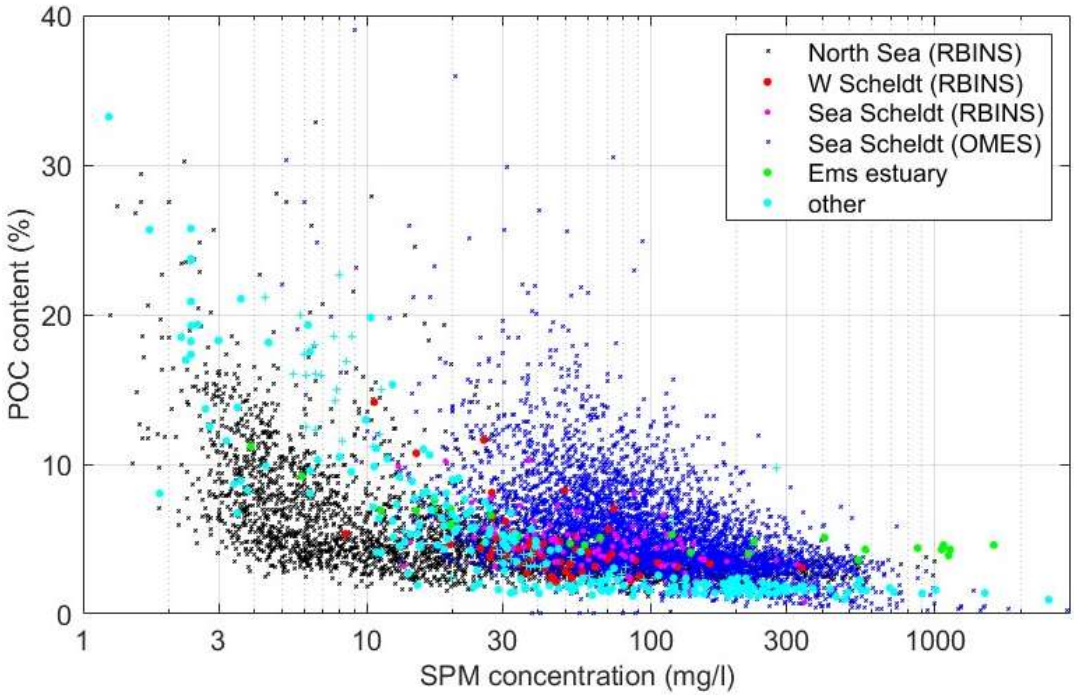

Figure 1: POC content of the SPM in the freshwater and brackish zones of the Sea Scheldt (OMES: 1995-2021, RBINS: 2004-2007), the saltwater zone in the Western Scheldt (RBINS: 2004-2018) and in the North Sea (2004-2023). Also shown are data from brackish and freshwater zones from the Ems estuary and from other areas (Godavari estuary, Guayas delta, Congo river, Huanghe estuary, Tokyo Bay).

APPENDIX 2

Bijdragen voor

EGU General Assembly, 27 April - 2 May 2025, Vienna (Austria)

EGU25-10712, updated on 13 Aug 2025
https://doi.org/10.5194/egusphere-egu25-10712
EGU General Assembly 2025

Intra-annual variability of marine floc morphology in southern North Sea coastal waters using in-situ high-resolution underwater imaging

Louise Delhaye, Céline Taymans, and Michael Fettweis
Royal Belgian Institute of Natural Sciences, OD Nature, Brussels, Belgium (ldelhaye@naturalsciences.be)

SPM concentration and composition is an indicator for the balance between physical (turbulence) and biogeochemical processes (production, remineralization). High SPM concentration coincides with a dominance of mineral particles and the occurrence of biomineral flocs. These high turbidity zones, generally located nearshore or in estuaries, are characterized by strong tidal currents, intensive resuspension and settling, flocculation in phase with the tides and high primary productions. With decreasing SPM concentration, organic matter becomes more dominant and biological flocs, for example phytoplankton cells or aggregates, are getting more prominent. Physical processes are less important, and flocculation occurs on seasonal time scales. Measuring SPM concentration and particle size distribution (PSD) using laser diffraction techniques (e.g. LISST-100x) has been a standard component of Belgium's monitoring for the past 20 years, resulting in a good knowledge of its spatial and temporal variability. However, despite its relevance to better understand and monitor the coastal pelagic environment, the PSD derived from laser diffraction do not provide insights into the origin (flocs, biological particles) and composition (mineral, organic matter) of the SPM. Yet, this information is crucial to better understand the SPM dynamics and to better predict the floc density and the fate and flux of minerals, carbon and pollutants.

High-resolution underwater particle cameras are gaining popularity as they capture larger particles and provide data on their morphology and origin. By doing so and enabling researchers to visually see SPM, they offer a promising complement to laser diffraction-based instruments. This however doesn't come without challenges, the main ones being related to image pre-processing (e.g. noise removal, histogram stretching, image reconstruction) and threshold definition as algorithms for particle detection and shape extraction may significantly impact PSD and derived parameters, requiring rigorous calibration and validation.

In this study, we address these gaps by developing a processing system using underwater high-resolution particle imagery and applying it on a test case: the intra-annual morphological variability of marine flocs. Images were taken *in-situ* four kilometers off the Belgian coast during

six oceanographic campaigns on board the RV Belgica between April 2023 and March 2024. An open-source user-friendly Python algorithm was developed to extract particles from images after validation in the lab against known-size particles. Floc morphologies were characterized using six shape indicators and were compared to *in-situ* SPM concentration, turbidity, LISST-100x and LISST-200x measurements as well as different parameters from water sample analyses taken at the same time.

EGU25-19833, updated on 13 Aug 2025
https://doi.org/10.5194/egusphere-egu25-19833
EGU General Assembly 2025

Budgeting the particulate organic matter from the suspended particulate matter in shelf seas

Xavier Desmit[1], Rolf Riethmüller[2], Saumya Silori[1], Markus Schartau[3], Dimitry Van der Zande[1], and Michael Fettweis[1]

[1]Royal Belgian Institute of Natural Sciences, Brussels, Belgium (xdesmit@naturalsciences.be)
[2]Institute of Coastal Ocean Dynamics, Helmholtz-Zentrum Hereon, 21502 Geesthacht, Germany
[3]GEOMAR Helmholtz Centre for Ocean Research Kiel, Kiel, Germany

Dissolved CO_2 and buried organic matter budgets have been studied in shelf seas to identify carbon fractions that are exported to the ocean interior or preserved in the sediment. However, the fate of suspended particulate organic matter remains less understood, particularly because its lability is difficult to identify. Analysis of the different fractions of particulate organic matter in the North Sea could contribute to understanding its fate. The particulate organic carbon (POC) concentration follows coastal-offshore gradients that can be predicted with the suspended particulate matter (SPM) concentration. The POC:SPM ratio indeed features a typical exponential decrease with the SPM concentration. While that ratio is higher offshore where SPM concentrations are minimum, it reaches low asymptotic values at the coast where SPM concentrations are high. Such a relationship is actually found in many different systems (coastal zones, estuaries) and at different latitudes. A semi-empirical model has been proposed to fit the observed data of that relationship in the southern North Sea (German Bight: Schartau et al., 2019; Belgian zone: Fettweis et al., 2022). Based on the model assumptions, it is possible to separate two fractions of POC: the fresh fraction, that is assumed to accumulate during the bloom and to be degraded within the season, and a more refractory POC fraction. More detailed calculations allow this latter fraction to be divided into a slow POC, which includes the refractory detritus, and a mineral POC, that is the POC adsorbed on the surfaces of clay minerals. We assume that suspended mineral particles in the North Sea provide a total surface area saturated with adsorbed organic matter, also considering an underlying dynamic equilibrium between adsorption and desorption of organic matter. We then calculate the SPM budget in the North Sea from satellite remote sensing and vertical concentration profiles obtained from in situ observations. On this basis, we can use the semi-empirical model to establish a budget of the fresh, refractory detrital and mineral fractions of POC on the shelf.

APPENDIX 3

Bijdrage voor

56th Int. Liège Coll. on Ocean Dynamics, 26-30 May, Liège (Belgium)

Environmental conditions for alkalinity enhancement in the Belgian part of the North Sea

Michael Fettweis[1], Jean-Philippe Belliard[1,2], Xavier Desmit[1], Saumya Silori[1], Duc Tran[1], Filip Meysman[3]

[1] Royal Belgian Institute of Natural Sciences, rue Vautier 29, 1000 Brussels (Belgium)

[2] ECOSPHERE, University of Antwerp, Universiteitsplein 1, 2140 Wilrijk (Belgium)

[3] Geobiology Research Group, Universiteitsplein 1, University of Antwerp, 2140 Wilrijk (Belgium)

Generation of ocean alkalinity occurs naturally through the weathering of rocks, specifically the dissolution of silicates or carbonates or the formation of pyrite from Fe-hydroxide minerals. Within the Blue Alkalinity project, we investigate how this natural weathering processes can be amplified through the guided disposal of large amounts of carbonate and iron oxide minerals at sea. The potential use of these materials as alkalinity enhancer depends on the local sediment geochemistry and local hydrodynamic conditions.

Calcite dissolution in marine is limited by the calcium carbonate saturation state, which is high in the North Sea. Therefore the calcite needs to be introduced into specific sediments where the pore water has a lower saturation state and thus enable $CaCO_3$ dissolution. The disposal of iron oxides will produce alkalinity through pyrite formation, which occurs through microbial sulphate reduction. This hence requires sediment locations with suitable anoxic conditions Moreover, successful alkalinity enhancement thus requires that sediments in which the iron oxides are mixed, remain stable over long time periods and are not resuspended during, for example, extreme events.

Therefore, we will present under what hydrodynamic conditions sediment particles are mobilized, transported and deposited in Belgian part of the North Sea. We will focus on the shallow, turbid and highly dynamic coastal region that contains mainly muddy sediments that are anoxic, and the offshore deeper regions that are less dynamic, and consists sandy sediments. Based on long-term continuous time series of SPM concentration and current velocity we can derive the probability of particles to be resuspended in both coastal and offshore environments. The impact of increased SPM concentrations due to the disposal of these minerals in both environments will be discussed.

APPENDIX 4

Reprint

Fettweis M, Silori S, Adriaens R, Desmit X. 2025. Clay minerals and the stability of organic carbon in suspension along nearshore to offshore transects. Geochimica et Cosmochimica Acta 395, 229-237

Geochimica et Cosmochimica Acta 395 (2025) 229–237

Contents lists available at ScienceDirect

Geochimica et Cosmochimica Acta

journal homepage: www.elsevier.com/locate/gca

Clay minerals and the stability of organic carbon in suspension along coastal to offshore transects

Michael Fettweis [a,*], Saumya Silori [a], Rieko Adriaens [b], Xavier Desmit [a]

[a] OD Natural Environment, Royal Belgian Institute of Natural Sciences, rue Vautier 29, 1000 Brussels, Belgium
[b] Qmineral, Gaston Geenslaan 1, 3001 Heverlee, Belgium

ARTICLE INFO

Associate editor: Xiaojuan Feng

Keywords:
Suspended particulate matter
Mineral-associated organic carbon
Clay minerals

ABSTRACT

Particulate (POC) and dissolved organic carbon (DOC) concentration, clay mineral content and composition and the suspended particulate matter (SPM) concentration have been analyzed in water samples taken along transects from the high turbid nearshore to the low turbid offshore on the North Sea shelf. The suspended POC has been classified into a mineral-associated ($POC_{mineral}$), a slowly degrading (POC_{slow}) and a fresh fraction (POC_{fresh}). The $POC_{mineral}$ has been estimated based on the clay mineral composition and on literature data of the mineral specific surface area per g and the OC content per specific surface area. It consists of organic molecules adsorbed onto mineral surfaces and is thereby the most refractory fraction. The POC_{fresh} content (% of POC_{fresh} in SPM) has been calculated using the semi-empirical POC-SPM model of Fettweis et al. (2022) and is intrinsically labile. The POC_{slow} content is refractory with variable rates of degradation. The total POC content of the SPM was between 2 and 11%, from which about 0.3–6.6% (0.1–2.1%) was POC_{fresh} in spring (resp., winter). The $POC_{mineral}$ content was between 0.4% and 1.1% and decreased towards the offshore, meaning that the POC offshore is less refractory than nearshore. The organic molecules adsorbed onto clay minerals, are dynamically exchanging with the DOC, and thus influencing its fate and concentration. However this process is not sufficient to explain the increasing POC/DOC ratio with increasing SPM concentration, which is further explained by primary production, advection and diffusion, density gradients and seabed erosion. Our results highlight the difficulty and the necessity of estimating the respective sample-POC and DOC concentrations, fluxes and fates along SPM concentration gradients in coastal zones. This is needed as organo-mineral interactions influence the vertical dynamics and horizontal transport of SPM and have an impact on particles and organic carbon fluxes.

1. Introduction

Minerals and organic matter (OM) are the major constituents of suspended particulate matter (SPM) in aquatic systems. Marine OM constitutes a mixture of plankton (phytoplankton, bacteria, etc.), exudates, detritus, fecal pellets, organic molecules originating from diverse autochthonous and allochthonous sources and organo-mineral associations (Arndt et al., 2013; Keil and Mayer, 2014). The lability of the OM ranges from high, for example living cells, to low, for example organo-mineral associations (Ittekkot, 1988; Mayer, 1994; Hedges and Keil, 1995; Etcheber et al., 2007; Singh et al., 2016; Hemingway et al., 2019). The relative content of these different forms of OM varies temporally and spatially, due to biogeochemical and physical processes.

In marine systems, minerals and OM come mostly together and organo-mineral interactions on molecular to mm scale are ubiquitous. Clay minerals are the major mineral component in organo-mineral associations. The primary interaction between them takes place on molecular to nano scale; they have been well described in reviews (for example Mitchel and Soga, 2005; Keil and Mayer, 2014; Deng et al., 2022; Zhao et al., 2023). These interactions occur in a variety of ways that goes from the adsorption of small and larger organic molecules onto surfaces by, for example, hydrogen bonds or van der Waals forces, to intercalation into expandable clay minerals and the occlusion into small clay mineral aggregates (flocculi). The resultant organo-mineral associations serve as building blocks or primary particles at a higher level of complexity known as biomineral flocs (Maggi, 2009; Lee et al., 2012; Shen et al., 2018). The interactions between organic molecules and minerals through adsorption/desorption kinetics show that a transition between the dissolved (organic molecules) and the particulate phase occurs (Kleber et al., 2021). Both the particulate (POM) and the

* Corresponding author.
E-mail address: mfettweis@naturalsciences.be (M. Fettweis).

https://doi.org/10.1016/j.gca.2025.03.003
Received 12 September 2024; Accepted 5 March 2025
Available online 8 March 2025

dissolved organic matter (DOM) fractions are therefore not necessarily constant in composition and concentration (Middelburg et al., 1993; Blattmann et al., 2019).

The OM plays an important role in many coastal and estuarine processes, such as the formation of biomineral deposits and the sequestration of carbon; the variation in water clarity and its influence on primary production; flocculation and the settling of biomineral flocs; or the transport of pollutants (see for example Pedersen and Calvert, 1990; Mayer, 1994; Chen et al, 2016; Singh et al., 2016; Blattmann et al., 2019; Hemingway et al., 2019; Opdal et al., 2019; Fettweis et al., 2022). The interactions of minerals and OM may stabilize part of the organic carbon or prevent further degradation (Hemingway et al., 2019). Organo-mineral association and other stable OM are found in marine sediments. Before being sequestered, they have been transported in suspension; an accurate estimation of this OM fraction in the SPM is up to now lacking.

We argue in this study that the organic matter in suspension can be classified into three groups: A mineral-associated, a slowly degrading or non-metabolizable, and a fresh and consumable fraction that encompasses the living cells and their exudates. This classification reflects the various organo-mineral interactions better than the two types of POM (mineral-associated and fresh) that were put forward by Schartau et al. (2019) in their semi-empirical POM-SPM model. We propose to split their 'mineral-associated' fractions into a slowly degrading fraction (POC_{slow}) and a truly mineral-associated fraction ($POC_{mineral}$). The latter comprises the organic carbon (OC) that is preserved from degradation through sorption of organic molecules to mineral surfaces and the intercalation into expandable clay minerals, and which depends mainly on the specific surface area of minerals (Keil and Mayer, 2014). The aim of our study is to estimate the content of the three POC groups in the SPM by collecting SPM from water samples and by analyzing the POC and DOC concentration and the mineral composition.

2. Methods

2.1. Sampling

The samples were taken in 12 stations all located along a cross-shore transect that ranges from the high turbid nearshore to the low turbid offshore in the English Channel and the southern North Sea in spring (March-April) and winter (December) 2023, see Fig. 1. The coordinates and the sampling date and time can be found in Table S1 (supplementary material). The Belgian stations MOW1, W05, W08 and Codevco and the UK stations West Gabbard and Sizewell are in the Southern Bight of the North Sea; stations Scenes and BS1 in the Seine Bay (France), stations HB2, HB1 and Helgoland in the German Bight and station Dogger Bank in the central North Sea.

The sampling was done with Niskin bottles and a centrifuge with a water inlet at about 4 m below the surface. The data set from Niskin bottles consists of 1.5 or 2 hourly samples at the surface and near the bed collected during 13 full tidal cycles and 8 half tidal cycles, and 2 times 2 samples in one location. To compare both samples, we will use here only the surface samples from the water samples. The centrifuge was collecting SPM during the full or half tidal cycle in all stations except for Dogger bank where the collection was done during transit (started 3 h before arrival until 3 after leaving the station). For station MOW1, W05 and W08 additional water samples data are available: MOW1 100 full tidal cycles since 2004, W05 40 full and half tidal cycles since 2018 and W08 37 full and half tidal cycles since 2019.

2.2. SPM, POC and DOC analysis

At every sampling occasion, three subsamples for SPM concentration were taken and filtered on board using pre-combusted (405 °C, 24 hr.), rinsed, dried for 24 hr. at 105 °C and pre-weighted 47 mm GF/C filters. After sampling the filters were rinsed with ultrapure water (resistivity

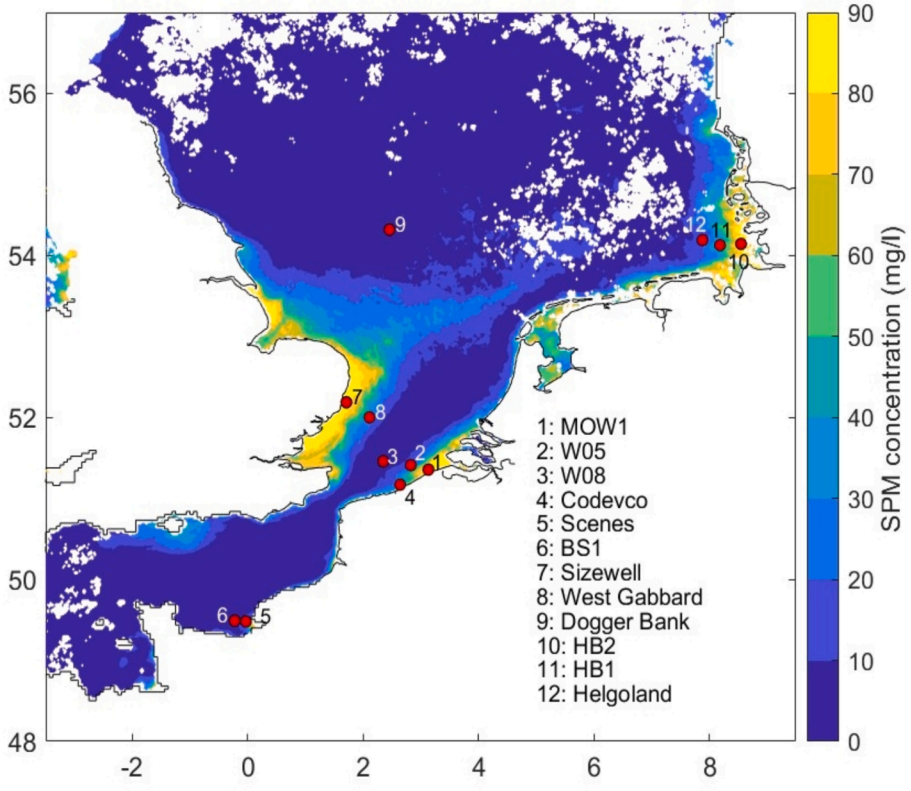

Fig. 1. Map of sampling stations in the North Sea and the English Channel. The background displays the averaged near surface SPM concentrations computed using the algorithm of Nechad et al. (2010) from Sentinel-3/OLCI images between November 2019 and March 2020.

18.2 MΩ cm normalized at 25 °C) and immediately stored at − 20 °C, before being dried for 24 hr. at 50 °C and weighted to obtain the concentration. The uncertainty (expressed as the RMSE of the triplicates divided by the mean value) decreases with increasing concentration from 8.5 % (SPM concentration < 5 mg/l) to 6.7 % (<10 mg/l), 3.5 % (10–50 mg/l), and 2.1 % (>100 mg/l) and represent the random error related to the lack of precision during filtrations. The samples for POC were filtered on board using 25 mm GF/C filters (pretreated as above for SPM), stored immediately at − 20 °C, before being analyzed using a Thermo Finnigan Flash EA1112 elemental analyzer (for details see Ehrhardt and Koeve, 1999). The analytical uncertainty is 12 %. The filtrates for the surface samples were collected in sample tubes for DOC and analyzed using standard spectrophotometric methods with a Skalar autoanalyzer, for details see van der Zee and Chou (2005).

2.3. Semi-empirical POC-SPM model

A characteristic feature of the SPM is that the organic matter content decreases exponentially with increasing SPM concentration and reaches an asymptotic value at high SPM concentration, which is about 3 % for the POC in the North Sea; at SPM concentration around 1 mg/l the POC content reaches values up to about 30 % (Fettweis et al., 2022). Schartau et al. (2019) proposed a semi-empirical model of the POM content of the SPM (measured as Loss on Ignition) as a function of SPM concentration, which allowed to calculate the POM concentration when SPM concentration is known. The conceptual basis of the POM-SPM model is that the POM concentration can be written as the sum of two fractions, a fresh and labile fraction (POM_{fresh}) and a less reactive and more refractory fraction (POM_{ref}). The first boundary condition of the model is that, when the SPM concentration approaches zero, the POM content of SPM converges to one, and POM is assumed to be mainly POM_{fresh}. The second one is that, at high SPM concentrations, the POM content converges towards an invariant POM fraction of the SPM, which is assumed to be mainly refractory POM (POM_{ref}). The remaining POM is described as a time varying fraction of the SPM, which can be attributed to the buildup (primary production) and decay (remineralization) of POM_{fresh}. The model was later extended for the POC, the particulate organic nitrogen and the transparent exopolymer particle contents of the SPM (Fettweis et al., 2022). When calibrated with observational data, the model can estimate the compositional changes of the POC fraction as a function of the SPM concentration.

2.4. Grain size, mineralogy and mineral-associated OC

2.4.1. Grain size analysis

The grain-size volume distribution of the samples was measured with laser diffraction using a Malvern Mastersizer-S in water with ultrasound sonication and after a thorough chemical treatment to remove the cementing agents such as the often poorly crystalline calcite cements by a moderate oxalic acid buffering solution, the organics with peroxide/hypochlorite and the free (Fe-)oxides and −hydroxides with the Citrate-Bicarbonate-Dithionite method. The method is based on Jackson (1975). Crystalline calcite and opal are preserved.

2.4.2. Mineralogical analysis method

For bulk mineralogy, a representative portion of each sample was mixed with a 10 % internal standard (ZnO) and 4 ml of ethanol. This mixture was milled for 5 min. using a McCrone micronizing mill and afterwards recuperated in porcelain cups (Środoń et al., 2001). The material was passed through a 250 μm sieve, side-loaded into alumina diffractometer holders to optimize the random orientation of crystallites. Bulk powders were measured by X-ray diffraction from 5 to 65° 2θ with steps of 0.02° lasting 2 s per step. Bulk powder diffraction patterns were analyzed and quantified using the Quanta software (© Chevron ETC) which combines summation of pure reference standards and the use of a ZnO internal standard.

Proven robust quantitative clay mineral analyses have been used following the approach outlined by Drits et al. (1997), Sakharov et al. (1999), Środoń et al. (2001) and Zeelmaekers et al. (2015). All collected samples were subjected to a systematic preparation procedure to characterize both bulk mineral composition and clay mineral composition using X-ray diffraction analysis. Approximately 100 g of each sample was dried at 60 °C and subsequently gently powdered and homogenized in a mortar. For clay mineral analysis, 15 g of powdered sample was subjected to a chemical preparation (modified after Jackson, 1975) during which carbonate cements, organic matter and free Fe-(hydr)oxides were removed using respectively acetic acid/Na-acetate buffer solution, 30 % H_2O_2 solution and Na-dithionite in a Na-citrate-bicarbonate environment respectively. Subsequently, clay material < 2 μm was extracted using a Thermo-Scientific SL-40R centrifuge and Ca-saturated using $CaCl_2$. Clay slides were prepared by sedimenting 160 mg of clay material < 2 μm on a glass slide. Both bulk powders and clay slides were measured using a Philips PW1050/37 goniometer connected to a PW1830 generator equipped with Cu-Kα radiation and PW3011/00 proportional detector in Bragg-Brentano θ–2θ setup. Clay slides were measured in air-dry conditions and saturated with ethylene glycol, each time from 2 to 47° 2θ with steps of 0.02° lasting 2 s per step. Clay slides were also exposed to 550 °C heating during 1 h and measured from 2 to 15° 2θ. Diffraction patterns of oriented slides were analyzed and quantified using the Sybilla clay modeling software (© Chevron ETC) (Adriaens et al., 2014; Zeelmaekers et al., 2015).

2.4.3. Mineral-associated OC content based on the mineral specific surface area

A strong positive correlation between the mineral specific surface area (SSA) and the OC content in sediments has been reported (Mayer, 1994; Keil and Mayer, 2014). Different techniques are used to determine the SSA, such as the gas adsorption method (including the N_2 method), the ethylene glycol monoethyl ether method, and the methylene blue method (Macht et al., 2011; Zhu et al., 2015). The variation in methods and in experimental conditions impact the SSA. However, studies consistently show that smectite has the highest SSA, followed by illite, kaolinite, and chlorite, see Table 1. By comparison, fine sand and silt sized minerals have SSA of 0.1 and 1 m^2/g, respectively. The OC content per SSA (mg/m^2) has been reported as 0.5–1 mg OC/m^2 SSA (Keil and Mayer, 2014) and 0.86 mg OC/m^2 Mayer (1994). Based on the mineral composition and assuming that the mineral surfaces are saturated with OC, we have calculated the OC associated with the minerals per g of SPM using the average values of SSA (Table 1) and OC content per SSA.

3. Results

3.1. Primary particle size

The primary particle size distribution is unimodal in winter in all stations, the median size is between 3.5 and 5.4 μm, showing that the SPM is composed of fine mineral particles (see Table S2, supplementary material). In spring, all stations except the coastal-offshore transect HB2, HB1 and Helgoland, have a bimodal distribution. The first mode corresponds to the winter one, whereas the second one is one order of magnitude larger (30–50 μm). These samples were taken during the

Table 1
Specific surface area (m^2/g) of different clay minerals.

	smectite	illite	kaolinite + chlorite
Zhao et al. (2023)	500–800	60–120	10–20
Macht et al. (2011)	346 ± 37	83 ± 5	–
White (2005)	750	100–200	5–40
Kohnke (1968)	500–800	60–200	20–40
Fripiat (1964)	700–800	100–200	5–20
Greene-Kelly (1962)	600–700	150–250	15–25

spring phytoplankton bloom and the second mode probably corresponds to the diatom skeletons, which have sizes of such magnitude. The vanishing of that second mode before the winter may be due to a combination of biogenic silica settling and dissolution.

3.2. Mineralogy

The bulk mineralogical composition of the SPM samples consists mainly of non-clay minerals (quartz and feldspars), biogenic minerals (carbonates and opal) and clay minerals, see Fig. 2 and Tables S3 and S4 (supplementary material). The other minerals in Fig. 2 are apatite, halite, rutile, anatase, pyrite and marcasite and are typical accessory minerals that occur in low quantities (<5%). The amorphous silica (opal) is from diatoms and is highest in spring, where it reached up to 20 % of the SPM in station W05. Changes in mineral composition are observed along the nearshore to offshore transects. We see generally a decrease of the clay minerals towards the offshore, which points to a dependence on the relative dominance of sandy or muddy lithologies. The latter is more abundant in nearshore areas. The clay mineral content was during both campaigns higher in the turbid nearshore stations Sizewell (41 %), MOW1 (35 %), Scenes (35 %) and in the German Bight stations HB2, HB1 and Helgoland (37 %) than in the low turbid Belgian stations W05, W08 and Codevco (22 %). In the remaining stations the clay mineral content was more variable between both campaigns (Dogger Bank: 19–47 % and West Gabbard: 17–40 %). The biogenic mineral fraction (carbonates and opal) increased generally towards the offshore, where it reached up to 50 %. It was always high (42–50 %) in stations MOW1, W05 and W08, and always low at Sizewell, Dogger Bank and HB2 (<30 %). In the other stations the content was significantly higher in spring than in winter.

The quantitative clay composition of the SPM consists of smectite, interstratified illite–smectite with about (65–75 % illite), illite, kaolinite and chlorite (see Tables S5 and S6, supplementary material). In the ternary diagram, smectite, illitic minerals (sum of illite and interstratified illite–smectite) and kaolinite + chlorite form the endmember compositions (Fig. 3). The clay mineral composition in all stations is on average 33.8 ± 8.8 % (interstratified illite–smectite), 25.5 ± 6.0 % (smectite), 16.6 ± 5.1 % (illite), 14.5 ± 4.2 % (kaolinite) and 2.1 ± 0.6 % (chlorite). The outliers in clay mineral composition are W08 in winter (low smectite content), Dogger Bank winter (high kaolinite + chlorite content) and Helgoland, Sizewell and BS1 in spring (high smectite content).

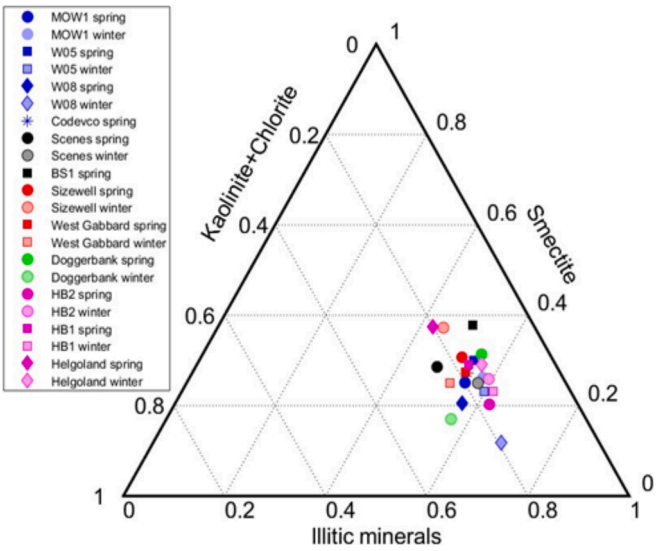

Fig. 3. Ternary diagram of the quantitative clay composition (<2µm) of the SPM in the North Sea with smectite, illitic minerals (illite + interstratified illite–smectite) and kaolinite + chlorite as endmember compositions, see Tables S5 and S6 in supplementary material for details.

3.3. OC content of the SPM

3.3.1. OC content derived from SSA and water samples

The OC content attached to minerals, called '$POC_{mineral}$ content', has been calculated using the SSA of the minerals (Table 1), the clay mineral fraction (Tables S3 and S4, supplementary material) and the clay mineral composition (Tables S5 and S6, supplementary material). This $POC_{mineral}$ content is compared with the mean surface POC content of the SPM (i.e., the POC:SPM ratio) obtained from water samples and called 'sample POC' (Table 2). The table shows that the sample POC content is always higher than the $POC_{mineral}$ content. The highest sample POC contents occur in spring during the phytoplankton bloom and can reach up to 12 % at the Dogger Bank station; in winter, the sample POC content is lower but remains about 5–10 times higher than the

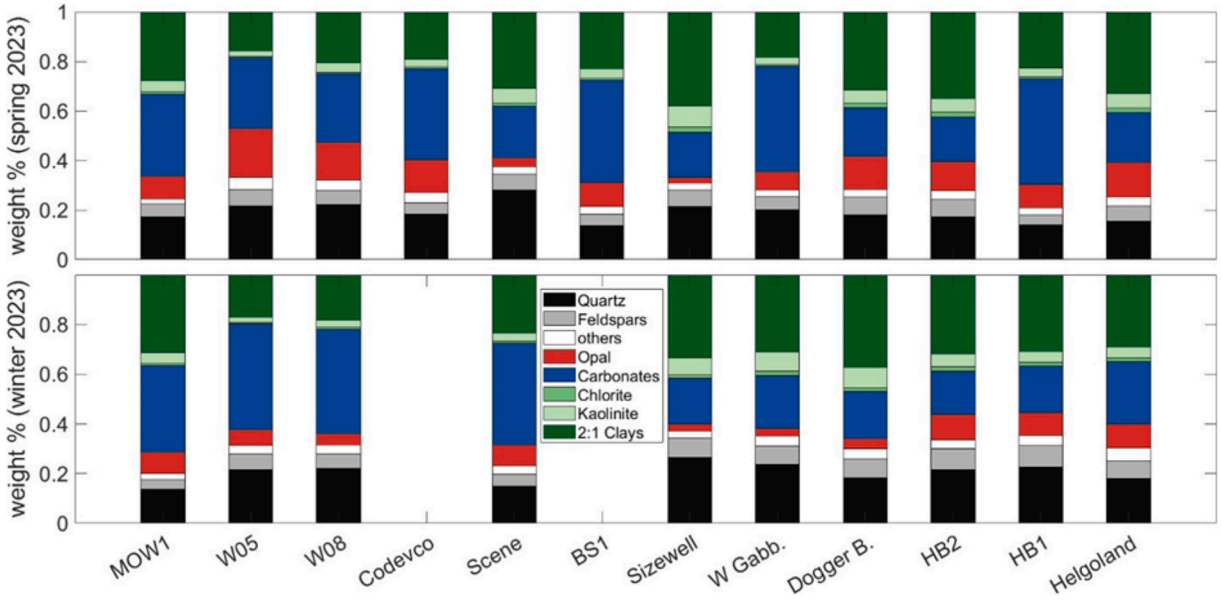

Fig. 2. Bulk mineralogy of the SPM in spring (above) and winter 2023 (below), see Tables S3 and S4 in supplementary material for details.

Table 2
POC content of the SPM (in %) derived from the mineral SSA ($POC_{mineral}$) and from the ratio of POC:SPM concentration from water sample (sample-POC). The standard deviation for $POC_{mineral}$ is based on the uncertainties in surface area and OC content of clay minerals found in the literature (see §2.4.3). The geometric mean and standard deviation of the POC content are obtained from averaging all data collected during a full or half tidal cycle.

	spring 2023		winter 2023	
	$POC_{mineral}$ (%)	sample-POC (%)	$POC_{mineral}$ (%)	sample-POC (%)
MOW1	0.71 ± 0.27	2.11*/2.7	0.86 ± 0.33	2.81*/1.1
W05	0.46 ± 0.18	5.12*/1.7	0.43 ± 0.17	2.79*/1.1
W08	0.48 ± 0.18	10.92*/1.6	0.39 ± 0.16	3.61*/1.2
Codevco	0.51 ± 0.20	7.54*/1.6	–	2.85*/1.1
Scene	0.82 ± 0.32	2.95*/1.5	0.62 ± 0.24	5.75*/1.2
BS1	0.77 ± 0.30	3.50*/1.5	–	–
Sizewell	1.18 ± 0.45	2.33*/1.3	1.10 ± 0.43	2.60*/1.4
West Gabbard	0.50 ± 0.19	3.34*/1.3	0.88 ± 0.34	4.62*/1.4
Dogger Bank	0.96 ± 0.37	11.82*/1.2	0.82 ± 0.31	5.07*/1.4
HB2	0.90 ± 0.35	4.00*/1.2	0.91 ± 0.35	3.81*/1.3
HB1	0.64 ± 0.25	3.58*/1.3	0.80 ± 0.31	5.44*/1.5
Helgoland	1.05 ± 0.41	5.27*/1.8	0.85 ± 0.33	6.12*/1.4

$POC_{mineral}$ content. The highest SSA derived OC content is found in the samples with highest smectite content.

3.3.2. Modeled POC content

The POC_{ref} and POC_{fresh} contents have been calculated using the semi-empirical POC-SPM model and the parameters given in Fettweis et al. (2022) applied to the SPM concentrations analyzed from the water samples, see Table 3. Whereas the refractory POC (POC_{ref}) content is quasi constant, the POC_{fresh} content varies with season (higher in spring) and SPM concentration. From the turbid inshore towards clearer offshore waters, the relative proportion of the POC_{fresh} versus the POC_{ref} content increases. Accordingly, at low SPM concentration the POC_{fresh} content is high, whereas at high SPM concentrations the POC_{ref} content dominates.

Table 3
Estimates of POC_{ref} and POC_{fresh} content (in %) of the SPM using the semi-empirical model of Fettweis et al. (2022). The values have been calculated using the measured SPM and sample-POC concentrations and are given as the geometric mean and standard deviation during a full or half tidal cycle.

	spring 2023			winter 2023		
	SPM (mg/l)	POC_{ref} (%)	POC_{fresh} (%)	SPM (mg/l)	POC_{ref} (%)	POC_{fresh} (%)
MOW1	121*/1.9	2.94*/2.4	0.27*/2.4	83*/2.0	3.01*/3.2	0.10*/3.2
W05	20*/2.1	2.94*/2.9	1.42*/2.9	9.6*/1.1	3.00*/1.3	0.79*/1.3
W08	5.1*/1.9	2.94*/2.4	4.01*/2.4	4.6*/1.1	3.00*/1.2	1.54*/1.2
Codevco	15*/1.3	2.94*/2.4	1.86*/2.4	14*/1.3	3.00*/1.5	0.60*/1.5
Scene	18*/1.6	2.91*/2.0	1.42*/2.0	8.7*/1.3	3.01*/1.4	0.92*/1.4
BS1	8.2*/1.8	2.92*/2.2	2.71*/2.2	–	–	–
Sizewell	31*/1.4	2.92*/1.6	0.91*/1.6	31*/1.4	3.01*/2.3	0.28*/2.3
West Gabbard	7.7*/1.5	2.92*/1.8	2.85*/1.8	7.2*/1.2	3.01*/1.3	1.08*/1.3
Dogger Bank	1.8*/1.3	2.93*/1.4	6.64*/1.4	3.4*/1.3	3.01*/1.3	2.05*/1.3
HB2	21*/1.2	2.93*/1.3	1.36*/1.3	22*/1.3	3.01*/2.8	0.37*/2.8
HB1	11*/1.3	2.93*/1.4	2.28*/1.4	5.3*/1.9	3.01*/2.3	1.37*/2.3
Helgoland	3.9*/1.8	2.93*/2.2	4.59*/2.2	3.4*/1.3	3.01*/1.6	2.00*/1.6

3.3.3. Variability of DOC and POC concentrations

The tidal averaged sample-POC and DOC concentrations are given in Table 4 and the sample-POC:DOC ratios are shown in Fig. 4. Additional sample-POC and DOC concentrations (2019–2023) from stations MOW1, W05 and W08 have been included in the figure. The figure shows that DOC concentrations exceed the POC concentration at low SPM concentration, while above about 30 mg/l the POC concentration is higher.

4. Discussion

We have derived the POC content of the SPM using three methods. The bulk POC content (sample-POC) is calculated from water samples (POC and SPM concentration) and provides a value that is based on the filterability of the particles (particles > 1.2 μm) and can be seen as a reference for the total POC content of the SPM. The SSA-derived OC is the mineral-associated fraction ($POC_{mineral}$ content) as described by Keil and Mayer (2014). This fraction is likely to be incorporated in marine sediments (Mayer, 1995; Middelburg and Meysman, 2007). The $POC_{mineral}$ fraction is, however, not necessarily constant in composition as it may occur in an actively reversible sorption equilibrium (Blattmann et al., 2019; Kleber et al., 2021). With the SPM-POC model, two fractions are obtained, one that contains the fresh and consumable fraction that encompasses the living cells and their exudates (Fettweis et al. 2022). This POC_{fresh} fraction has a seasonal cycle driven by phytoplankton production – and hence light, nutrient availability and temperature – and a large fraction of it is rapidly recycled (Muylaert et al., 2006; Schartau et al., 2019). The other fraction, POC_{ref}, contains the mineral-associated fraction and a fraction with a longer, but variable, turnover time. It may consist amongst others of POC that is protected by occlusion into small clay mineral aggregates (flocculi) and other slowly degradable OM. The partitioning of organic carbon into two pools has been widely used in the literature, however, no clear definition exists on what constitutes labile or refractory material as it depends on the interactions between the OM and the environment. Therefore, many authors

Table 4
Sample-POC and DOC concentrations (in mg/l) analyzed from water samples. The (geometric for POC, arithmetic for DOC) mean and standard deviation of the POC and DOC concentration is from the averaging of all data collected during a full or half tidal cycle.

	spring 2023		winter 2023	
	sample-POC (mg/l)	DOC (mg/l)	sample-POC (mg/l)	DOC (mg/l)
MOW1	4.90*/2.5	1.61 ± 0.15	2.32*/2.0	1.48 ± 0.18
W05	0.82*/1.4	1.31 ± 0.03	0.25*/1.2	0.82 ± 0.01
W08	0.56*/1.2	1.09 ± 0.13	0.17*/1.1	0.69 ± 0.04
Codevco	1.04*/1.3	1.42 ± 0.09	0.39*/1.3	1.02 ± 0.07
Scene	0.53*/1.4	–	0.50*/1.2	2.06 ± 0.65
BS1	0.29*/1.4	–	–	–
Sizewell	0.71*/1.3	–	0.79*/1.2	1.05 ± 0.10
West Gabbard	0.26*/1.4	–	0.33*/1.2	0.93 ± 0.06
Dogger Bank	0.21*/1.5	–	0.17*/1.1	0.99 ± 0.10
HB2	0.80*/1.2	–	0.83*/1.3	2.40 ± 0.43
HB1	0.39*/1.2	–	0.29*/1.4	1.26 ± 0.10
Helgoland	0.20*/1.3	–	0.20*/1.1	1.02 ± 0.03

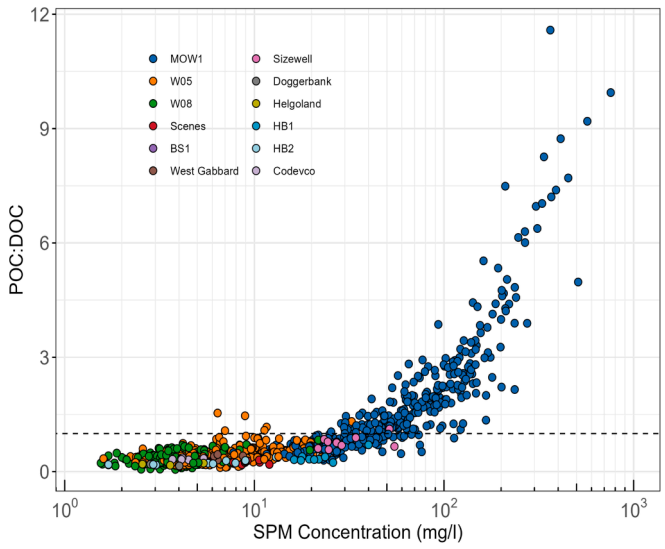

Fig. 4. Sample-POC:DOC ratio (1:1 dashed line shown) as a function of SPM concentration. Additional data have (2019–2023) been added for stations MOW1, W05, and W08.

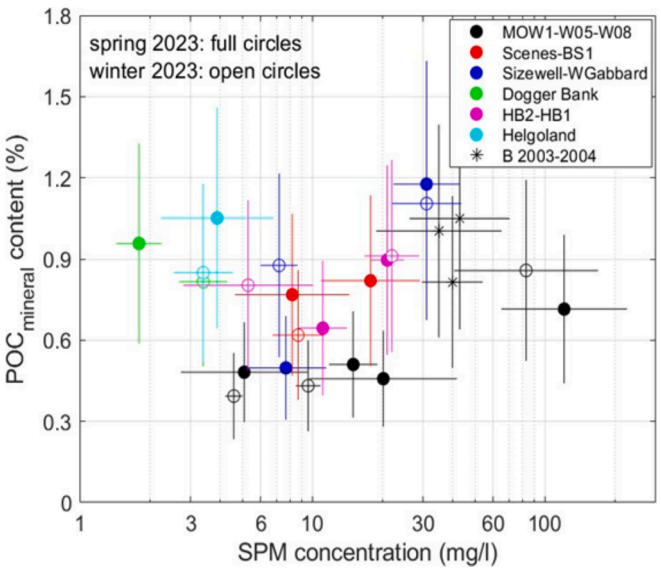

Fig. 5. $POC_{mineral}$ content of the SPM derived from mineral SSA as a function of SPM concentration. The vertical error bars are the standard deviation from the SSA of the minerals (Table 1) and the horizontal ones the standard deviation from the full or half tidal averaging. 'B 2003-2004' are additional data from the Belgian part of the North Sea, see § 4.2.

consider the degradability of the POC as a continuum between two different extremes: fast degradation within hours to days and preservation on geological time scales (Middelburg et al, 1993; Mayer, 1995; Dauwe et al., 1999; Liu and Xue, 2020; Baltar et al., 2021). Our approach makes a distinction within the non-fresh fraction. The $POC_{mineral}$ fraction is the most refractory one and is only varying with the mineral composition of the SPM (considering that available mineral surfaces are always saturated with their associated OM). The POC fraction that remains after subtraction of the $POC_{mineral}$ from the bulk POC concentration can be split into a fresh and labile fraction (POC_{fresh}) and a fraction that is slowly degradable (POC_{slow}). The total POC concentration can then be written as:

$$POC = POC_{mineral} + POC_{slow} + POC_{fresh}$$

Hereunder we explore three questions: 1) How does the $POC_{mineral}$ content vary with SPM concentration, i.e., in the cross-shore axis; 2) What is the mineralogical variability of SPM in time; and 3) Is the $POC_{mineral}$ the missing DOC at high SPM concentration?

4.1. $POC_{mineral}$ content along a nearshore to offshore transect

The dynamic nature of shelf seas is responsible for variations in SPM concentration (Fig. 1) and POC content (Desmit et al., 2024). The $POC_{mineral}$ content of the SPM in the measuring stations as a function of SPM concentration is shown in Fig. 5. The large spread in the data is related to the heterogeneity in clay mineral content (% of clay in SPM) and clay mineral composition (types of clay). This variability may occur on spatial and temporal scales, for instance when comparing Helgoland to the nearshore HB2, or HB1 in winter and in spring. Despite the large spreading, an increase in $POC_{mineral}$ content with increasing SPM concentration can be observed in most areas, with the exceptions of Dogger Bank, Helgoland and HB1 in winter. Irion et al. (1987) report that under normal conditions (without human activities), river sediments are trapped in the estuaries (Elbe, Weser). They argue that the recent mud accumulation SE of Helgoland is the result of loss of SPM by dredging operations in the estuaries, increasing the natural sediments discharge and thus favoring export of SPM towards the German Bight. This finding might explain the peculiar result from Helgoland and/or HB1, which are more typical for the nearshore. The differences between regions, for example the lower increase in $POC_{mineral}$ content in the Belgian stations (MOW1-W05-W08 and Codevco) when compared to the German and UK stations indicates the heterogeneity of SPM composition in the study area, and underlines that the SPM in the North Sea has different provenances (Adriaens et al., 2018). A detailed mineralogical composition in space and time is therefore needed to differentiate accurately between the more refractory POC fractions ($POC_{mineral}$ and POC_{slow}).

A typical feature of shelf seas is the persistence of a horizontal cross-shore gradient, with higher SPM concentrations in the shallow coastal waters and lower concentrations offshore. Desmit et al. (2024) confirmed the concept of 'line of no return' of Postma (1984) by using the POM composition and content of the SPM. Such a line is located at some distance from the coast and functions as a zone with low cross transport of SPM. The data from the Belgian (MOW1, W05, W08), UK (Sizewell, West Gabbard) and German (HB2, HB1) stations show a decrease in clay mineral content towards the offshore and confirm that a transition zone exists, not only in the POC content and composition but also in the mineral content and composition. The line of no return can be interpreted as the outer limit to a transition zone where similar concentrations of POM_{fresh} and POM_{ref} prevail (Desmit et al., 2024), changes in phytoplankton order richness take place (Jung et al., 2017) and lowering of the mineral specific surface area per unit of SPM occur. We can distinguish two $POC_{mineral}$ contents: one offshore and one inshore the transition zone, see Table 5. The POC is thus less refractory offshore than nearshore.

4.2. Temporal variability of SPM mineralogy

The SPM concentration and composition is highly variable and depends on hydrodynamics, wind, waves, season, seafloor composition and human activities. Seasonal changes drive biological processes that

Table 5
Averaged $POC_{mineral}$ content (±uncertainty) in cross-shore direction for 4 regions in the North Sea and English Channel based on Fig. 5 (data 2023).

	high turbid	low turbid
Belgian transect	0.79 ± 0.22	0.45 ± 0.09
UK, F and G transect	0.98 ± 0.17	0.58 ± 0.13
Helgoland	–	0.90 ± 0.20
Dogger Bank	–	0.89 ± 0.24

change the POC content, of which a major part is POCfresh. Spring-neap cycles, storm frequency and wind direction, have an influence on the transport, resuspension or erosion of the seabed and may alter the mineral composition. For the Belgian nearshore area Adriaens et al. (2018) concluded that the SPM originates from the erosion and resuspension of the muddy seafloor, which has the same clay mineral composition as the SPM. This conclusion was supported by 15 centrifuge samples that have been collected during four sampling campaigns in 2003, 2004 and 2007 in the Belgian part of the North Sea (Zeelmaekers, 2011). The clay minerals were analyzed using the method described above, bulk mineralogy was only determined on five samples and SPM concentration on only three. In Fig. 6, these clay mineral compositions are presented with the 2023 data. The figure shows that the sum of kaolinite and chlorite remains constant (about 20 %), but that there are large variations in the smectite and illitic minerals content. In the older data the smectite content is between 39 % and 53 % while in 2023 smectites represent only between 12 % and 26 %. A lower smectite content decreases the SSA significantly and thus the $POC_{mineral}$ content. The older data align with the UK, German and French data from 2023, see Fig. 5. The reason for the difference between 2023 and 2003–2007 could be an increase of the SPM transport from the English Channel towards the North Sea caused by higher frequency of S, SW and W weather types. An increase of southwesterly winds in the Southern Bight of the North Sea has been reported by van den Eynde et al. (2012). Fettweis et al. (2012) have argued that changes in the frequency of these weather types change the SPM concentration distribution and thus possibly also the SPM mineral composition. SPM from the English Channel contain 10–30 % less smectite than the 2003–2007 SPM samples and have a higher carbonate content due to the erosion of cretaceous cliffs (Adriaens et al., 2018). The latter is supported by the higher carbonate content (35 %) in the recent samples from the Belgian part of the North Sea than in the samples from 2003 to 2007 (29 %).

4.3. $POC_{mineral}$ and DOC

The traditional classification of organic matter into particulate and dissolved components is based on size and filtration properties. However, this classification can be distorted by the interaction of smaller dissolved molecules with mineral particles (Keil et al., 1994). These molecules, though intrinsically bound to be dissolved or colloidal, may be retained on filters due to their association with minerals, increasing the measured amount of POC. From a compositional point of view, only POC_{fresh} and POC_{slow} depend on phytoplankton production, remineralization, erosion or terrestrial input as opposed to $POC_{mineral}$, which depends only on the mineral composition. This effect is likely to be pronounced in nearshore turbid waters, which have higher mineral particle concentrations compared to clearer offshore waters.

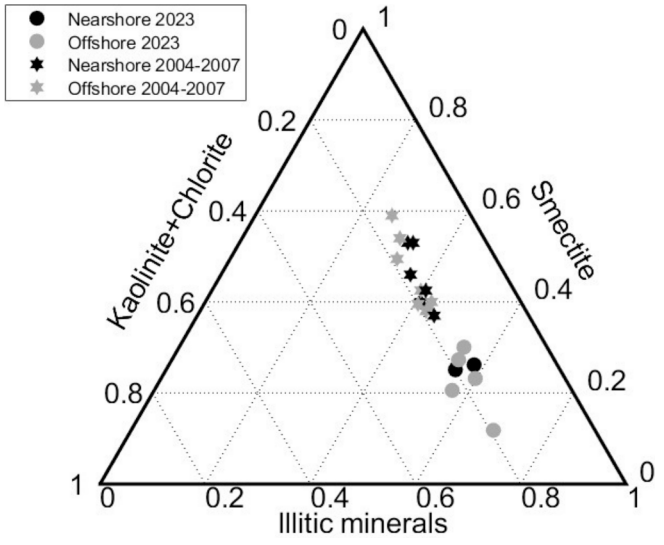

Fig. 6. Ternary diagram of the longer-term quantitative clay composition (<2μm) of the SPM limited to the Belgian part of the North Sea with smectite, illitic minerals (illite + interstratified illite–smectite) and kaolinite + chlorite as endmember compositions. We compare 15 samples from 2004 to 2007 with the 7 samples from 2023 (stations MOW1, W05, W08 and Codevco).

Offshore waters generally exhibit sample-POC/DOC ratios well below 1, indicating a dominance of the DOC fraction (Osterholz et al., 2021), whereas ratios greater than 1 are often reported in turbid waters (Abril et al., 2002; Zhao and Gao, 2019). Herman and Heip (1999) demonstrated systematic variation in sample-POC/DOC ratios as a function of SPM concentrations in European estuaries, suggesting significant exchange between particulate and dissolved pools through adsorption and desorption processes. Similarly, along the Belgian transect, sample-POC/DOC ratios greater than 1 are frequently observed at MOW1 (Fig. 4) but become less common at comparatively deeper and less turbid stations like W05 and W08. The OC adsorbed onto mineral particles is dynamically exchanging with the DOC, and thus influencing its fate and concentration. Clearly, such adsorption stabilizes the organic compound and may delay its degradation and loss (Keil et al., 1994; Hemingway et al., 2019), although some transformation of the adsorbed OC continuously occur (Kleber et al., 2021). The desorption of organic compounds can lead to their further transformation and replacement by other organic compounds present in the marine system (Blattmann et al., 2019). However, this process is not sufficient to explain the variation in POC/DOC ratio along the SPM concentration gradient as suggested by Herman and Heip (1999) for estuaries. Subtracting $POC_{mineral}$ (estimated from the mineral SSA) from the sample-POC and adding it to the DOC concentration results in a lower POC/DOC ratio, however, it still remains 2–4 times higher nearshore than offshore. This higher nearshore $(POC\text{-}POC_{mineral})/(DOC + POC_{mineral})$ ratio can be further explained by phytoplankton production, advection and diffusion, density gradients and seabed erosion. The production of POC and DOC is higher nearshore because of a higher phytoplankton production due to higher nutrient concentration. This higher production will be affected by down-gradient diffusion, tidal or wind-driven advection and by the occurrence of a horizontal density gradient, initiated by fresh water inflow by rivers that causes a net particle transport towards the coast (see Desmit et al., 2024). For the Belgian nearshore, additional input of POC results from the erosion of OM rich muddy sediments (see Adriaens et al., 2018).

5. Conclusions

The SPM is composed of both mineral and organic particles that interact constantly. The organic fraction of the SPM is composed of labile and refractory material. To better understand these interactions on the North Sea shelf, we have analyzed at different locations the mineralogical composition of clays and have estimated the mineral SSA, which is correlated with the amount of adsorbed organic compounds. Assuming these mineral surfaces are always saturated with organic matter, we calculated the mineral-associated POC linked to the SPM concentration at each location. The resulting mineral-associated POC is consistently lower than the one estimated in a previous model study (Fettweis et al., 2022). This led us to consider three different fractions of POC, which are the $POC_{mineral}$, that is the organic molecules adsorbed onto mineral surfaces and thereby less exposed to degradation, the POC_{slow}, that is an intrinsically refractory fraction with variable rates of degradation, and the POC_{fresh}, that is an intrinsically labile fraction. The OC adsorbed onto mineral particles is dynamically exchanging with the DOC, and thus influencing its fate and concentration. However this process is not sufficient to explain the variation in POC/DOC ratio along the SPM concentration gradient, which is further explained by primary production, advection and diffusion, density gradients and seabed erosion.

CRediT authorship contribution statement

Michael Fettweis: Writing – original draft, Visualization, Project administration, Methodology, Investigation, Funding acquisition, Formal analysis, Conceptualization. **Saumya Silori:** Writing – original draft, Visualization, Methodology, Investigation, Formal analysis, Conceptualization. **Rieko Adriaens:** Writing – review & editing, Resources, Methodology. **Xavier Desmit:** Writing – review & editing, Methodology, Formal analysis, Conceptualization.

Data availability

Data of in situ SPM, POC and DOC concentrations are available at https://doi.org/10.24417/bmdc.be:dataset:2900.

Declaration of competing interest

The authors declare that they have no known competing financial interests or personal relationships that could have appeared to influence the work reported in this paper.

Acknowledgements

The research was supported by the Belgian Science Policy (BELSPO) within the BRAIN-be PiNS (contract nr RV/21/PiNS) and the Ministry of the Flemish Community (Belgium) (MOMO project). Ship time with the RV Belgica was provided by BELSPO and the Royal Belgian Institute of Natural Sciences (OD Natural Environment).

Appendix A. Supplementary material

Supplementary data to this article contain the coordinates of the stations and the sampling dates, the primary particle size parameters, the bulk mineralogy and the quantitative clay mineral composition of the clays in the SPM.

Supplementary material to this article can be found online at https://doi.org/10.1016/j.gca.2025.03.003.

References

Abril, G., Nogueira, M., Etcheber, H., Cabeçadas, G., Lemaire, E., Brogueira, M.J., 2002. Behaviour of organic carbon in nine contrasting European estuaries. Estuar. Coast. Shelf Sci. 54, 241–262.

Adriaens, R., Vandenberghe, N., Elsen, J., 2014. Natural clay-sized glauconite in the Neogene deposits of the Campine Basin (Belgium). Clays Clay Miner. 62, 35–52.

Adriaens, R., Zeelmaekers, E., Fettweis, M., Vanlierde, E., Vanlede, J., Stassen, P., Elsen, J., Środoń, J., Vandenberghe, N., 2018. Quantitative clay mineralogy as provenance indicator for recent muds in the southern North Sea. Mar. Geol. 398, 48–58.

Arndt, S., Jørgensen, B.B., LaRowe, D.E., Middelburg, J.J., Pancost, R.D., Regnier, P., 2013. Quantifying the degradation of organic matter in marine sediments: a review and synthesis. Earth Sci. Rev. 123, 53–86.

Baltar, F., Alvarez-Salgado, X.A., Arístegui, J., Benner, R., Hansell, D.A., Herndl, G.J., Lønborg, C., 2021. What is refractory organic matter in the ocean? Front. Mar. Sci. 8, 642637.

Blattmann, T.M., Liu, Z., Zhang, Y., Zhao, Y., Haghipour, N., Montlucon, D.B., Plötze, M., Eglinton, T.I., 2019. Mineralogical control on the fate of continentally derived organic matter in the ocean. Science 366, 742–745.

Chen, Y.-M., Gao, J.-B., Yuan, Y.-Q., Ma, J., Yu, S., 2016. Relationship between heavy metal contents and clay mineral properties in surface sediments: implications for metal pollution assessment. Cont. Shelf Res. 124, 125–133.

Dauwe, B., Middelburg, J.J., Herman, P.M.J., Heip, C.H.R., 1999. Linking diagenetic alteration of amino acids and bulk organic matter reactivity. Limnol. Oceanogr. 44, 1809–1814.

Deng, Z., Huang, D., He, Q., Chassagne, C., 2022. Review of the action of organic matter on mineral sediment flocculation. Front. Earth Sci. 10, 965919.

Desmit, X., Schartau, M., Terseleer, N., Van der Zande, D., Riethmüller, R., Fettweis, M., 2024. The transition between coastal and offshore areas in the North Sea unraveled by the suspended particle composition. Sci. Total Environ. 915, 169966.

Drits, V.A., Lindgreen, H., Sakharov, B.A., Salyn, A.L., 1997. Sequential structure transformation of illite-smectite-vermiculite during diagenesis of Upper Jurassic shales. North Sea. Clay Miner. 33, 351–371.

Ehrhardt, M., Koeve, W., 1999. Determination of particulate organic carbon and nitrogen. In: Grasshoff, K., Kremling, K., Ehrhardt, M. (Eds.), Methods of Seawater Analysis, 3rd ed.,. Wiley, pp. 437–444.

Etcheber, H., Taillez, A., Abril, G., Garnier, J., Servais, P., Moatar, F., Commarieu, M.-V., 2007. Particulate organic carbon in the estuarine turbidity maxima of the Gironde, Loire and Seine estuaries: origin and lability. Hydrobiol. 588, 245–259.

Fettweis, M., Monbaliu, J., Nechad, B., Baeye, M., Van den Eynde, D., 2012. Weather and climate related spatial variability of high turbidity areas in the North Sea and the English Channel. Meth. Oceanogr. 3–4, 25–39.

Fettweis, M., Schartau, M., Desmit, X., Lee, B.J., Terseleer, N., Van der Zande, D., Parmentier, K., Riethmüller, R., 2022. Organic matter composition of biomineral flocs and its influence on suspended particulate matter dynamics along a nearshore to offshore transect. J. Geophys. Res. Biogeosci. 127, e2021JG006332.

Fripiat, W.F., 1964. In: Bradley, W.F. (Ed.), Clay and clay minerals, proc. 12th nat. conf.. Macmillan, New York, pp. 327–358.

Greene-Kelly, R., 1962. The identification of montmorillonoids in clay. J. Soil Sci. 4, 233–237.

Hedges, J.I., Keil, R.G., 1995. Sedimentary organic matter preservation: an assessment and speculative synthesis. Mar. Chem. 49, 81–115.

Hemingway, J.D., Rothman, D.H., Grant, K.E., Rosengard, S.Z., Eglinton, T.I., Derry, L.A., Galy, V.V., 2019. Mineral protection regulates long-term global preservation of natural organic carbon. Nature 570, 228–231.

Herman, P.M.J., Heip, C.H.R., 1999. Biogeochemistry of the Maximum Turbidity Zone of Estuaries (MATURE) Some Conclusions. J. Mar. Syst. 22, 89–104.

Irion, G., Wunderlich, F., Schwedhelm, E., 1987. Transport of clay minerals and anthropogenic compounds into the German Bight and the provenance of fine-grained sediments SE of Helgoland. J. Geol. Soc. 144, 153–160.

Ittekkot, V., 1988. Global trends in organic matter in river suspensions. Nature 332, 436–438.

Jackson, M.L., 1975. Soil chemical analysis. 2nd Ed. Parallel Press, University of Wisconsin, 895pp.

Jung, A.S., Bijkerk, R., Van Der Veer, H.W., Philippart, C.J.M., 2017. Spatial and temporal trends in order richness of marine phytoplankton as a tracer for the exchange zone between coastal and open waters. J. Mar. Biol. Assoc. 97, 477–489.

Keil, R.G., Montluçon, D.B., Prahl, F.G., Hedges, J.I., 1994. Sorptive preservation of labile organic matter in marine sediments. Nature 370, 549–552.

Keil, R.G., Mayer, L.M., 2014. 12.12 - Mineral matrices and organic matter. Treatise Geochem. (2nd Ed.) 12, 337–359.

Kohnke, H., 1968. Soil physics. McGraw-Hill Book Co., New York.

Kleber, M., Bourg, I.C., Coward, E.K., Myneni, S.C.B., Nunan, N., 2021. Dynamic interactions at the mineral–organic matter interface. Nature Rev. Earth Environ. 2, 402–421.

Lee, B.J., Fettweis, M., Toorman, E., Molz, F., 2012. Multimodality of a particle size distribution of cohesive suspended particulate matters in a coastal zone. J. Geophys. Res. Ocean 117, C03014.

Liu, Z., Xue, J., 2020. The lability and source of particulate organic matter in the Northern Gulf of Mexico Hypoxic Zone. J. Geophys. Res. Biogeosci. e2020JG005653.

Maggi, F., 2009. Biological flocculation of suspended particles in nutrient-rich aqueous ecosystems. J. Hydrol. 376, 116–125.

Macht, F., Eusterhues, K., Pronk, G.J., Totsche, K.U., 2011. Specific surface area of clay minerals: comparison between atomic force microscopy measurements and bulk-gas (N2) and -liquid (EGME) adsorption methods. Appl. Clay Sci. 53, 20–26.

Mayer, L.M., 1994. Surface area control of organic carbon accumulation in continental shelf sediments. Geochim. Cosmochim. Acta 58, 1271–1284.

Mayer, L.M., 1995. Sedimentary organic matter preservation: an assessment and speculative synthesis - a comment. Mar. Chem. 49, 123–126.

Middelburg, J.J., Vlug, T., Vandernat, F., 1993. Organic-matter mineralization in marine systems. Global Planet. Change 8, 47–58.

Middelburg, J.J., Meysman, F.J.R., 2007. Burial at sea. Science 316, 1249–1295.

Mitchel, J.K., Soga, K., 2005. Fundamentals of Soil Behavior. John Wiley, p. 558.

Muylaert, K., Gonzales, R., Franck, M., Lionard, M., Van der Zee, C., Cattrijsse, A., Vyverman, W., 2006. Spatial variation in phytoplankton dynamics in the Belgian coastal zone of the North Sea studied by microscopy, HPLC-CHEMTAX and underway fluorescence recordings. J. Sea Res. 55, 253–265.

Nechad, B., Ruddick, K.G., Park, Y., 2010. Calibration and validation of a generic multisensor algorithm for mapping of total suspended matter in turbid waters. Remote Sens. Environ. 114, 854–866.

Opdal, A.F., Lindemann, C., Aksnes, D.L., 2019. Centennial decline in North Sea water clarity causes strong delay in phytoplankton bloom timing. Global Change Biol. 25, 3946–3953.

Osterholz, H., Kilgour, D.P.A., Storey, D.S., Lavik, G., Ferdelman, T.G., Niggemann, J., Dittmar, T., 2021. Accumulation of DOC in the South Pacific Subtropical Gyre from a molecular perspective. Mar. Chem. 231, 103955.

Pedersen, T., Calvert, S., 1990. Anoxia vs. productivity: what controls the formation of organic-carbon-rich sediments and sedimentary rocks? Am. Assoc. Pet. Geol. Bull. 74, 454–466.

Postma, H., 1984. Introduction to the symposium on organic matter in the Wadden Sea. Neth. Inst. Sea Res. - Publ. Ser. 10, 15–22.

Sakharov, B.A., Lindgreen, H., Salyn, A.L., Drits, V.A., 1999. Determination of illite smectite structures using multispecimen X-ray diffraction profile fitting. Clays Clay Miner. 47, 555–566.

Schartau, M., Riethmüller, R., Flöser, G., van Beusekom, J., Krasemann, H., Hofmeister, R., Wirtz, K., 2019. On the separation between inorganic and organic fractions of suspended matter in a marine coastal environment. Progr. Oceanogr. 171, 231–250.

Shen, X., Toorman, E.A., Lee, B.J., Fettweis, M., 2018. Biophysical flocculation of suspended particulate matters in Belgian coastal zones. J. Hydrol. 567, 238–252.
Singh, M., Sarkar, B., Biswas, B., Churchman, J., Bolan, N.S., 2016. Adsorption-desorption behavior of dissolved organic carbon by soil clay fractions of varying mineralogy. Geoderma 280, 47–56.
Środoń, J., Drits, V.A., McCarty, D.K., Hsieh, J.C.C., Eberl, D.D., 2001. Quantitative XRD analysis of clay-rich rocks from random preparations. Clays Clay Miner. 49, 514–528.
Van den Eynde, D., De Sutter, R., Haerens, P., 2012. Evolution of marine storminess in the Belgian part of the North Sea. Nat. Hazards Earth Syst. Sci. 12, 305–312.
van der Zee, C., Chou, L., 2005. Seasonal cycling of phosphorus in the Southern Bight of the North Sea. Biogeosci. 2, 27–42.
White, R.E., 2005. Principles and Practice of Soil Science: The Soil as a Natural Resource, 4th Edition. Blackwell Publishing.
Zeelmaekers, E., 2011. Computerized qualitative and quantitative clay mineralogy: Introduction and application to known geological cases. KULeuven, Belgium. PhD thesis.
Zeelmaekers, E., Honty, M., Derkowski, A., Środoń, J., De Craen, M., Vandenberghe, N., Adriaens, R., Ufer, K., Wouters, L., 2015. Qualitative and quantitative mineralogical composition of the Rupelian Boom clay in Belgium. Clay Miner. 50, 249–272.
Zhao, L., Gao, L., 2019. Dynamics of dissolved and particulate organic matter in the Changjiang (Yangtze River) Estuary and the adjacent East China Sea shelf. J. Mar. Sys. 198, 103188.
Zhao, T., Xu, S., Hao, F., 2023. Differential adsorption of clay minerals: implications for organic matter enrichment. Earth Sci. Rev. 246, 104598.
Zhu, X., Cai, J., Song, G., Ji, J., 2015. Factors influencing the specific surface areas of argillaceous source rocks. Appl. Clay Sci. 109–110, 83–94.